SCIENCE CHINA
Chemistry

•INVITED REVIEWS•

October 2025 Vol.68 No.10: 4552–4594
https://doi.org/10.1007/s11426-025-2942-5

Artificial intelligence for nanomedicine

Xiaolin Song[1,2,3], Xingfa Gao[1*], Hui Wang[1], Fangzhi Yu[4], Mengmeng Qin[4], Yiye Li[4], Yixuan Liu[4], Wei Feng[5], Caiyu Zhou[6], Nikita N. Chukavin[7,8], Liming Wang[9], Xuejing Cui[4], Xinghua Shi[1*], Lele Li[4*], Huan Meng[4*], Guangjun Nie[4*], Hao Wang[4*], Jinming Hu[10*], Liang Yan[4*], Yu Chen[5*], Lizeng Gao[6*], Anton L. Popov[7*], Hui Wei[8,11,12*], Chunying Chen[4*] & Yuliang Zhao[3*]

[1]*Laboratory of Theoretical and Computational Nanoscience, National Center for Nanoscience and Technology of China, Beijing 100190, China*
[2]*University of Chinese Academy of Sciences, Beijing 100049, China*
[3]*Institute of Nanotechnology and Intelligence (inAI), College of Chemistry and Materials Science, Jinan University, Guangzhou 511443, China*
[4]*CAS Key Laboratory for Biomedical Effects of Nanomaterials and Nanosafety, National Center for Nanoscience and Technology, Beijing 100190, China*
[5]*School of Life Sciences, Shanghai University, Shanghai 200444, China*
[6]*CAS Engineering Laboratory for Nanozyme, Key Laboratory of Biomacromolecules, Institute of Biophysics, Chinese Academy of Sciences, Beijing 100101, China*
[7]*Institute of Theoretical and Experimental Biophysics, Russian Academy of Sciences, Pushchino 142290, Russia*
[8]*Department of Biomedical Engineering, College of Engineering and Applied Sciences, Nanjing National Laboratory of Microstructures, Jiangsu Key Laboratory of Artificial Functional Materials, Nanjing University, Nanjing 210023, China*
[9]*CAS Laboratory for Biomedical Effects of Nanomaterials and Nanosafety, Institute of High Energy Physics, Chinese Academy of Sciences, Beijing 100049, China*
[10]*Hefei National Research Center for Physical Sciences at the Microscale, Department of Polymer Science and Engineering, University of Science and Technology of China, Hefei 230026, China*
[11]*Nanozyme Laboratory in Zhongyuan, Henan Academy of Innovations in Medical Science, Zhengzhou 451163, China*
[12]*State Key Laboratory of Analytical Chemistry for Life Science, School of Chemistry and Chemical Engineering, Chemistry and Biomedicine Innovation Centre (ChemBIC), ChemBioMed Interdisciplinary Research Centre at Nanjing University, Nanjing University, Nanjing 210023, China*

Received July 1, 2025; accepted August 6, 2025; published online September 11, 2025

Nanomedicine has emerged as a dynamically evolving frontier in contemporary medical research. However, the development of nanomedicine is impeded by significant challenges due to its complex, multidisciplinary nature, necessitating the exploration of innovative solutions. Artificial intelligence (AI) has established itself as a pivotal and rapidly advancing domain within nanomedicine research. By leveraging its robust data processing and analytical capabilities, AI can efficiently analyze large datasets and accurately predict the properties and medical functions of nanomaterials. Over the past years, AI applications have proliferated across critical nanomedicine subdomains, including intelligent nanobiosensors for precision diagnostics, AI-optimized nanocarriers for targeted drug delivery, machine learning-guided adjuvant therapy systems, and predictive computational models for nanosafety evaluation. This review aims to provide a thorough analysis of AI's influence throughout the entire spectrum of nanomedicine, as well as the formidable challenges and extraordinary potential for pioneering researchers.

*Corresponding authors (email: gaoxf@nanoctr.cn; shixh@nanoctr.cn; lilele@nanoctr.cn; mengh@nanoctr.cn; niegj@nanoctr.cn; wanghao@nanoctr.cn; jmhu@ustc.edu.cn; yanliang@ihep.ac.cn; chenyuedu@shu.edu.cn; gaolizeng@ibp.ac.cn; antonpopovleonid@gmail.com; weihui@nju.edu.cn; Chenchy@nanoctr.cn; zhaoyl@nanoctr.cn)

nanomaterials, artificial intelligence, biosensors, drug delivery, adjuvant therapy, nanosafety

Citation: Song X, Gao X, Wang H, Yu F, Qin M, Li Y, Liu Y, Feng W, Zhou C, Chukavin NN, Wang L, Cui X, Shi X, Li L, Meng H, Nie G, Wang H, Hu J, Yan L, Chen Y, Gao L, Popov AL, Wei H, Chen C, Zhao Y. Artificial intelligence for nanomedicine. *Sci China Chem*, 2025, 68: 4552–4594, https://doi.org/10.1007/s11426-025-2942-5

CONTENTS

1 Introduction

Every technological revolution opens up new possibilities for scientific advancement by providing innovative tools and redefining research paradigms. The ongoing artificial intelligence (AI) revolution is no exception. It has the potential to significantly lower the barriers to the development of nanomedicine.

Nanomedicine [1,2], a pivotal frontier branch of modern medicine, has achieved remarkable progress in the fields of disease diagnosis, prognosis, and treatment in recent years [3]. This progress is largely attributed to its unique ability to integrate multidisciplinary knowledge and technologies through finely designed nano-platforms [4–6]. These platforms enable targeted medical functions and minimize systemic toxicity. A prime example is the lipid nanoparticle (LNP) delivery of mRNA technology, which stands as one of the landmark achievements in nanomedicine [7,8]. This technology has been successfully applied to the treatment of COVID-19. The nanocarrier delivery system is one of the key factors that enabled the success of mRNA. This breakthrough was awarded the Nobel Prize in Physiology or Medicine in 2023 [9–11].

However, the development of nanomedicine is impeded by significant challenges due to its complex, multidisciplinary nature [12,13]. Nanomedicine research integrates materials science, chemistry, biology, and medicine, presenting

intricate interdisciplinary challenges that have become a major bottleneck [14]. These bottleneck issues are difficult to overcome using a single classical research approach, such as experimentation, theory, or simulation. Traditional nanomedicine research methods, which rely heavily on extensive trial-and-error experimentations, are not only time-consuming and labor-intensive but also result in a low success rate. Fundamental theories, often applicable within a single discipline, face open-ended difficulties when applied to this interdisciplinary field of nanomedicine. Additionally, although molecular simulations have the potential to elucidate microscopic mechanisms and structure-activity relationships, the inherent complexity of nanobiology often leads to a scarcity of detailed molecular-level information, making it difficult to effectively conduct these simulations [15]. These limitations collectively hinder the rapid advancement of nanomedicine, necessitating the exploration of innovative solutions.

The rapid advancement of AI technologies has emerged as a transformative force in addressing the multifaceted challenges of scientific research and lowering the barriers to its development [16], such as in the field of nanomedicine [17] and synthetic chemistry [18]. Unlike classical theory and simulation technologies, which rely heavily on intermediate physical mechanisms to establish quantitative cause-and-effect relationships, AI operates on an end-to-end basis. It relies solely on data without the need to understand the underlying mechanisms. As long as sufficient cause-and-effect data are available, AI can establish mathematical models to quantitatively elucidate these relationships. This data-driven paradigm is exemplified by large language models (LLMs) [19,20], which leverage vast amounts of text data to generate human-like responses without explicit programming of linguistic rules or world knowledge. This characteristic makes AI particularly well-suited to nanomedicine, a field where the intrinsic mechanisms are often difficult to fully elucidate.

By leveraging its robust data processing and analytical capabilities, AI can efficiently analyze large datasets and accurately predict the properties and medical functions of nanomaterials. This enables AI to optimize the design of nanomedicine systems, thereby significantly enhancing development efficiency, reducing costs, and accelerating the clinical translation of nanomedicines. Moreover, the application of AI in nanomedicine extends beyond the design phase. AI can also be used to optimize the manufacturing processes of nanomedicines, thereby improving production efficiency and quality control. Additionally, AI can analyze clinical data to provide intelligent diagnostic support, enabling precision medicine [21]. In summary, AI has the potential to revolutionize various aspects of nanomedicine, from design and manufacturing to clinical application.

Consequently, the integration of AI into nanomedicine has ignited a global surge in research activity, particularly in the development of innovative AI-driven frameworks for nanodrug design and high-throughput screening. This synergy has yielded ground-breaking advances across diverse domains, including the creation of nanosensors for disease detection and diagnosis [22], the optimization of nanocarriers for targeted drug delivery [23], the screening of inorganic nanoparticles (NPs) for adjuvant therapies, and the safety assessment of engineered nanomaterials (Figure 1). Several recent reviews have summarized these developments, emphasizing AI's transformative role in reshaping nanomedicine. For instance, Schroeder *et al.* [24] systematically surveyed the integrated application of AI and nanotechnology in precision cancer medicine, with a focus on how AI optimizes nanomaterial design, patient diagnosis, and personalized treatment plan formulation, while Serov and Vinogradov [25] reviewed the applications of AI and machine learning (ML) in nanomedicine and explores how data-driven approaches can optimize the physicochemical properties and clinical translation of nanomedicines. Collectively, these analyses deliver critical insights into specialized subfields, underscoring AI's strategic importance as a catalyst for innovation and paradigm shifts within the discipline.

AI has established itself as a pivotal and rapidly advancing domain within nanomedicine research. Ongoing investigations are actively exploring optimal methodologies for integrating AI across diverse subdomains of nanomedicine. The exponential increase in scholarly publications in this area not only reflects the field's robust growth but also highlights the necessity for a comprehensive summary. This review aims to address this need by providing a thorough analysis of AI's influence throughout the entire spectrum of nanomedicine. This includes data acquisition, AI-enhanced diagnostic nanosystems, intelligently engineered therapeutic delivery platforms, and AI-driven nanotoxicology assessment. By critically evaluating current methodological approaches, persistent interdisciplinary challenges, and emerging future directions, we elucidate how AI is funda-

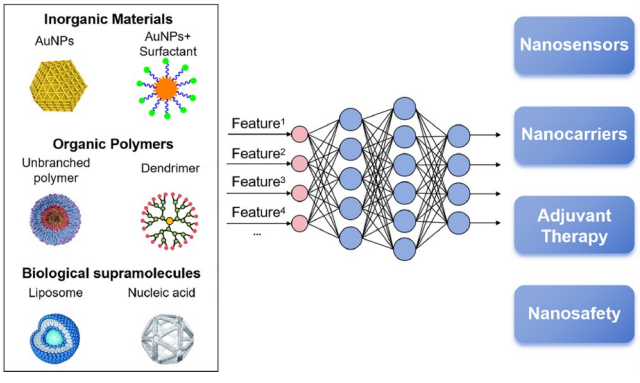

Figure 1 (Color online) Integration of artificial intelligence with functional materials: AI bridges inorganic/organic/biological material systems (left) to advanced applications in sensing, drug delivery, and therapeutics (right), demonstrating cross-disciplinary synergy in nanotechnology.

mentally reshaping the innovation landscape in nanomedicine. It is not merely accelerating discovery but also actively expanding the theoretical and practical boundaries of the field.

2 AI-based new research paradigm for nanomedicine

2.1 Datasets

The structural composition of nanomedicine systems typically exhibits considerable complexity, often comprising diverse components ranging from small organic molecules and macromolecular biomolecules to inorganic nanomaterials. To systematically elucidate the structure-activity relationships (SARs) of these nanomedicines, AI-based computational approaches have emerged as powerful tools. The construction of an AI-driven SAR model generally involves four critical phases: (i) data collection, (ii) encoding, (iii) algorithm selection, (iv) validation.

The successful implementation of AI-driven SAR modeling in nanomedicine research heavily relies on the availability of high-quality, well-organized datasets. To ensure that scientific data can be effectively utilized for computational analysis, the FAIR (Findable, Accessible, Interoperable, Reusable) principles have been widely adopted as a guiding framework [26]. The core objective of FAIR is to enhance data reusability by requiring that datasets be accompanied by comprehensive metadata, assigned persistent identifiers (*e.g.*, DOIs), and indexed in searchable repositories. This structured approach not only facilitates rapid data retrieval but also enables seamless integration across different computational workflows, thereby supporting more robust AI-based SAR predictions. As the field progresses, adherence to FAIR principles becomes increasingly critical in bridging the gap between experimental nanomedicine research and AI-driven drug discovery.

AI for science and drug development [27] provides a systematic review of earlier advancements, including comprehensive lists of databases and models for comparison. The current discussion focuses primarily on research progress from the past three years. Recent developments in high-accuracy machine learning interatomic potentials (MLIPs) have been reviewed elsewhere (*e.g.*, Wan *et al*. [28]) and are not repeated here. The first part introduces key databases and automated data acquisition methods, while the second part examines AI algorithms and models, with particular attention to their interpretability and computational efficiency in drug discovery applications.

The datasets used to construct AI models are typically derived from experimental measurements, computational simulations, and existing databases. Table 1 summarizes the key datasets relevant to nanomedicine applications. While experimental and simulation datasets can often be directly utilized for machine learning, literature-derived datasets require substantial preprocessing, including text extraction, data annotation, information retrieval, and data mining operations. Recent advances have led to the development of automated workflows leveraging large language models (LLMs) for dataset preparation. Current scientific LLMs employ core NLP pretraining methodologies, exemplified by GPT-based architectures [29] (*e.g.*, MolXPT [30]) and BERT-based frameworks [31] (*e.g.*, KV-PLM [32]). Domain-specific adaptations such as BioGPT, Bio-MedLM [33], and med-PALM [34] demonstrate enhanced performance in biomedical question-answering through fine-tuning of foundational models like GPT-2 [35] and PaLM [36]. Supervised fine-tuning with limited paired data has also proven effective, as demonstrated by DrugChat [37]. General-purpose LLMs (*e.g.*, DeepSeek, ChatGPT) have been successfully applied to dataset preparation through specialized workflows [38]. The CrystaLLM model represents a significant advancement in bridging natural-language processing with materials informatics [39]. BERT-based variants, including BioBERT, ChemBERT, MaterialBERT, LLM-Prop [40], and MatKG, have established new benchmarks in materials science knowledge representation [41,42]. The MatSci-BERT [43] framework specifically addresses materials science dataset preparation through SciBERT adaptations. Additionally, manually curated literature datasets have enabled the training of specialized machine learning models to support nanodrug development initiatives [44,45].

AI systems like Coscientist [46] and AI-Chemist [47] have enabled robotic automation of chemical experiments. These integrate with high-throughput density functional theory workflows (*e.g.*, AFLOW [48]), accelerating nanomedicine development through efficient experimentation and computational modeling.

The development of small molecule databases can be achieved by integrating molecular graph representations with quantum mechanical (QM) calculations. A prominent example is the GEOM dataset [49], which contains high-quality molecular conformers. In this database, 3D molecular structures are initially generated using RDKit [50] and subsequently refined through geometry optimization with ORCA [51] and CREST [52]. The dataset includes two widely used subsets, GEOM-QM9 and GEOM-Drugs, which serve as standard benchmarks for evaluating molecular conformation generation methods.

Several globally recognized advanced materials databases have been developed through density functional theory (DFT) calculations. Notable examples include the Materials Project datasets, which contain a Γ-phonon database comprising approximately 146,000 materials [53] and a partial density of states (PDOS) database derived from density

Table 1 Publicly accessible databases for small molecules, proteins, and materials

NAME	Description	URL
Propedia	A database for protein-peptide identification based on a hybrid	http://bioinfo.dcc.ufmg.br/propedia2/
sc-PDB	A database for identifying variations and multiplicity of "druggable" binding sites in proteins	http://bioinfo-pharma.u-strasbg.fr/scPDB/
ACCDB	A collection of chemistry databases for broad computational purposes	https://doi.org/10.1002/jcc.25761
SCOP	A structural classification of proteins database for the investigation of sequences and structures	https://www.ebi.ac.uk/pdbe/scop/
PubChemQC project	A large-scale first-principles electronic structure database for data-driven chemistry	https://nakatamaho.riken.jp/pubchemqc.riken.jp/
GDB-17	Enumeration of 166 billion organic small molecules in the chemical universe database	https://gdb.unibe.ch/downloads/
AlphaFold Protein Structure Database	Massively expanding the structural coverage of protein-sequence space with high-accuracy models	https://alphafold.com/
Atomly	AI-driven computational material data with wide coverage to support predictive modeling	https://www.atomly.net
Materials Project	Open source DFT database, community contribution-based	https://legacy.materialsproject.org/
OQMD	Focus on material stability and formation prediction	https://www.oqmd.org/
AFLOWLIB	Structure and property repository from high-throughput *ab initio* calculations of inorganic materials	https://aflowlib.org
Computational Materials Repository	Infrastructure to enable the collection, storage, retrieval and analysis of data from electronic-structure codes	https://cmr.fysik.dtu.dk
GDB	Databases of hypothetical small organic molecules	https://gdb.unibe.ch/downloads
Harvard Clean Energy Project	Computed properties of candidate organic solar absorber materials	https://cleanenergyproject.org
Materials Project	Computed properties of known and hypothetical materials were carried out using a standard calculation scheme	https://materialsproject.org
NOMAD	Input and output files from calculations using a wide variety of electronic-structure codes	https://nomad-repository.eu
Open Quantum Materials Database	Computed properties of mostly hypothetical structures were carried out using a standard calculation scheme	https://oqmd.org
NREL Materials Database	Computed properties of materials for renewable-energy applications	https://materials.nrel.gov
TEDesignLab	Experimental and computed properties to aid the design of new thermoelectric materials	https://doi.org/10.1016/j.commatsci.2015.11.006
ZINC	Commercially available organic molecules in 2D and 3D formats	https://zinc15.docking.org
ChEMBL	Bioactive molecules with drug-like properties	https://www.ebi.ac.uk/chembl
ChemSpider	Royal Society of Chemistry's structure database, featuring calculated and experimental properties from a range of sources	https://chemspider.com
Citrination	Computed and experimental properties of materials	https://citrination.com
Crystallography Open Database	Structures of organic, inorganic, metal-organic compounds and minerals	https://crystallography.net/cod
CSD	Repository for small-molecule organic and metal-organic crystal structures	https://www.ccdc.cam.ac.uk
ICSD	Inorganic Crystal Structure Database	https://icsd.fiz-karlsruhe.de
MatNavi	Multiple databases targeting properties such as superconductivity and thermal conductance	https://mits.nims.go.jp
MatWeb	Datasheets for various engineering materials, including thermoplastics, semiconductors and fibers	https://matweb.com
NIST Chemistry WebBook	High-accuracy gas-phase thermochemistry and spectroscopic data	https://webbook.nist.gov/chemistry
NIST Materials Data Repository	Repository to upload materials data associated with specific publications	https://materialsdata.nist.gov/
PubChem	Biological activities of small molecules	https://pubchem.ncbi.nlm.nih.gov
CATH 4.2	151 million protein domains	https://www.cathdb.info/
ProFold	Protein fold classification with additional structural features and a novel ensemble classifier	https://doi.org/10.1155/2016/6802832
Gene Ontology	The world's largest source of information on the functions of genes	https://www.geneontology.org/
ENZYME	A repository of information relative to the nomenclature of enzymes	https://enzyme.expasy.org/

perturbation functional theory (DPFT) calculations for 1,521 semiconductor compounds [54]. Additionally, the Atomly platform provides an extensive collection of 340,000 calculated band structures [55], further expanding the available computational materials data resources.

2.2 AI models related to nanomedicine

2.2.1 AI for organic small molecules

Machine learning approaches for modeling 2D molecular representations have demonstrated considerable potential in computational chemistry [56,57]. These techniques offer viable alternatives to resource-intensive quantum chemical (QM) calculations for determining 3D molecular configurations, thereby substantially improving the efficiency of molecular simulation workflows. The key distinction between 2D and 3D molecular representations lies in their structural encoding: 2D representations capture the molecular graph topology with node and edge attributes, whereas 3D representations incorporate atomic spatial coordinates. These coordinates enable precise calculation of geometric parameters such as interatomic distances, bond angles, and torsion angles. Given the profound influence of molecular conformation on physicochemical properties, 3D structural information significantly enhances the accuracy of property predictions. Such spatial data is particularly valuable for applications including molecular property prediction, molecular dynamics simulations, and protein-ligand docking studies.

However, acquiring accurate 3D molecular geometries through quantum mechanical calculations remains highly challenging due to their substantial computational demands, which significantly restricts the broad application of 3D structural data. Consequently, machine learning-based reconstruction of 3D molecular geometries has emerged as a promising alternative approach, offering the potential to substantially reduce computational costs while improving accessibility to 3D structural information. Considerable progress has been achieved in developing machine learning models for molecular conformation generation. Nevertheless, with ongoing advancements in computational capabilities, the increasing availability of QM-derived datasets will play a pivotal role in enhancing these models, particularly for drug discovery applications where accurate structural data is crucial.

2.2.2 AI for proteins

As demonstrated in Table 2, ML approaches for protein structure modeling have advanced significantly through the integration of diverse structural data sources, including monomeric, homodimeric, and heterodimeric protein structures from the Protein Data Bank (PDB). The field has witnessed substantial progress through the application of graph neural networks, diffusion models, and three-dimensional geometric learning techniques, which collectively enable more efficient discovery and design of novel protein structures. A transformative development has been the implementation of deep learning-based generative approaches, particularly diffusion models, which have fundamentally altered protein design methodologies by achieving unprecedented levels of accuracy, efficiency, and structural diversity. The key innovation of these approaches involves the direct generation of atomic coordinates within three-dimensional space while incorporating physical constraints, contrasting with conventional methods that depend on energy function optimization. This coordinate-based generation more accurately reflects real physical space. The denoising process employed by diffusion models, analogous to techniques used in image generation, facilitates exploration of broader conformational landscapes while producing structurally viable and diverse protein architectures. Notably, diffusion models exhibit particular effectiveness in addressing symmetry-related challenges, such as those encountered in symmetric protein complex arrangements, and demonstrate superior capability in designing complex multimeric structures that have proven difficult to achieve through traditional design approaches.

As demonstrated experimentally, various 3D structural representations (including atomic coordinates, reference frames, and internal angles) at different resolution levels (Cα, backbone, or full-atom representations) exhibit distinct computational requirements and diffusion dynamics. A landmark achievement published in Science by David Baker's research group demonstrated the capability of AI systems to design functional enzymes *de novo*, with catalytic efficiencies surpassing previous designs by a factor of 60,000. Parallel developments have yielded specialized computational workflows, including an AlphaFold-based pipeline for cyclic peptide structure prediction and design [58], and ColabDock's innovative adaptation of AlphaFold's architecture for protein-protein docking applications incorporating experimental constraints [59].

2.2.3 AI for inorganic materials

The application of AI in material structure analysis has progressed significantly, as comprehensively documented in Table 3. For solid-state systems, traditional crystallographic representations employing translation vectors and fractional atomic coordinates prove inadequate for machine learning applications. This limitation has driven the evolution of graph-based representations for crystalline materials, progressing from basic 2D depictions to sophisticated crystal graphs. Current graph neural network architectures for crystals fall into two categories: those without periodic boundary condition integration (including CGCNN, SchNet, and MEGNet) and periodic-aware models (such as

Table 2 ML-based protein conformation generation models

Subtasks	Approaches	Name
Protein folding	Two-stage learning	RaptorX-Contact, AlphaFold1, trRoseTTA
Protein representation	End-to-end learning	AlphaFold3, AlphaFold2, RoseTTAFold, ESMFold, OpenFold
Learning	Invariant networks	IEConv, HoloProt, MaSIF, dMaSIF, ProteinMPNN, GearNet, ProNet, PiFold, CDConv GVP-GNN, GBPNet
Protein	Equivariant networks Structure representation: coordinates	ProtDiff, Chroma, Genie, LatentDiff
Backbone	Structure representation: frames	RFdiffusion, FrameDiff
Generation	Structure representation: internal angles	FoldingDiff

Table 3 ML-based protein(material)-small molecule conformation generation models

Subtasks	Approaches	Name
Protein-ligand binding prediction	Predict coordinates	RaptorX-Contact, AlphaFold1, trRoseTTA
Structure-based drug design	End-to-end learning	AlphaFold3, AlphaFold2, RoseTTAFold, ESMFold, OpenFold
Molecule and material interactions	Invariant networks	IEConv, HoloProt, MaSIF, dMaSIF, ProteinMPNN, GearNet, ProNet, PiFold, CDConv GVP-GNN, GBPNet

Matformer, PotNet, and Ewald-MP). These frameworks enable property prediction at multiple structural levels: graph-level predictions encompass formation energy, band gaps, Ehull, bulk moduli, and shear moduli; node-level analyses capture atomic forces and charges; while edge-level computations describe bond energies [60].

2.2.4 AI for protein(material)-ligand interactions

While AI applications for individual molecular systems have been extensively investigated, it is crucial to recognize that molecular physical and biological functionalities are predominantly governed by intermolecular interactions. This section consequently focuses on AI methodologies specifically developed for analyzing molecular interaction systems, with particular emphasis on small molecule-protein interactions and small molecule-material interfaces.

Protein-ligand binding prediction and structure-based drug design represent both fundamental and challenging aspects of modern drug discovery. Recent advances in geometric deep learning and generative modeling have enabled more effective representation of protein-ligand complexes as three-dimensional structures, where complex interaction patterns and symmetry requirements can be accurately encoded. Current state-of-the-art approaches can be systematically categorized into two distinct paradigms: (1) context-aware atomic generation methods that sequentially build molecular structures based on binding site characteristics and previously generated atoms, and (2) coordinate-based generation techniques that directly predict complete 3D atomic configurations, as exemplified by diffusion modeling approaches. Notably, the AlphaFold3 framework incorporates diffusion-based structure generation, demonstrating unprecedented capability in predicting complex molecular assemblies comprising proteins, nucleic acids, small molecules, ions, and post-translational modifications. Comparative analyses reveal that these advanced AlphaFold implementations achieve substantial improvements in prediction accuracy over conventional computational tools [61].

Regarding small molecule-material interactions, current research has predominantly focused on predictive tasks, with limited exploration of generative or design-oriented approaches. Several computational methodologies have been developed to characterize material-molecule interactions, including NPCoronaPredict—a specialized framework for modeling NP-coronavirus interactions (*e.g.*, SARS-CoV-2) with direct applications in therapeutic delivery systems, vaccine development, and antiviral material engineering [62]. Table 3 systematically summarizes existing computational approaches for predicting key interaction parameters including binding energies, interfacial forces, and molecular adsorption configurations in material systems.

Explainable artificial intelligence (XAI) plays a crucial role in drug discovery by identifying critical molecular substructures or functional groups that influence target properties. While significant progress has been made in developing XAI methods for conventional 2D graph neural networks, interpretability techniques for geometric deep learning (GDL) models operating on 3D molecular graphs remain relatively underdeveloped. Current GDL interpretation approaches [63,64] primarily focus on analyzing and visualizing learned representations through systematic ar-

chitectural examination. A recent advancement introduced a perturbation-based interpretation method specifically designed for 3D point clouds [65]. This technique employs a trainable interpreter model that introduces controlled noise to individual 3D coordinates while jointly training with the target GDL model. The resulting noise patterns generate importance scores for each spatial point, providing local interpretability. However, this framework currently only addresses invariant prediction tasks and does not account for the fundamental geometric constraints of equivariance in its interpretations [66]. Consequently, there exists a pressing need for novel XAI methodologies specifically tailored to equivariant GDL architectures that preserve the geometric consistency of both predictions and their explanations.

3 AI-based new research paradigm for nanomedicine

The integration of AI and nanotechnology has driven groundbreaking advancements in medical diagnostics, enabling rapid, precise, and scalable solutions for disease detection. This section explores two critical domains—nanosensors and micro/nanofluidics—and their synergy with AI to overcome challenges related to sensitivity, specificity, throughput, and real-time biomarker analysis for more accurate and efficient disease diagnosis.

3.1 Nanosensors

The fusion of AI and nanotechnology has transformed disease detection and diagnosis. By integrating the unique physicochemical properties of nanomaterials with the biorecognition units, nanosensors achieved exceptional sensitivity and specificity in detecting disease-associated biomarkers [67–69]. Beyond identifying native biomarkers, nanosensors can also be engineered as synthetic biomarkers that generate molecular reporters in response to specific biological targets *in vivo*. This innovation addresses key challenges such as low sensitivity, poor specificity, and the absence of detectable signals in early-stage diseases, marking a paradigm shift in diagnostic strategies [70]. Capitalizing on their X-ray attenuation, magnetic, and optical properties, various nanoprobes have been developed to enhance biomedical imaging techniques, including computed tomography (CT), magnetic resonance imaging (MRI), and optical imaging. For instance, quantum dots (QDs) have been extensively used for biomedical imaging, even within the near-infrared (NIR) window [71,72]. Recently, Fang *et al*. [73] synthesized an erbium-based rare-earth nanoprobe (pEr) that exhibits distinct emission properties in response to oxyhemoglobin saturation (sO_2) levels. Using this nanoprobe, they developed a non-invasive bioimaging technique to evaluate tumor vessel oxygenation within the NIR-IIb (1,500–1,700 nm) window. Their findings revealed that cancer cell oxygen consumption modulates vessel sO_2 levels during early tumorigenesis and that a positive response to immunotherapy is often accompanied by a remarkable decrease in tumor vessel sO_2 levels.

Despite the progress achieved, nanosensor technology still faces challenges in clinical disease detection, including limitations in sensitivity, specificity, and real-time data analysis. Recent developments in AI offer promising solutions for these challenges, enabling the creation of intelligent diagnostic platforms with enhanced accuracy and efficiency. One of AI's most successful applications in this domain is biomedical image processing, encompassing automatic segmentation, structure identification, feature extraction, and report generation [74–76]. For instance, convolutional neural network (CNN)-based deep learning (DL) models have been employed to detect and quantify a broad range of gold NP (AuNP) concentrations used as contrast agents in CT imaging [77]. Magnetic particle imaging (MPI), a noninvasive and radiation-free diagnostic technique that leverages the nonlinear magnetic response of superparamagnetic NPs, has emerged as a valuable imaging modality [78]. However, challenges in image reconstruction have limited its clinical applicability. To address this, AI-driven approaches, including machine learning (ML) and DL techniques, have been integrated into MPI workflows, enhancing image reconstruction, resolution and diagnostic accuracy [79,80]. Notably, a unified hybrid DL system was recently developed to improve breast cancer risk stratification using multimodal data, demonstrating superior performance compared to experienced radiologists [81].

Although NIR fluorescence imaging enhances tumor visualization, it remains susceptible to interference from light scattering and autofluorescence, leading to reduced clarity and contrast. To address these issues, several AI-based solutions have been developed. For instance, Ma *et al*. [82] utilized generative adversarial network (GAN), a class of DL models capable of generating high-quality synthetic data, to transform fluorescence images from the NIR-I/IIa window (900–1,300 nm) into higher resolution images in the longer-wavelength NIR-IIb window, significantly improving resolution and signal-to-noise ratio. Additionally, the integration of task-assisted GAN into microscopy acquisition pipelines enables selection of regions of interest and optimization of imaging sequences, eliminating the need for manual parameter adjustments during image acquisition [83]. By coupling neuromorphic detection with CNN-based DL models, researchers have achieved real-time tracking of fluorescent NPs with 50 nm spatial resolution and millisecond temporal resolution, highlighting AI's potential to advance both fundamental research and clinical diagnosis [84].

Most nanosensors are designed to detect specific targets. However, disease diagnosis based on individual biomarkers often suffers from low specificity and poor positive predictive value. To overcome this challenge, in 2022, Kim *et al*. [85] proposed a perception-based strategy that enhances diagnostic accuracy by integrating multiple sensory inputs with a pre-learned pattern library. Perception systems accomplish target recognition through the alignment of multiple sensory inputs, each encoding distinct characteristics, with a pre-learned pattern library. This approach utilizes organic color center (OCC)-functionalized, single-stranded DNA (ssDNA)-encapsulated single-walled carbon nanotubes (SWCNTs) to construct nanosensor arrays (OCC-DNAs, Figure 2A). By training multiple ML models, including artificial neural networks (ANNs), random forest (RF), and support vector machines (SVMs), to analyze the diverse emissions of OCC-DNA nanosensors in response to various biofluid characteristics, this strategy enabled classification of high-grade serous ovarian carcinoma (HGSOC) based on disease-specific molecular fingerprint (Figure 2B). The optimized SVM model (Figure 2C) demonstrated exceptional diagnostic performance, achieving a sensitivity of 87% and a specificity of 98%, outperforming conventional protein biomarker-based tests (Figure 2D).

3.2 Microfluidics and nanofluidics

Microfluidics and nanofluidics, which enable precise control of fluids at the microliter to picoliter scale [86], offer miniaturized lab-on-a-chip systems for disease detection and diagnosis. These systems facilitate multiplexed analysis of blood, saliva, sweat, or other body fluids while minimizing sample consumption. For instance, microfluidic purification chips allow for the capture and label-free detection of multiple disease biomarkers from a blood sample, significantly enhancing target capture and release efficiency compared to conventional methods [87]. Beyond sample collection and transport, microfluidic colorimetry enables RNA/DNA amplification at the single-nucleotide level, allowing for the quantification of nucleic acid biomarkers associated with viral diseases such as COVID-19 and H1N1 influenza A from saliva [88]. The miniaturization of microfluidic chips has also led to the development of portable health monitoring systems. For example, a reported wearable composition detection system integrates a microfluidic module for dynamic sweat sampling, enabling real-time monitoring of uric acid and tyrosine levels [89]. At the clinical level, a microfluidic-based thermophoretic profiling system facilitates early cancer detection by precisely profiling extracellular vesicle surface proteins [90]. These advancements in microfluidics and nanofluidics are revolutionizing disease detection and diagnosis by enabling precise fluid manipulation, real-time monitoring, and integration into cost-effective, miniaturized, and even wearable diagnostic devices. The ability to collect, transport, and process minimal fluid volumes with high accuracy improves reproducibility, while rapid data generation with minimal reagent consumption enhances efficiency and affordability.

While microfluidic and nanofluidic systems offer significant advantages in precision and high-throughput analysis, they also present challenges, particularly in optimizing complex parameters and managing the vast data streams they generate. The integration of AI provides a transformative solution, enhancing the accuracy, efficiency, and scalability

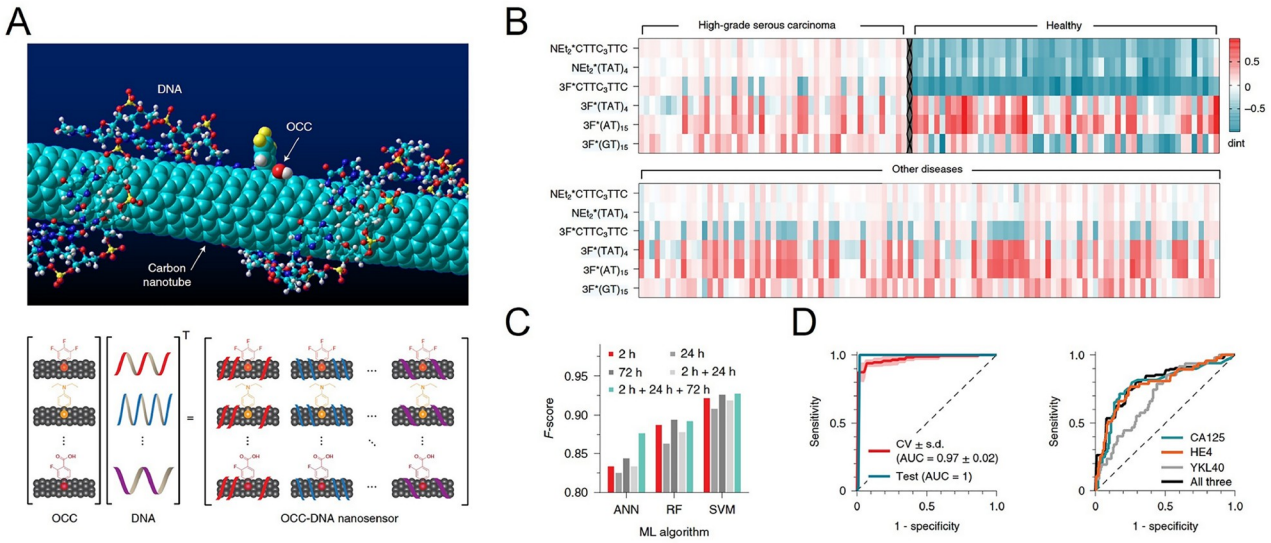

Figure 2 (Color online) (A) Schematic representation of an OCC-DNA nanosensor array. (B) Intensity changes in each OCC-DNA sensors responding to 215 serum samples from patients with HGSOC, other diseases, and healthy donors. (C) Performance comparison of ANN, RF, and SVM models for HGSOC classification. (D) Classification accuracy of the optimized SVM model (left) *versus* a conventional biomarker-based test (right). Reproduced with permission from Ref. [85]. Copyright©2022, Springer Nature.

of these systems. AI-driven microfluidic and nanofluidic platforms enable real-time, automated, high-throughput, and high-precision screening of biological and pathological samples, and significantly advance point-of-care (PoC) diagnostics. DL models have been incorporated into microfluidic platforms for high-throughput single-cell analysis, flow cytometry, and organ-on-a-chip (OoC) applications, facilitating blood analysis, omics studies, and pathological cell sorting. In 2018, a DL-assisted microfluidic cell sorting system (Figure 3A) was developed, integrating high-throughput cell microscopy, focusing, and sorting within a single automated platform [91]. Powered by a CNN model, the system achieved real-time data acquisition, processing, decision-making, and actuation within 32 ms, enabling precise sorting of microalgal and blood cells based on intracellular protein localization and cell-cell interactions. Given their capability to analyze image arrays, neural networks have been widely applied in microfluidic flow cytometry for cell classification. For instance, CNNs can generate t-distributed stochastic neighbor embedding (t-SNE) plots from stimulated Raman scattering (SRS) images collected via flow cytometry, allowing for differentiation of cell types and pathological conditions (Figure 3B) [92]. Additionally, integrating refractive index (RI) tomography with neural networks has demonstrated high accuracy in lymphocyte classification [93]. Pathological cell screening is a fundamental component of single-cell disease diagnosis. In 2020, a CNN-driven image analysis architecture was employed for cell localization and segmentation in an omics analysis system, facilitating single-cell analysis under experimental conditions [94]. In phenotyping applications, ML approaches have been integrated with real-time fluorescence and deformability cytometry (RT-FDC), a novel microfluidic technique capable of generating multi-dimensional datasets, to differentiate cancerous from healthy tissue (Figure 3C) [95]. Given the large volumes of image-based and multi-dimensional data produced by RT-FDC, AI-driven analysis has proven particularly effective for this application. The

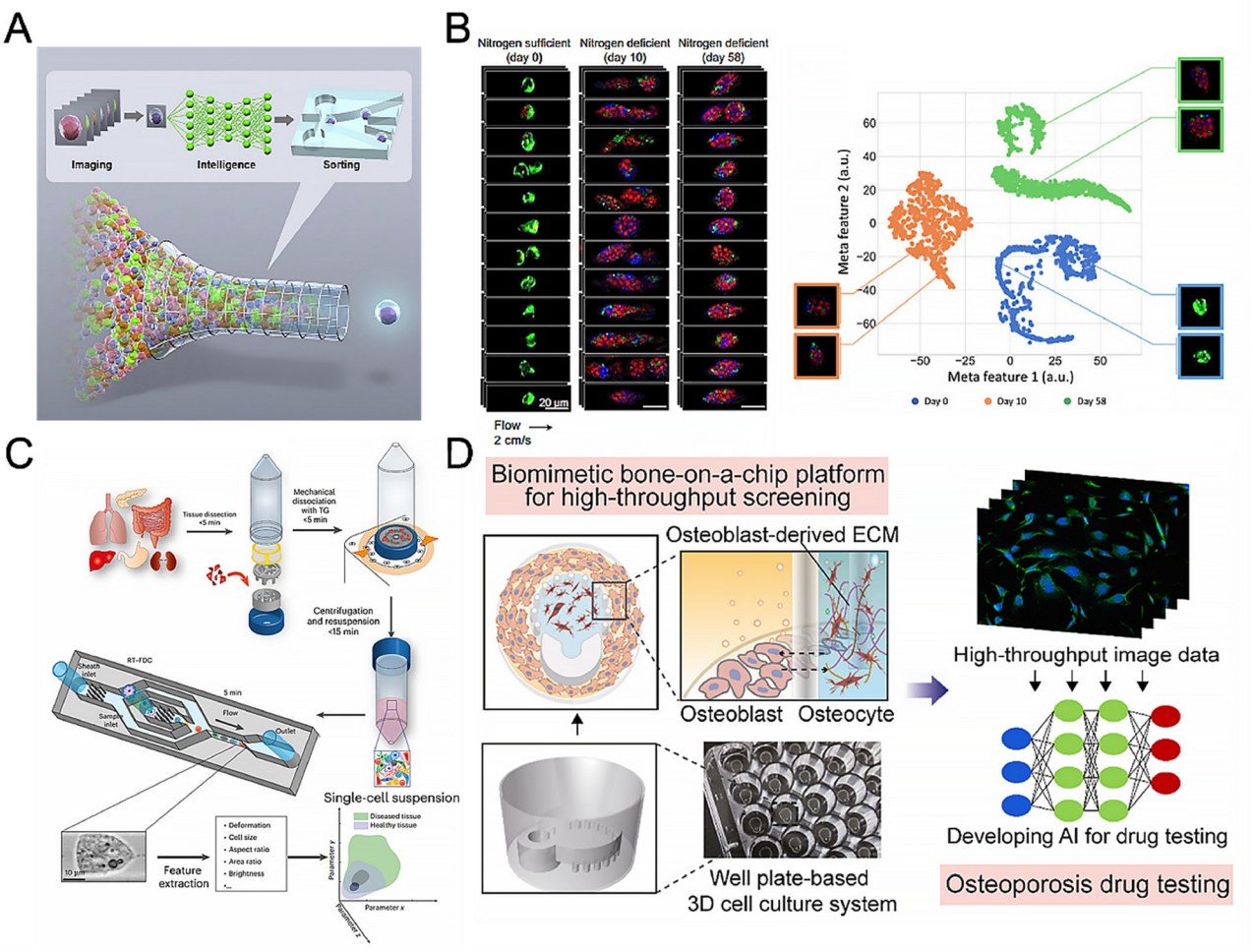

Figure 3 (Color online) (A) Schematic representation of a deep-learning-assisted microfluidics cell sorting system. Reproduced with permission from Ref. [91]. Copyright©2018, Cell Press. (B) SRS images of *E. gracilis* cells cultured under 3 different conditions, with a CNN-generated t-SNE plot for cell classification. Reproduced with permission from Ref. [92]. Copyright©2019, the Author(s). (C) Machine learning-based phenotyping system for distinguishing cancerous tissue from healthy tissue. Reproduced with permission from Ref. [95]. Copyright©2023, the Author(s). (D) Workflow for osteoporosis drug screening using a bone-on-a-chip system. Reproduced with permission from Ref. [97]. Copyright©2023, the Author(s).

miniaturized and cost-effective nature of microfluidic chips makes them valuable tools for a wide range of medical applications, particularly in resource-limited settings. AI-assisted microfluidic platforms hold the potential to overcome key challenges in personalized medicine and disease detection. Moreover, these systems facilitate *in vitro* rapid drug screening. For instance, OoC models, which replicate human physiological environments and simulate complex pathological conditions, have been integrated with AI to predict adverse cutaneous drug reactions and assess osteoporosis treatments (Figure 3D) [96,97]. This convergence of AI and microfluidics opens new avenues for disease diagnosis and personalized drug screening, enhancing both therapeutic development and precision medicine.

4 Nanocarriers for drug delivery

4.1 Lipid NPs

Lipid-based NPs (LBNPs) represent one of the most widely utilized nanocarriers in clinical practice, particularly for cancer therapies and nucleic acid delivery [98]. This diverse category encompasses liposomes, LNPs, solid lipid NPs (SLNs), and lipid nanoemulsions, among others [99]. Notable examples include Doxil®—the first FDA-approved liposomal nanomedicine for cancer—and the COVID-19 mRNA vaccine, which relies on LNP technology [7,8]. Despite their clinical success, the development of lipid-based nanomedicines has been remarkably slow [100]. Over the past three decades, only approximately 20 lipid-based formulations have gained regulatory approval, a stark contrast to the approximately 20-fold higher number of approved small-molecule drugs. The development of lipid-based NPs faces multifaceted challenges: optimizing biocompatibility, achieving tissue-specific targeting, delivering therapeutic efficacy, minimizing immunogenicity, and ensuring scalable manufacturing. Traditional approaches, dependent on empirical trial and error, struggle to navigate the high-dimensional design space defined by lipid chemistry, formulation parameters, and biological interactions. In recent years, advances in the integration of AI and machine learning (ML) have improved efficacy in LBNP design, optimization, and application in nanomedicine.

4.1.1 AI-driven rational design of functional lipids

Functional lipids, such as ionizable lipids, charged lipids, and PEGylated lipids, influence key properties of LBNPs, including stability, encapsulation efficiency, biodistribution, and cellular uptake [101]. The design and screening of optimal functional lipids require a comprehensive understanding of their molecular structures, physicochemical properties, and interactions with drug payloads and other components. However, traditional lipid discovery and screening methods are often labor-intensive, time-consuming, and limited in their ability to design, synthesize and evaluate a vast number of lipid candidates [102,103]. These limitations highlight the critical need for advanced, high-throughput, and AI-driven approaches to accelerate functional lipid innovation.

By integrating ML, deep learning, and molecular dynamics simulations, AI can systematically analyze complex datasets, propose new lipid structures, predict lipid behavior, and optimize lipid properties for specific therapeutic applications [104]. For example, AI-driven virtual screening approaches have been applied in the rational design of ionizable lipids. The AI-guided ionizable lipid engineering (AGILE) platform, combined with deep learning and combination chemistry, was used to streamline ionizable lipid development with efficient library design, *in silico* lipid screening via deep neural networks, and adaptability to diverse cell lines. With AGILE, researchers identified a potent ionizable lipid, H9, from 12,000 virtual structures [105]. Furthermore, researchers have gathered various structures of ionizable lipids from literature sources and patents to predict apparent pK_a and mRNA delivery efficiency of LNPs. AI-driven generation and screening led to the design and evaluation of nearly 20 million ionizable lipids, identifying several candidates that demonstrated robust experimental performance [106]. In another study, a dataset of over 9,000 LNP activity measurements was used to train a directed message-passing neural network for predicting nucleic acid delivery with diverse lipid structures. By evaluating 1.6 million lipids *in silico*, two lipids with promising local mRNA delivery efficacy were identified [107]. These examples highlight the power of AI in rational functional lipid design.

4.1.2 AI-driven formulation design and optimization of lipid-based NPs

Unlike many other nanocarriers, lipid-based NPs typically comprise more than two different types of lipids. For instance, FDA-approved Doxil® liposomes contain hydrogenated soy phosphatidylcholine (HSPC), cholesterol, and PEG-DSPE in a 56:39:5 molar ratio [108]. Similarly, Moderna's COVID-19 LNP formulation comprises four lipid components at optimized molar ratios: ionizable lipid (SM-102, 50%), helper lipid (DSPC, 10%), cholesterol (38.5%), and PEG-lipid (DMG-PEG, 1.5%) [109]. The complex lipid composition poses significant challenges in the formulation design of lipid-based nanocarriers, making traditional empirical, low-throughput formulation approaches inefficient. AI models can optimize lipid compositions using empirical data to achieve ideal physicochemical properties (*e.g.*, size, surface charge, stability) [110]. By feeding historical data on formulations into machine learning models, researchers can predict the most effective lipid ratios and combinations for specific applications, such as drug delivery, gene therapy, or

vaccine development. Furthermore, when combined with the automated high-throughput screening (HTS) workflow, AI-screened formulation candidates can be efficiently evaluated [111].

AI has emerged as a transformative tool for navigating the complexity of LBNPs. For example, Eugster *et al*. [112] demonstrated this potential by training XGBoost models on over 1,300 liposome formulations, achieving robust predictions for vesicle size and formation probability. This highlights a paradigm shift from empirical formulation design to AI-driven rational engineering, with profound implications for vaccine development, gene therapy, and precision oncology.

4.1.3 AI for lipid-based NPs preparation and production

The preparation and large-scale production of LBNPs present significant challenges, particularly in achieving precise control over particle size, polydispersity, encapsulation efficiency, and batch-to-batch reproducibility [113,114]. These challenges make exploring the application of AI in lipid-based NP production highly significant, especially after the rise of microfluidic manufacturing during the COVID-19 pandemic.

AI algorithms, particularly deep learning and reinforcement learning models, can analyze high-dimensional data from experimental and production settings to predict the ideal conditions for NP assembly. Thus, they hold great promise for optimizing the preparation parameters for NP synthesis. For instance, AI can optimize solvent selection, lipid composition, mixing speed, temperature, and flow rates in microfluidic systems [115]. Researchers have applied XAI to predict the complex interactions between formulation and process parameters, enhancing lipid behavior prediction during microfluidic production. Through model training, a reliable framework has been established for transitioning from traditional liposome production to microfluidic techniques [112].

In addition to optimizing preparation parameters, AI-driven techniques are being integrated into real-time monitoring systems to improve quality control. By utilizing AI-enhanced characterization and imaging techniques, such as Raman spectroscopy, dynamic light scattering (DLS), and transmission electron microscope (TEM), AI models can detect suboptimal production conditions and deviations in NP characteristics [116]. Automated feedback mechanisms can dynamically adjust process variables, ensuring high reproducibility and minimizing batch failures. This is particularly crucial for pharmaceutical applications, where stringent regulatory compliance requires precise control over NP specifications.

Furthermore, AI also plays a pivotal role in scaling up LBNP production for clinical and commercial applications, addressing critical challenges such as batch-to-batch reproducibility that arise during the transition from laboratory to industrial manufacturing. The AI-assisted autonomous, integrated microfluidic (AIM) platform streamlines LBNP production by combining continuous-flow synthesis, inline purification, real-time monitoring, and AI-driven Bayesian optimization [117]. It enables rapid, autonomous production of tailored liposomal NPs with precise size and encapsulation control, ensuring reproducibility. These AI-based predictive models facilitate process adjustments before actual scale-up, reducing material wastage and improving cost-efficiency.

4.1.4 AI for predicting interactions between lipid-based NP and biological systems

The interactions between lipid-based NPs and biological systems play a crucial role in determining their *in vivo* stability, biodistribution, therapeutic efficacy, and safety [118,119]. Upon administration, NPs encounter complex biological environments, including plasma proteins, immune cells, physiological barriers, and intracellular trafficking organelles [120]. Understanding these interactions is essential for optimizing NP formulations to achieve precise drug delivery while minimizing off-target effects and immunogenicity.

One significant application of AI in this field is the prediction of NP-protein corona formation [121]. When LBNPs enter biological fluids, proteins from plasma rapidly adsorb onto their surface, forming a "protein corona". This corona alters the biological identity of the NPs, influencing cellular uptake, immune recognition, and biodistribution [122]. AI-driven predictive models, particularly deep learning, can analyze high-throughput proteomics data to forecast the specific plasma proteins likely to bind to different LBNP formulations. For instance, machine learning (*e.g*., random forest and neural network) models were used to learn the complex relationships between NP properties and corona composition and then to comprehensively and quantitatively predict the formation of protein coronas and the related cell responses [44]. This predictive ability helps researchers design LBNP formulations to avoid off-target effects and unintended immune outcomes.

In addition to predicting the protein corona formation, AI can help predict the cellular uptake and intracellular trafficking of LBNPs. Machine learning algorithms (*e.g*., univariate analyses and random forest algorithms) have been used for analyzing data acquired by pooled screening with multiomic annotation to identify features of the cancer cells and NPs that could predict successful NP delivery. This method identified the SLC46A3 gene as a negative regulator and predictive biomarker for LBNP uptake [123]. The AI-driven insights are particularly useful in predicting the targeting efficiency for specific tissues of NPs, such as the liver, spleen, or tumor. For example, a supervised deep

neural network has been trained to predict the organ accumulation of NPs by analyzing mass spectrometry data on the protein corona composition [124]. These approaches allow the rational design of LBNPs to improve targeting efficiency, particularly in cancer therapy and gene delivery applications.

Furthermore, AI is also being used to assess the potential toxicity of LBNPs. AI models trained on large datasets of NP compositions and their immunogenic profiles can predict the likelihood of adverse reactions. Being trained on datasets that include the physicochemical properties of NPs, exposure conditions, and cellular responses of different cell lines, AI-driven models (*e.g.*, Random Forest) exhibited the highest performance in the given dataset and can be used to predict NP toxicity, leading to cost and time savings for toxicity analysis [125].

AI shows significant potential in LBNPs research by enabling the rational design of functional lipids, optimizing formulations, enhancing large-scale production efficiency, and predicting biological interactions. However, many challenges still remain in this area, including the need for standardized datasets and high-throughput experimental validation. Overcoming these challenges will require interdisciplinary collaboration across computational science, materials chemistry, pharmaceutical science, engineering science, and biomedical science. With continuous advancements, AI-driven methodologies are expected to accelerate the development of next-generation LBNPs, paving the way for more effective and personalized therapeutic solutions.

4.2 Nucleic acid-based nanocarriers

Nucleic acid-based nanocarriers are a class of nanoscale architectures assembled from DNA, RNA or DNA/RNA hybrids leveraging nucleic acid nanotechnology, which has been emerging as a robust framework for next-generation therapeutics and precision diagnostic systems [126]. As a best-known paradigm of nucleic acid-based nanocarriers, two- or three-dimensional DNA origami, which is self-assembled from a long single-stranded DNA molecule into nearly arbitrary shapes and patterns by employing hundreds of short oligonucleotides [127], is becoming a robust tool possessing great potential in the biomedical and drug delivery sectors [128].

In the past fifteen years, nucleic acid nanostructures, especially DNA origami, have evolved from small oligonucleotide assemblies into megadalton-scale architectures composed of hundreds to thousands of nucleic acid strands [129,130]. And characterization of the nanostructures produces complex datasets. Advances in computational power have enabled the simulation-based prediction of the nanoproperties across diverse design configurations. As a transformative tool in scientific analytics, AI has fundamentally transformed conventional approaches to molecular structure analysis and design. Machine learning is increasingly employed to optimize synthesis and characterization processes. By using machine learning algorithms supported by plenty of open-source machine learning/AI packages, researchers can analyze vast nanoscience datasets, uncover new patterns, and accelerate nucleic acid nanostructure discovery through active learning, which is fundamentally reshaping experimental planning, data characterization, storage, and interpretation in nucleic acid nanotechnology.

The most demanding aspect of machine learning implementation involves the accurate identification and extraction of relevant feature descriptors. In DNA origami specifically, key descriptors in the machine learning pipeline typically include structural characteristics (*e.g.*, shape, size, compactness, *etc.*), biological interactions (*e.g.*, cell type, *etc.*), or synthesis process parameters (*e.g.*, temperature, duration, concentration, *etc.*) [131]. Taking into account internalization and *in vivo* biostability of DNA origami, a more sophisticated yet highly informative input feature space can be established. These descriptors are domain-specific and span the parameter space of interest-whether for novel material discovery or performance optimization, thus ascertaining the right structure of the DNA origami.

A relatively extensive application of AI in nucleic acid nanotechnology is relieving data analysis of complicated nucleic acid nanostructures, which is time-consuming and prone to operator-dependent variability. Intra-image structural characterization of nucleic acid assemblies constitutes a critical requirement for efficient prototyping and quality assessment in the nano-scaffold fabrication. As a subfield of machine learning, computer vision (CV) develops intelligent software with human-like visual recognition and comprehension capabilities based on machine learning algorithms, which helps to resolve the critical limitation of manual structure annotation in image characterization, such as atomic force microscopy (AFM) [132]. Convolutional neural network (CNN)-based CV has been utilized in the detection, classification, and prediction of DNA origami nanostructures in recent years.

Kim *et al*. [133] propose an integrated approach combining systematic data acquisition protocols with deep learning-enhanced image super-resolution to enable accurate and high-throughput AFM characterization. The established workflow for AFM image acquisition and preprocessing requires only one matched low- and high-resolution image pair for effective training of conventional super-resolution models, significantly reducing data requirements. Implementation for DNA nanostructure metrology reveals nearly tenfold acceleration in AFM scanning without appreciable precision loss. The integrated transfer learning module facilitates on-demand optimization for diverse target samples. This approach proves particularly valuable for the comprehensive characterization of structurally analogous

sample variants across diverse environmental parameters or design iterations.

Using the You Only Look Once (YOLO) v5 deep convolutional neural network, Chiriboga *et al*. [132] outline a generalized protocol for the rapid automation of DNA structure detection and classification in raw AFM image data6. From molecular design to predictive analytics of DNA nanostructure, a complete pipeline including AFM imaging, data annotation, data augmentation, model training, and inference is presented, with a methodology integrating data acquisition and preparation, model building and training, prediction generation and evaluation, and data curation. The method reduces AFM image annotation duration by three orders of magnitude (hours to less than 30 s) with high repeatability compared with conventional manual approaches.

Deep neural networks are also utilized by Chen *et al*. [134] to develop a YOLOx-based feature enhancement method (YOLOx+3BiFPNc+attention) for DNA origami, especially the defective origamis, detection and yield estimation. A feature enhancement fusion network is proposed with the attention mechanism. The presence of impurities, including salt crystals, secondary structures, and noise, does not diminish the robustness and accuracy of the approach, which is confirmed by AFM images from wide-area scans to zoomed-in regions. The method demonstrates the capability for yield estimation of the DNA origami in a complex environment, achieving millisecond-level detection speeds.

Addressing the demand for rapid, high-throughput screening of fluorescence intensity trajectories, Deep-LASI (deep-learning assisted single-molecule imaging analysis), another software suite assisted by deep neural networks, is introduced by Wanninger *et al*. [135] for single-, two- and three-color single-molecule imaging data analysis of multicolor DNA origami structures. Deep-LASI performs automated trace sorting, Förster resonance energy transfer (FRET) correction factor determination, and dynamic state transition classification with a processing time of 20–100 ms per trajectory. On the basis of a highly tunable L-shaped DNA origami structure, Deep-LASI is used to conduct titration and characterize protein conformational dynamics, validating its capability in total internal reflection fluorescence microscopy and confocal single-molecule FRET (smFRET) data analysis.

Truong-Quoc *et al*. [136] present a deep-learning-based graph neural network for rapidly inferring the three-dimensional conformation of DNA origami assemblies. The graph neural network demonstrates the base-pair connectivity, sequence-dependent geometric and mechanical properties of base-pair steps, and electrostatic repulsive forces of DNA origami. To minimize the data-driven loss and the physics-informed loss, it is designed a hybrid data-driven and physics-informed approach is designed by incorporating the mechanical energies into the loss function, besides a detection for the structural variance. The model achieves near real-time inference of monomeric DNA origami structure and enables analysis of supramolecular assemblies comprising hundreds of DNA building blocks through an unsupervised approach. The model also makes it possible to design DNA origami structures inversely with a given target shape.

Except for above researches which demonstrate the feasibility of deep neural networks in automatically recognizing static DNA nanostructures in AFM or fluorescence microscopy, Wang *et al*. [137] conduct a deep neural networks-based pipeline for quantifying the structure and mechanical properties of dynamic DNA origami devices, which is important to enable their applications in molecular diagnostics, force sensing, and nanorobotic systems. A YOLOv5 deep neural network is used to detect the nanostructures from TEM images of DNA origami (*i.e*., particle detection), then a Resnet50 deep neural network is used to detect the conformation from individual images (*i.e*., pose estimation). The pipeline is also applied to a "Hinge-Nucleosome" system and a three-arm device to demonstrate its robustness in multiple dynamic DNA origami devices.

In addition to expediting labor-intensive analytical processes, AI has been employed to optimize the design of nucleic acid-based nanostructures. Sidestepping quantum molecular modeling, which is difficult to execute quantum chemistry calculations on large molecular structures of nucleic acids [138], machine learning enables systematic exploration of the nanostructure design space across diverse geometries and spatial patterns, reducing the required number of experimental iterations while maximizing the probability of achieving target nanocarriers for specific drug delivery.

Benson *et al*. [139] present a method for *in silico* stimulating wireframe DNA nanostructure and assessing their rigidity by applying the coarse-grained molecular dynamics package oxDNA. An iterative evolution of the more rigid nanostructure is autonomously generated by inducing structural mutants through the addition or removal of base pairs in designated helices or by repositioning of internal supports. Using the simulation dataset, a graph neural network is trained to predict the beneficial mutations to local or overall DNA nanostructures and achieve shape fidelity to target profiles.

In addition, a machine learning model based on an equivariant Euclidean neural network framework is developed by Lee *et al*. [140] to provide quantum-accurate *ab initio* electron density profiles for arbitrary DNA nanostructures up to ~225 kDa. Training on B-DNA basepair steps to capture base interaction, the model obtains the electron densities with typical errors of less than 1%, and it can extrapolate to the A- and Z-DNA configurations. It is demonstrated that the computational scaling for the model is linear

by the calculation of several large-scale DNA nanostructures. In comparison to conventional force field approaches, this machine learning electron density model can produce more accurate electrostatic potentials for the prediction of structural properties of designed-DNA nanostructures.

AI is helpful to identify and program the internal behavior and function of nucleic acid-based nanostructures for biomedical applications. Protein corona is the proteins adsorbing on nanostructures in complex biological fluids [141]. It has been a long-term challenge in nanomedicine to predict and control protein corona and even engineer their functions. Most recently, Huzar *et al*. [142] developed a machine learning model to predict the protein corona composition with priority enrichment on a DNA nanostructure based on properties of both the nanostructures and proteins. Based on a prepared library of DNA nanostructures with diverse sizes, shapes, charges, and surface modifications, two machine learning models are developed to predict whether a protein will appear in the corona of a DNA nanostructure with 92% accuracy, which supports the design of DNA nanocarriers with functionalized protein corona for improved drug delivery *in vivo*.

Overall, the integration of AI in nucleic acid nanotechnology has progressed gradually. It is imperative to build a comprehensive database or standardized platform for sharing DNA nanostructure data and developing models, which is a goal that has not yet been achieved at present, and will promote the development of nucleic acid-based nanostructures from simple proof-of-concept into biomedical applications. Some promising resources, such as Nanobase, an online database of nucleic acid nanostructures introduced by Poppleton *et al*. [143], are encouraging the process of machine learning in the field by sharing existing designs and promoting data accessibility.

4.3 Peptides and proteins

4.3.1 Fundamentals of AI in peptides and proteins nanocarrier design

In recent years, AI technologies have achieved breakthrough progress in the biomedical field, particularly demonstrating enormous potential in peptide and protein nanocarrier design. Traditional peptide and protein design primarily relied on experimental trial and error and limited rational design approaches, while the introduction of AI has significantly improved design efficiency and accuracy, accelerating the translation from design to application. The emergence of AlphaFold2 represents a major breakthrough for AI in the field of protein structure prediction. Developed by the DeepMind team, this system employs deep learning algorithms to predict three-dimensional protein structures with near-experimental accuracy [144]. For drug delivery nanocarrier design, accurate prediction of peptide and protein structures is crucial for understanding their self-assembly behavior, drug binding properties, and biocompatibility. RoseTTAFold, as another powerful structure prediction tool, integrates multi-scale structural information and demonstrates excellent performance in predicting complex structural domains [145]. Moreover, advanced evolutionary algorithms and neural networks have further enhanced our capability to design peptide structures with precise folding properties [146]. These AI-driven structure prediction tools provide a solid structural foundation for nanocarrier design, enabling researchers to understand nanocarrier behavior at the molecular level. Recent work by Lin *et al*. [147] on evolutionary-scale prediction of atomic-level protein structure with a language model has further expanded our ability to predict complex protein structures with unprecedented accuracy (Figure 4) [148].

Deep learning methods have been widely applied to reveal the sequence-structure-function relationships of peptides and proteins. Transformer architecture from natural language processing has been utilized to build embedding representations capable of capturing protein language through pre-training on large-scale protein sequence data, providing a powerful tool for function prediction [149,150]. In nanocarrier design, understanding how to sequence variations affect carrier drug loading capacity, stability, and targeting performance is particularly important. Comprehensive machine learning analysis of NPs in cancer research has provided data-driven insights into nanocarrier performance across different design parameters [151]. This work systematically evaluated the relationship between NP properties and *in vivo* behavior, establishing a foundation for predictive nanocarrier design. Peptide self-assembly behavior is key to constructing nanocarriers. Recent advances in machine learning approaches have overcome human bias in the discovery of self-assembling peptides [152]. This research revealed how AI can identify non-intuitive sequence patterns that lead to effective self-assembly, expanding the design space beyond traditional heuristics (Figure 5).

Large language models have demonstrated remarkable capabilities in generating functional protein sequences across diverse families [153]. Madani *et al*. [153] showed how models pre-trained on protein sequence data can capture fundamental principles of protein design, enabling the generation of novel sequences with desired functionalities for nanocarrier applications. Building on this foundation, Ferruz and Höcker [154] demonstrated controllable protein design with language models, allowing for precise engineering of proteins with specific properties—a critical advancement for designing peptide-based delivery systems.

The translation of AI-designed peptides and proteins to clinical applications requires understanding their *in vivo* behaviors. Wang and Höcker [155] developed tumor-selective

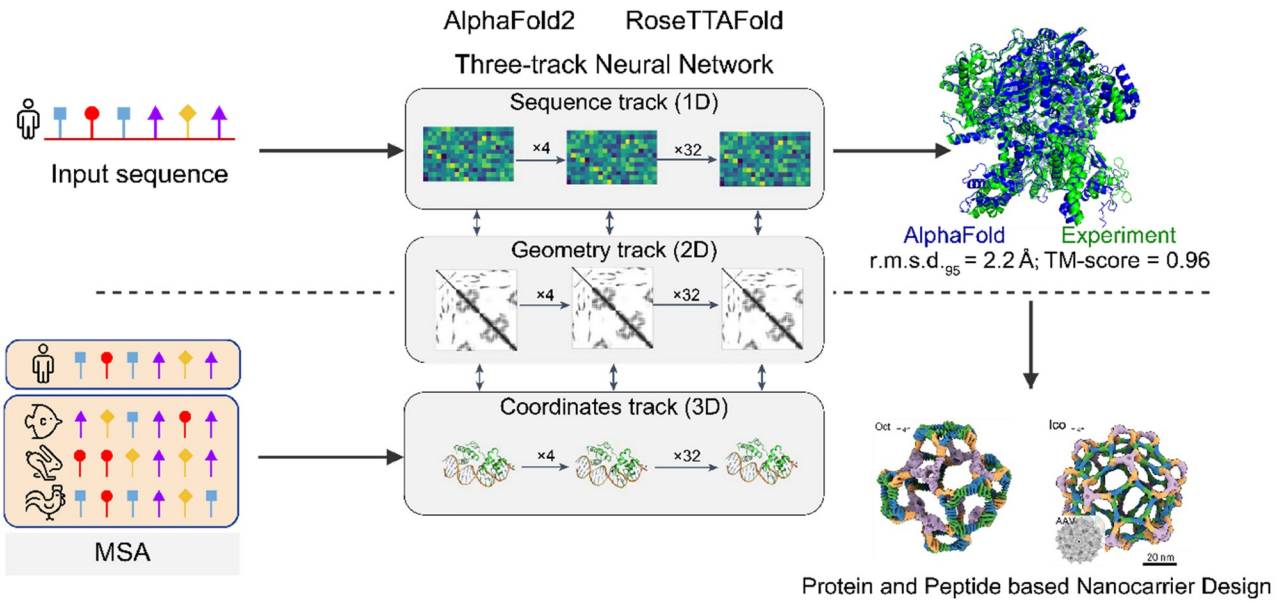

Figure 4 (Color online) Structure prediction models for peptide and protein nanocarriers. Artificial intelligence algorithms including AlphaFold2 (Reproduced with permission from Ref. [144]. Copyright©2021, the Author(s)) and RoseTTAFold (Reproduced with permission from Ref. [145]. Copyright©2021, the Author(s)) accurately predict three-dimensional molecular conformations, providing essential structural insights that guide the rational design and optimization of peptide and protein-based nanocarrier systems. Reproduced with permission from Ref. [148]. Copyright©2025, the Author(s).

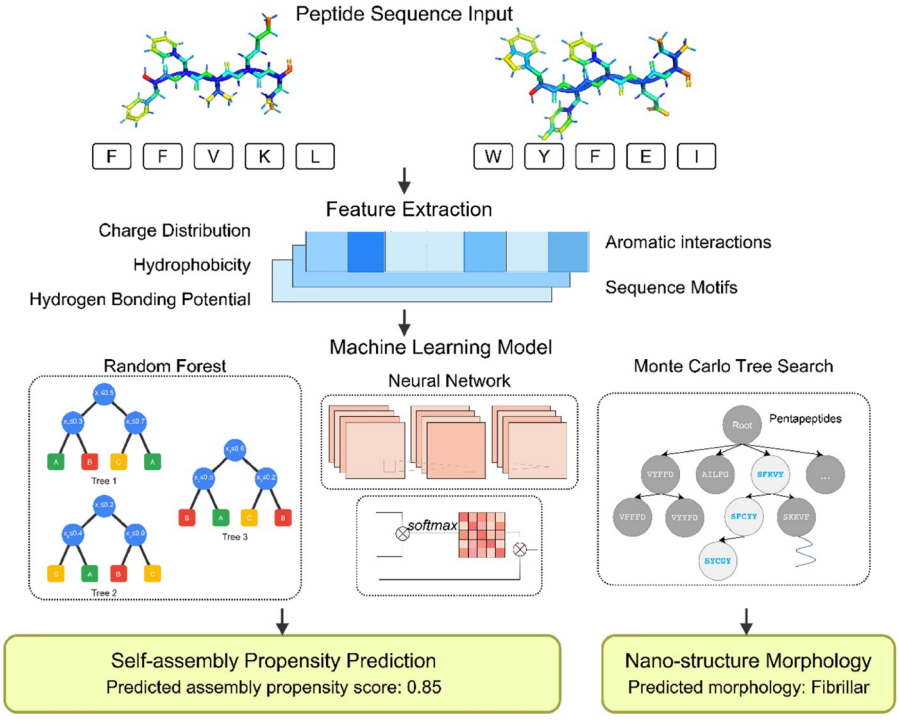

Figure 5 (Color online) AI algorithms for predicting peptide self-assembly. Machine learning models analyze sequence features to predict assembly propensity and resulting nanostructure morphologies. Reproduced with permission from Ref. [152]. Copyright©2022, Springer Nature.

cascade-activatable self-detained nanocarrier systems for rational design and efficient peptide delivery. Their integrated theoretical and experimental approach provided valuable insights into complex delivery processes and established design principles for optimizing nanocarrier performance [156]. Supporting these developments, Gao *et al.* [157] conducted a systematic review on integrating machine learning with molecular modeling for drug delivery

nanocarrier design, highlighting how computational approaches can accelerate next-generation delivery system development by establishing predictive relationships between nanocarrier properties and therapeutic outcomes.

4.3.2 Protein engineering and optimization via AI

Proteins as drug delivery carriers possess high specificity, biocompatibility, and multi-functionality. AI technology has significantly accelerated the engineering and optimization process of protein carriers. Natural proteins such as albumin and ferritin are ideal drug carriers. Recent advances in language models have guided the modification of natural proteins to enhance their drug delivery properties [154]. By identifying conservation patterns and functional motifs, these models can predict modifications that maintain structural integrity while enhancing drug binding capacity. Groundbreaking work by Cao *et al*. [158] has developed methods for designing protein-binding proteins from target structure alone, enabling the creation of small, stable proteins that can bind to specific targets with high affinity and specificity. This approach opens new possibilities for designing targeted drug delivery systems with enhanced binding properties. Comprehensive research on the self-assembly of peptides to nanostructures has provided insights into how various non-covalent interactions drive the formation of different nanoarchitectures that can serve as effective drug carriers [146].

Protein cages are a class of nanocarriers with hollow structures capable of encapsulating drug molecules. Recent advances in protein structure prediction through AlphaFold21 and RoseTTAFold2 have enabled the precise design of protein cage assemblies with controlled interior volumes and surface properties. Yang *et al*. [159] have developed computational methods for designing non-porous pH-responsive antibody NPs that can package a variety of molecular payloads and undergo tunable pH-dependent disassembly in the range of pH 5.9–6.7, providing new routes for targeted delivery of biologics. These AI-guided approaches have significantly expanded the design space for protein-based nanocarriers. Research investigating structure-induced functional changes in self-assembled peptide nanofibers has revealed how such modifications can be leveraged for targeted drug delivery, demonstrating how subtle structural modifications can dramatically alter the drug release profiles and targeting capabilities of peptide nanocarriers [160].

Controlling protein-protein interfaces is key to constructing complex protein nano-components. Recent evolutionary language models trained on sequence data can capture the subtle patterns that govern protein-protein interactions [147]. This approach enables the design of complementary interfaces for the precise assembly of multi-component protein nanostructures. Baker *et al*. [161] have developed a hierarchical design method for pseudosymmetric protein nanocages, creating large self-assembling protein nanomaterials with diameters of up to 96 nm, which are the largest bounded computationally designed protein assemblies generated to date. Similarly, Lee *et al*. [148] have developed four-component protein nanocages through programmed symmetry breaking, achieving complex structures with tetrahedral, octahedral, and icosahedral symmetries. These approaches significantly expand the possibilities for designing sophisticated drug delivery vehicles. Functionalized PLGA-PEG NPs for *in vivo* targeted drug delivery have established important principles for the formulation of polymer-protein hybrid nanocarriers that can be optimized using AI-based approaches [162].

4.3.3 AI-optimized functional peptides for targeted delivery

Targeted delivery is a key strategy for improving therapeutic effects and reducing side effects. AI technology has greatly accelerated the discovery and optimization process of functional targeting peptides. Utilizing deep learning, a peptide nanocarrier with improved penetration efficiency can be designed for antisense oligomers, even RNA and DNA, with the prediction of nuclear-targeting properties [163]. For specific targeting, Baker *et al*. [164] have significantly improved the design of protein binders using deep learning, increasing the success rate of designed binders nearly 10-fold by combining AlphaFold2 or RoseTTAFold. Kolodziejski *et al*. [165] have developed a machine learning-driven approach for multifunctional peptide engineering, creating peptides with high melanin binding, efficient cell penetration, and low cytotoxicity for sustained ocular drug delivery. Engineering of bacteria-derived outer membrane vesicles as vaccines using bacterial glycoengineering has provided insights into how protein and peptide-based nanostructures can be designed for targeted immune responses that could be further optimized using AI-driven approaches [166,167] (Figure 6).

Tumor-homing peptides can specifically recognize tumor tissues and are important components for targeted tumor therapy. Machine learning analyses of large datasets have identified NP properties that correlate with enhanced tumor accumulation [151]. Advanced language models can generate sequences with specific binding affinities to target receptors [153]. By training on known receptor-ligand interactions, these models can design novel peptides with enhanced specificity and binding strength. Shen *et al*. [168] have developed advanced machine learning approaches for designing nanotheranostics, combining therapeutic and diagnostic functions in a single nanoplatform.

Designing peptides with both targeting and efficient delivery capabilities requires balancing multiple competing design objectives. Modern AI approaches, particularly those

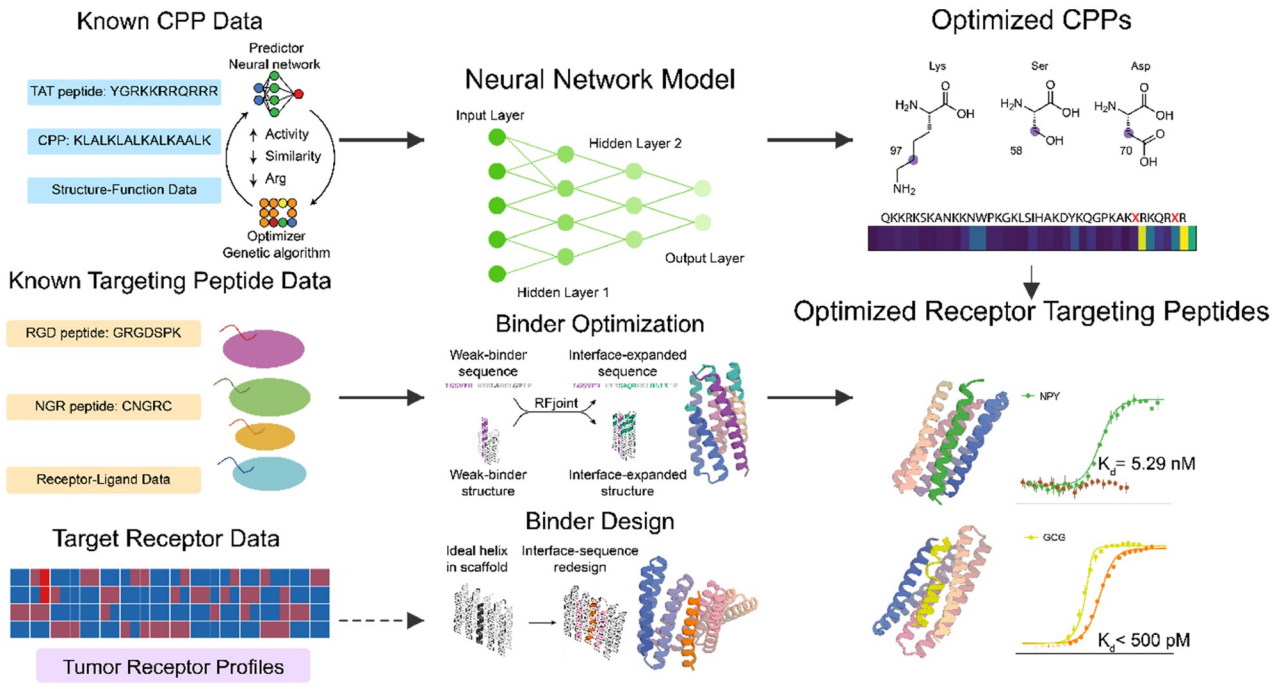

Figure 6 (Color online) AI for designing cell-penetrating and tumor-homing peptides. Reproduced with permission from Ref. [167]. Copyright©2024, the Author(s). Neural networks analyze structure-function relationships to optimize peptides for cellular penetration and tumor targeting.

incorporating Pareto optimization frameworks, can effectively balance these competing objectives to identify optimal peptide sequences that maintain high performance across all relevant metrics. Self-play reinforcement learning has emerged as a powerful technique for protein engineering, as demonstrated by Yang *et al*. [169], allowing for the optimization of complex protein functions through sequential decision-making processes. Recent advances in standardizing protein building blocks, as shown by Courbet *et al*. [170], have enabled the blueprint approach to designing extendable nanomaterials with predictable properties, which can significantly improve nanocarrier design in protein and peptide.

4.3.4 AI-optimized functional peptides for targeted delivery

Drug loading efficiency and controlled release are key indicators for evaluating nanocarrier performance. AI technology provides powerful tools for optimizing these processes. Understanding the interactions between drugs and carriers is crucial for optimizing loading efficiency. Gao *et al*. [157] demonstrated how molecular modeling combined with machine learning can predict drug-carrier interactions with high accuracy. This approach enables the rational design of nanocarriers with enhanced affinity for specific drug molecules.

By combining structural biology and machine learning, smart materials can design stimuli-responsive nanocarriers for precise drug release and optimized loading efficiency. Comprehensive machine learning analyses of large datasets of NPs in preclinical cancer research, as conducted by Conde *et al*. [171], have provided valuable insights into how NP properties influence their therapeutic performance, guiding the rational design of drug delivery systems (Figure 7).

Cleavable peptide linkers are important components for achieving controlled drug release. Machine learning models trained on protease specificity data can design peptide sequences with precise degradation kinetics in response to disease-specific enzymes. These linkers enable the development of intelligently responsive drug delivery systems that release their cargo selectively at disease sites. Maximizing drug loading capacity is a key goal in nanocarrier design. The development of nanotheranostics guided by machine learning has further expanded the functionality of drug delivery nanocarriers by integrating therapeutic and diagnostic capabilities [168].

4.3.5 Future perspectives in AI-designed peptide/protein nanocarriers

The application of AI in peptide and protein nanocarrier design is in a stage of rapid development and will further promote the development of personalized precision medicine in the future. End-to-end platforms integrating design, optimization, and validation are future development directions. Pandi *et al*. [172] demonstrated the combination of cell-free biosynthesis with deep learning, which offers a powerful approach to accelerate the de novo development of functional peptides. Human-in-the-loop approaches developed by Xu *et al*. [173], can significantly accelerate the prediction

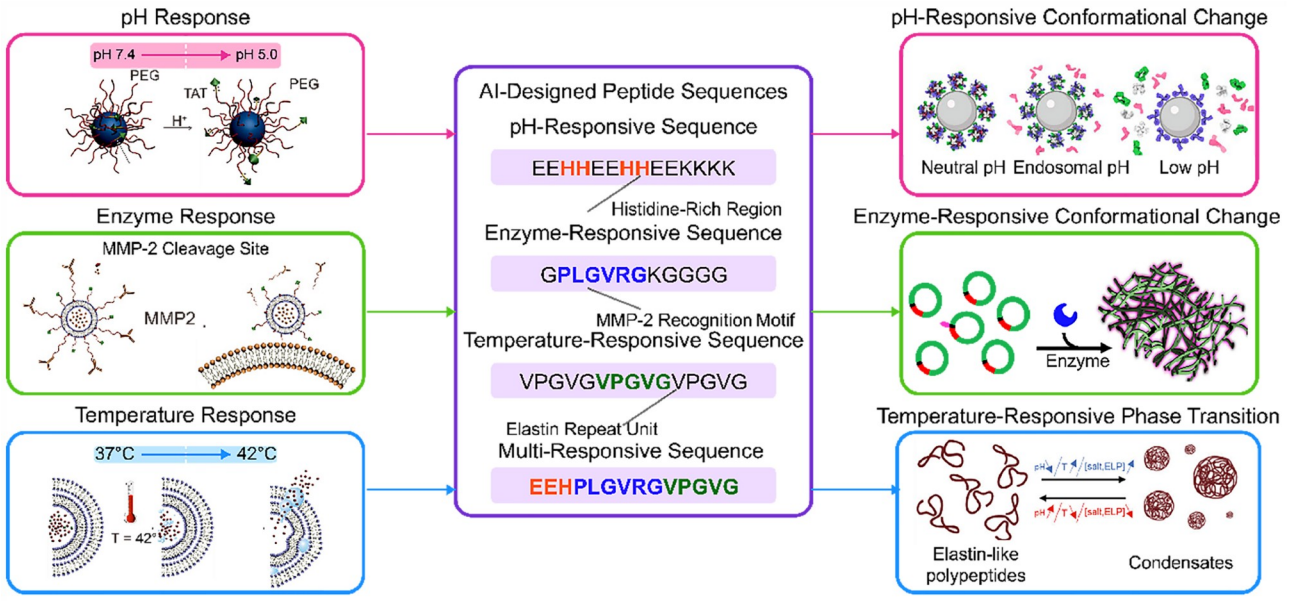

Figure 7 (Color online) AI design of stimuli-responsive release mechanisms. AI algorithms design peptide sequences that respond to environmental triggers (pH, temperature, enzymes) for controlled drug release at target sites.

and discovery of peptide hydrogels by integrating expert knowledge with computational predictions. These comprehensive platforms that combine multiple AI technologies for automated design, optimization, and validation of peptide/protein nanocarriers will significantly accelerate the development cycle from concept to clinical application.

Transfer learning can accelerate the design of novel nanocarriers. By leveraging knowledge gained from related domains, transfer learning approaches can significantly reduce the amount of experimental data required to design effective nanocarriers for new applications or target diseases. This approach is particularly valuable for developing personalized delivery systems based on limited patient-specific data. Improving the explainability of AI decisions is crucial for rational design. As machine learning models become increasingly complex, ensuring transparency in their decision-making processes becomes essential for scientific progress. Advanced interpretability methods can reveal the molecular features that drive model predictions, providing valuable insights for rational nanocarrier design.

Personalized medicine is a future development trend. AI-driven approaches that integrate multi-omics patient data with nanocarrier design principles can enable the development of personalized delivery systems tailored to individual patient profiles. These systems can account for variations in disease presentation, metabolism, and immune responses to optimize therapeutic outcomes. The integration of quantum computing with AI techniques promises to unlock new capabilities for designing highly complex nanocarrier systems with unprecedented precision and functionality. Quantum algorithms offer the potential to efficiently explore the vast conformational spaces of proteins that remain challenging for classical computing approaches, which could revolutionize the field of protein nanocarrier design in the coming years (Figure 8).

4.4 Polymers

Polymeric nanocarriers have shown great potential in drug delivery due to their advantages, such as controlled drug release, biocompatibility, and targeted delivery [174]. However, designing optimized polymeric drug delivery systems requires precise control over material properties, drug loading efficiency, and release kinetics. Traditional trial-and-error methods are time-consuming and inefficient, highlighting the need for advanced computational approaches. AI is transforming the field of polymeric nanomedicine by accelerating material screening, optimizing formulations, and predicting *in vivo* behavior [175]. This section provides an overview of the role of AI in the design, optimization, and biomedical applications of polymeric nanocarriers for drug delivery.

4.4.1 AI-based design and optimization of polymeric nanocarrier formulations

AI is increasingly applied in nanomedicine, particularly in the design and optimization of polymeric nanocarriers for drug delivery [176]. AI techniques such as big data analysis, machine learning (ML), and computational simulations enable the efficient prediction of key nanocarrier parameters, including solubility, biodegradability, and drug binding capacity, facilitating optimized carrier formulations. Supervised learning models can select polymeric nanocarriers with the best drug encapsulation efficiency and stability,

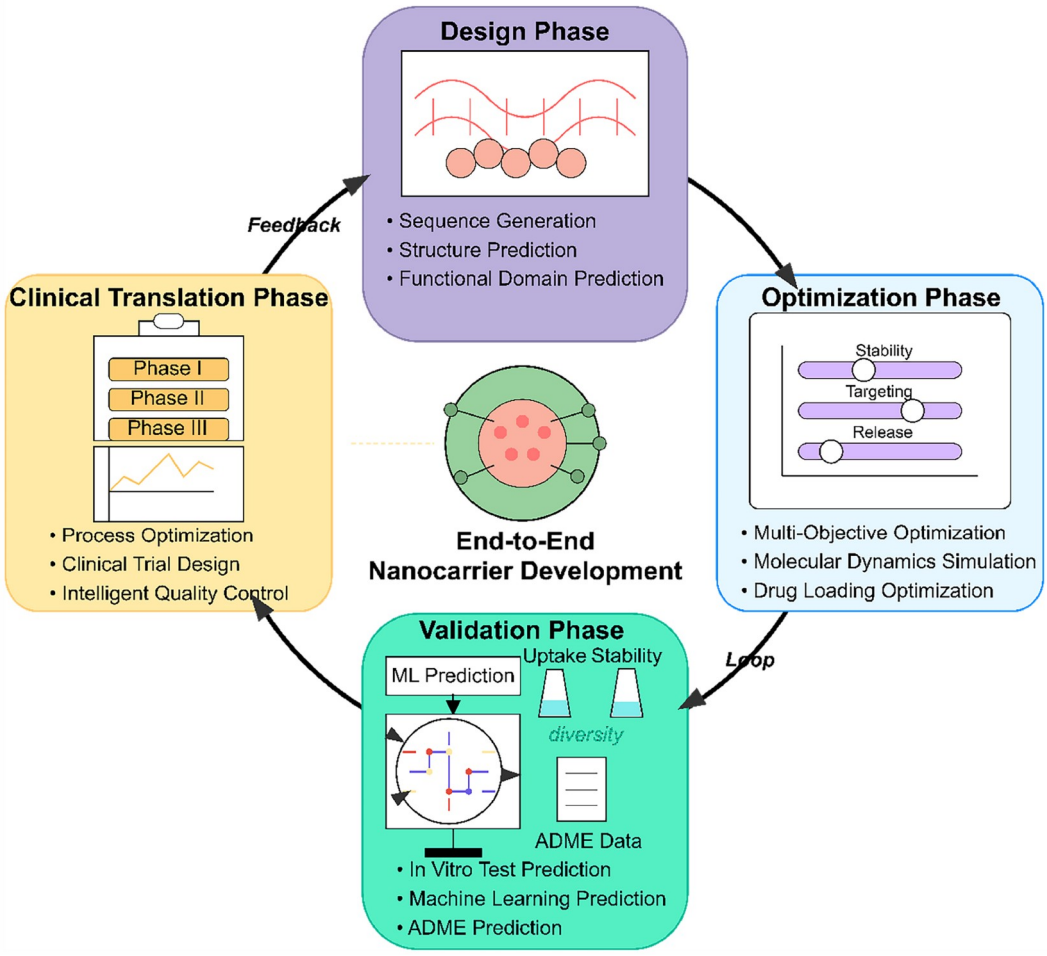

Figure 8 (Color online) Integrated AI platforms for end-to-end nanocarrier development. A comprehensive platform that combines multiple AI technologies for automated design, optimization, and validation of peptide/protein nanocarriers.

enabling precise and efficient drug delivery strategies [175].

AI is useful in the early design phase of nanocarriers, predicting drug-carrier interactions and optimizing formulations [177]. For example, Hathout and Metwally [178] proposed a computer-assisted drug formulation design method. They used molecular dynamics simulations to model nanocarriers of trimyristin and poly(lactide-*co*-glycolide) (PLGA), studied drug-carrier interactions through molecular docking, and correlated binding energies with drug loading. Using an artificial neural network (ANN), they analyzed the effects of drug molecular descriptors on binding energy and drug loading, showing that AI could accurately predict drug loading, saving experimental time and effort. Machine learning combined with experimental design also plays a significant role in optimizing drug delivery systems. Raza *et al*. [179] used an artificial neural network and design of experiments (ANN-DoE) approach to optimize sorafenib-loaded self-assembled NPs based on fucoidan and polyethyleneimine. Their study revealed that the ANN-DoE model accurately predicted the relationship between polymer concentration and NP size, leading to stable NPs with high encapsulation efficiency, offering a promising solution for anticancer drug delivery. AI is also used to predict drug release behavior and guide formulation design. Ainslie *et al*. [180] focused on AI-assisted drug release from polymeric NPs. They developed a diffusion-erosion model to describe drug release based on drug diffusion and polymer degradation. Using machine learning to estimate the diffusion coefficient, they could accurately predict *in vitro* drug release, which helped design Ace-DEX-based formulations. In combination therapy, optimizing dual-drug-loaded NPs is crucial. Zhao *et al*. [181] used machine learning combined with sequential nanoprecipitation to prepare dual-drug-loaded polymeric NPs. Their study identified hydrophobicity as a key factor influencing formulation performance, with polymer selection also playing a significant role. Most of the evaluated formulations showed good stability, with dual-drug NPs achieving high loading efficiency, providing new insights for combination therapy.

While significant progress has been made in drug delivery, challenges remain in gene delivery, particularly in developing efficient polymers to replace viral vectors [182,183].

Reineke *et al*. [184] synthesized 43 polymers via reversible addition-fragmentation chain transfer polymerization and identified the polycationic carrier P38 as efficient for plasmid DNA delivery. ML methods like SHapley Additive exPlanation and causal modeling revealed different design requirements for pDNA and ribonucleoproteins, offering guidance for the design of polymeric carriers tailored for specific therapeutic needs (Figure 9). AI is revolutionizing the design and optimization of polymeric nanocarriers, significantly enhancing the precision, efficiency, and therapeutic potential of drug and gene delivery systems.

4.4.2 AI-driven controlled synthesis of polymeric nanocarriers

Polymeric nanocarriers enable targeted drug delivery but require precise control of size, drug-loading, and surface charge. AI optimizes synthesis parameters via data-driven models, establishing quantitative structure-property relationships for programmable release and targeting. This reduces trial-and-error, accelerating tailored nanomedicine development with reproducible, scalable production.

As a practical polymeric carrier, the controlled synthesis of PLGA is frequently investigated using AI-driven data models [185–187]. Huwaimel and Alqarni [185] developed an AI framework to optimize PLGA NP synthesis via nanoprecipitation. Integrating antisolvent properties, polymer parameters, and concentration gradients, a three-phase model was implemented: data preprocessing (outlier removal, normalization), hybrid regression (LASSO-SVR with ensemble learning) for size prediction, and glowworm swarm optimization for hyperparameter tuning, achieving high zeta potential accuracy ($R^2 > 0.9$). This AI-driven approach enables precise control of NP size and surface charge while minimizing synthesis variability, advancing programmable nanocarriers for tailored therapeutics.

ANN enables controlled polymeric nanocarrier synthesis

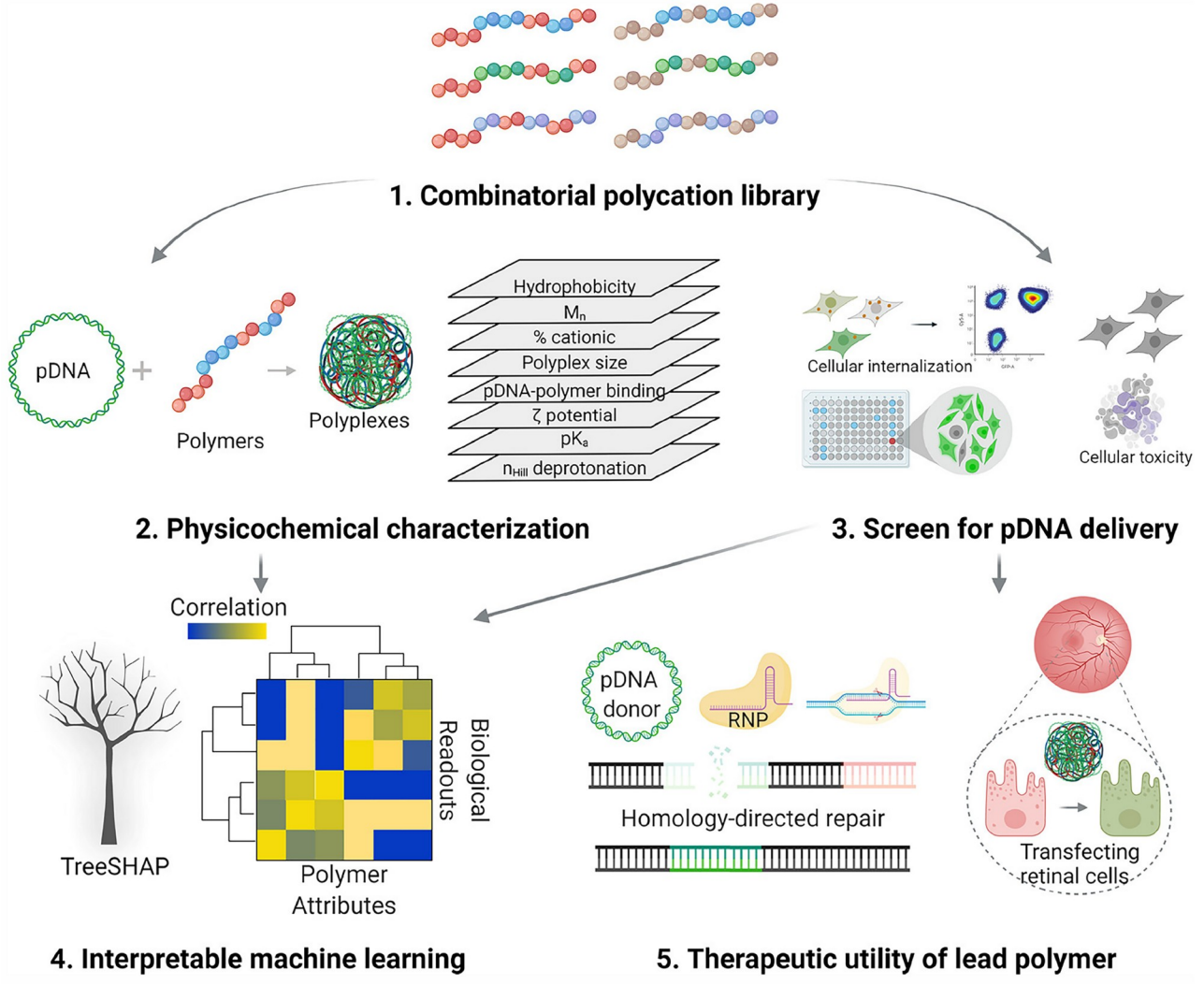

Figure 9 (Color online) Combinatorial library polymers with characterized pDNA loading and multimeric assembly, enabling rapid evaluation of internalization, delivery efficiency, and toxicity. Interpretable ML methods derive structure-function relationships. Reproduced permission from Ref. [184]. Copyright©2022, the Author(s).

through nonlinear mapping of polymer properties (molecular weight, hydrophobicity) and process parameters [188–190]. By establishing "synthesis-structure-performance" models, ANN predicts particle size, polydispersity, and surface charge while optimizing nanoprecipitation and microfluidics. This data-driven approach reduces trial-and-error, advancing programmable nanodrug delivery systems via end-to-end design.

Hashad *et al*. [190] developed an ANN to optimize chitosan-tripolyphosphate NP synthesis. By linking chitosan-TPP ratios to synthesis outcomes, the ANN model achieved precise control over particle size, zeta potential, and yield while preventing aggregation. This study demonstrated ANN's capability in simultaneously predicting NP characteristics and process efficiency, establishing a data-driven framework for controllable nanocarrier design. The approach enables reproducible fabrication of functional drug delivery systems through intelligent parameter optimization.

4.4.3 AI-driven controlled release of polymeric nanocarriers

AI is transforming polymeric nanocarrier release kinetics research from empirical to computational approaches by decoding multifactorial release mechanisms. Traditional methods, limited by nonlinear material-process-environment interactions (*e.g.*, polymer crystallinity, drug hydrophobicity, and pH), fail to systematically resolve release regulation. ML algorithms like ANN build quantitative models linking multiscale parameters to release dynamics, enabling two breakthroughs: nonlinear interaction decoding through graph theory-integrated deep learning reveals hidden material-environment-kinetics relationships, while inverse design using ANN and Bayesian optimization reverse-engineers process parameters (solvent ratios, emulsification) to optimize drug loading and burst suppression [191]. This AI-driven framework enables predictive nanocarrier engineering with tailored release profiles, advancing intelligent drug delivery systems [188,192–195].

Narasimhan *et al*. [192] developed an AI-driven framework to optimize drug release kinetics in polyanhydride nanocarriers. By integrating polymer chemistry, drug properties, and NP parameters, the hybrid model combined linear manifold learning with nonlinear graph-theoretic analysis. While linear methods identified key descriptors (*e.g.*, polymer hydrophobicity), nonlinear modeling achieved high-precision predictions (<10% error) for novel antibiotics, even with untrained atomic groups. The model maintains robustness ($\Delta R^2 < 0.05$) when incorporating new formulations. Leveraging DrugBank data and minimal experimental inputs, this framework enables virtual screening of polymer-drug pairs and programmable release kinetics, accelerating antibacterial nanomedicine development with controlled burst suppression and sustained delivery.

4.4.4 AI-driven multiscale modeling of polymeric nanocarrier-biointeractions for precision drug delivery

The delivery efficiency and safety of polymeric nanocarriers are governed by their structural characteristics, biological barrier penetration capacity, and microenvironmental responsiveness. Clinical translation challenges primarily stem from insufficient mechanistic insights into hierarchical nano-bio interactions across tissue-cellular-molecular scales. Off-target risks can be attributed to sequential biological barriers, including systemic clearance, tissue permeation, and intracellular delivery [13]. AI-enhanced quantitative structure-activity relationship (QSAR) models integrate multi-omics data with polymeric carrier parameters to dynamically simulate biointerfacial interactions. This paradigm bridges structure-function relationships of polymeric architectures with tissue-organ delivery dynamics, establishing a predictive multiscale framework that correlates physicochemical properties of nanocarriers with therapeutic efficacy outcomes [25].

In gene delivery system optimization, poly(β-amino ester) (pBAE) has garnered significant attention due to its biocompatibility and tunable chemical architecture. However, its delivery efficiency is constrained by multifaceted factors including polymer internal structure, compositional distribution, and cellular uptake mechanisms, rendering conventional experimental screening approaches labor-intensive and inefficient. The integration of AI technology provides novel strategies to decode pBAE's structure-performance relationships. Current studies explore AI applications in pBAE optimization from multiple perspectives. Initial work quantitatively analyzed pBAE component distributions, revealing synergistic effects between high- and low-molecular-weight fractions to guide structural refinement [188]. Subsequent research expanded to large-scale pBAE libraries, employing ML to construct cross-cell-line transfection and toxicity prediction models, thereby enhancing screening efficiency and applicability [196]. Further investigations integrated AI to elucidate pBAE cellular uptake mechanisms, identifying critical determinants (backbone configuration, terminal oligopeptides, particle size) of endocytic pathways [197]. This progression from polymer composition optimization to high-throughput modeling and cellular interaction mechanism decoding establishes a theoretical foundation and technical roadmap for intelligent design of advanced gene delivery vectors.

Chan's seminal research [124] on the correlation between polymeric nanocarrier structure and biodistribution demonstrates that polyethylene glycol-coated gold NPs exhibit complex cascading distribution behaviors in biological systems. These behaviors are governed not only by surface chemistry but also by dynamic protein corona evolution, vascular network permeation efficiency, and extracellular matrix interactions. By integrating proteomics with

supervised deep learning, the team pioneered a hierarchical QSAR model linking surface modifications to organ-specific biodistribution. This model quantitatively established that distinct patterns of surface-adsorbed proteins drive hepatic and splenic targeting. Further extending QSAR analysis to micrometastases, ML revealed that microenvironmental parameters such as vascular density and matrix heterogeneity regulate diffusion kinetics, which directly govern cellular uptake efficiency (Figure 10) [198]. Early-stage micrometastases, characterized by immature vasculature and simplified stromal architecture, demonstrated a 50% increase in NP penetration compared to primary tumors. Collectively, these studies established a multiscale QSAR framework integrating systemic biological analysis of organ-level distribution and microenvironment-focused cellular delivery mechanisms. The framework reconciles active modulation of macroscopic biological barriers with passive targeting strategies at microscopic scales. Future developments in multi-omics-driven dynamic QSAR modeling are poised to become pivotal for achieving precision nanomedicine delivery and overcoming complex biological barriers.

5 Inorganic NPs for adjuvant therapy

5.1 Tumor radiosensitizers

As a clinically feasible regime, radiotherapy is at the forefront in curing various solid tumors through directly or indirectly damaging DNA of malignant cancer cells as well as their other intracellular biomacromolecules including proteins [199]. High-Z nanoparticles (NPs) have emerged as promising nanoscale radiosensitizers due to their strong radiation attenuation capabilities and ability to enhance local energy deposition through secondary electron generation and reactive species production. A wide range of high-Z NPs—such as Au, Bi, Hf, and W—have demonstrated significant improvements in radiotherapeutic efficacy, particularly in overcoming the resistance of hypoxic tumor cells. Experimental evidence highlights that the radiosensitization effects of these NPs are strongly influenced by their size, shape, and surface chemistry. Studies have reported size-dependent enhancement in DNA damage and tumor suppression, shape-dependent cellular uptake efficiencies, and surface-ligand-dependent variations in ROS generation and cell death pathways. For instance, PEGylated AuNPs show superior radiosensitization compared to citrate-coated counterparts, and nanospike geometries functionalized with cell-penetrating peptides yield higher sensitization ratios. Collectively, these findings underscore the complex relationship between the physicochemical characteristics of high-Z NPs and their biological performance under ionizing radiation (see Supporting Information online for detailed discussion and references, Section S1).

Despite these advances made, much remains largely unknown regarding the influence of morphology features and surface functionalization on the radiosensitization by high-Z NPs, thereby it is difficult to define the desired size, shape, and surface properties to improve their radiotherapeutic

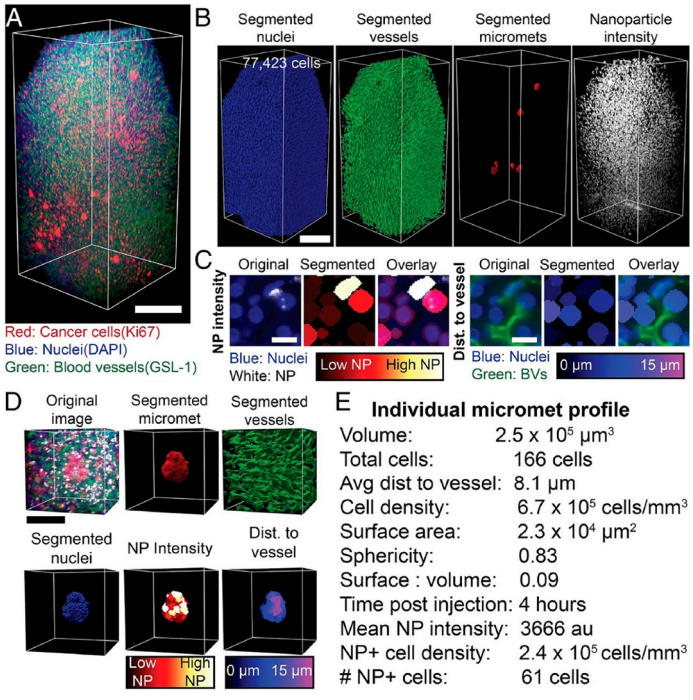

Figure 10 (Color online) (A–E) ML image segmentation technology was used to analyze 3D microscopic images of liver, quantitatively characterize the spatial distribution of nuclei, blood vessels and NP strength in micrometastases, and analyze the distance between cells and blood vessels to construct an individualized quantitative feature map of micrometastases. Reproduced with permission from Ref. [198]. Copyright©2019, the Author(s).

efficacy. In this case, the central issue of current research should be to consider the precise control over the morphology features and surface properties of high-Z NPs. Current synthesis of high-Z NPs primarily includes hydrothermal, solvothermal, precipitation, chemical reduction, and thermal decomposition processes. Generally, most of the experimental parameters involved in these methods, such as temperature, concentration, reaction time, and surface ligand, are strongly interdependent upon each other during the formation of high-Z NPs. Therefore, lots of trial-and-error approaches are required to understand the complex interdependence effects, experimentally making the synthesis of desired high-Z NPs rather laborious, time-consuming, and resource-intensive. For example, a small disturbance of reagent concentrations and pH could cause a drastic difference in the size of AuNPs, and therefore hundreds of synthetic experiments are needed to ascertain the optimum parameters for better radiosensitization effects [200].

To circumvent these bottlenecks and simultaneously expedite the discovery of novel nanoscale radiosensitizers, integration of AI, especially deep learning algorithms, with the methods mentioned above, offers a powerful tool to relate experimental parameters to the morphology features of high-Z NPs and thereby develop efficient protocols for their synthesis [201,202]. During process development, experimental conditions/results serve as input to machine learning algorithms, learning the mathematical relationships between the morphology features of interest (*e.g.*, shape, size, or crystalline structure) and a set of experimental conditions (*e.g.*, temperature, concentration, or reaction time), the surface propertied of interest (*e.g.*, zeta potential) and a set of experimental conditions, or even the radiosensitization effect and physicochemical properties of high-Z NPs. These established relationships are particularly useful to guide the synthesis of high-Z NPs with tight specifications in terms of shape and size and to help understand the influence of morphology features and physicochemical properties on their radiosensitization effects. For the former case, some efforts have been devoted recently to providing new insights into the synthesis of high-Z metal NP. Schletz *et al*. [203] used interdependent variation parameters such as precursor, capping agent, reducing agent, and the amount of gold seeds as input conditions and the size of AuNPs as output targets. These were trained with tree-based machine learning algorithms including Linear Regression, Random Forest Regression, AdaBoost, and XGBoost, to learn the algorithms on the semi-batch, seed-mediated synthesis of AuNPs, finally establishing the correlation between synthesis parameters and size to predict the synthetic outcomes and optimize experiment planning. Li *et al*. [204] presented a machine learning model by stacking Siamese neural networks with the graph convolutional neural networks. By training the limited data (only 54 examples), more chemical insights could be acquired from the decision tree to understand the synthesis process and help guide the synthesis of desired AuNPs. The hybrid model, achieved by combining artificial neural network and modified particle swarm optimization, could establish the relationships between the size of silver NPs (AgNPs) and practical parameters including temperature, pH, feed rate, $AgNO_3$ to opium ratio, and agitation speed, finally producing optimal conditions to yield AgNPs with the average diameter of approximately 4 nm [205]. By extracting experimental data from an eight-dimensional chemical space (Au-Ag-Cu-Co-Ni-Pd-Sn-Pt) as inputs, Wahl *et al*. [206] used the Bayesian optimization algorithm to predict the synthesis of polyelemental nanomaterials and guide their synthesis to achieve targeted structural properties. Unfortunately, artificial intelligence-assisted synthesis has yet to be used for the fabrication of high-Z NPs as nanoscale radiosensitizers, and, so far, no studies have been devoted to understanding how the morphology features and physicochemical properties affect their radiosensitization effects and interact with each other. Given the complicated properties of high-Z NPs and the complexity of the biological responses, the introduction of AI into the field of nanoscale radiosensitizers could provide an effective alternative way to achieve better decision-making to design high-Z NPs with ideal features and explore corresponding mechanisms of radiosensitization. In fact, during the radiotherapy workflow, considerable studies have demonstrated a proof of principle that AI could be used to extract robust features such as radiomics and genomics, effectively establishing predictive models for treatment response [207–210]. For example, a novel artificial neural network with selective connection based on gene patterns could learn the gene pattern information and provide insights into radiosensitivity and radiocurability [211]. The nomogram based on radiomics signature showed proper sensitivity to predict the risk of local recurrence after intensity-modulated radiotherapy.

5.2 Tumor catalytic therapy

Catalytic tumor therapy has emerged as a transformative paradigm in tumor treatment, leveraging *in situ* catalytic reactions to selectively eliminate cancer cells [212]. This approach utilizes engineered catalytic biomaterials that exploit endogenous tumor microenvironment (TME), such as acidic pH and elevated hydrogen peroxide (H_2O_2) levels [213], or respond to exogenous stimuli including light, ultrasound, magnetic field, X-rays or thermal triggers to generate cytotoxic agents/species at the tumor site [214]. Especially, Huang and Chen [215] recently proposed the concept of pancatalytic medicine by holistic management of catalytic biomaterial preparation (P), catalytic biological effect activation (A) and non-toxic (N) catalytic therapy of tumor or other diseases, which further significantly promotes

the clinical translation of catalytic biomaterials for versatile disease treatment. Although a wide spectrum of catalytic biomaterials, including nanozymes [216], photosensitizers, sonosensitizers, magnetic NPs, and thermoelectric agents [217], have demonstrated the desirable therapeutic potential, clinical translation remains impeded by several challenges. Chief among these are the inherent complexity and variability of the TME, limited predictive understanding of biomaterial behavior *in vivo*, and the need for personalized therapeutic regimens tailored to individual patient profiles, which have significantly hindered the translation of catalytic tumor therapy from bench to bedside.

Recent breakthroughs in AI have catalyzed innovation across biomedical disciplines, including drug discovery and materials science, by offering data-centric approaches capable of resolving nonlinear high-dimensional problems. In the context of catalytic tumor therapy, AI is rapidly gaining traction for its ability to optimize catalytic biomaterial design, predict tumor-specific catalytic reactions, and enable individualized therapeutic strategies. By integrating heterogeneous datasets ranging from experimental assays to quantum mechanical simulations to public repositories, AI algorithms can uncover latent patterns and generate predictive models of materials-biological system interactions. This facilitates the rational design of next-generation catalytic agents, enhances mechanistic understanding of their biological fate, and circumvents the inefficiencies of traditional trial-and-error methodologies. Consequently, AI is poised to accelerate the development of more efficient, adaptable, and clinically viable catalytic tumor therapies, ushering in a new era of precision oncology.

The implementation of AI in catalytic tumor therapy typically adheres to a systematic, multi-step process, encompassing data aggregation, feature engineering, model development, performance validation, and clinical applications (Figure 11). Initially, diverse data types, such as physicochemical measurements, theoretical calculations (*e.g.*, density functional theory, Monte Carlo simulations), high-throughput screening outputs, and multi-omics data derived from patient biopsies, are curated to capture the multi-dimensional nature of both catalytic biomaterials and tumor biology. From these inputs, a range of descriptors is constructed to encode structural, electronic, and biological attributes. Subsequently, machine learning (ML) models, spanning conventional algorithms (*e.g.*, random forests, support vector machines) to advanced deep learning architectures (*e.g.*, graph neural networks, Transformers), are trained to map these features to therapeutic outcomes, including drug loading efficiency, catalytic efficiency, and tumor responsiveness. Interpretability methods such as SHapley Additive exPlanations are employed to identify key drivers for performance, thereby guiding iterative optimization of materials and treatment regimens. This closed-loop pipeline integrates *in silico* predictions with experimental feedback, enabling continuous refinement and broader applicability across various therapeutic contexts.

Among the most impactful applications of AI in catalytic tumor therapy is the rational design and high-throughput screening of catalytic biomaterials. Traditionally reliant on heuristics and labor-intensive methods, the development of catalytic biomaterials is undergoing a paradigm shift enabled by AI-driven prediction of structure-function relationships. Machine learning models can correlate key physicochemical features, such as particle size, surface area, band gap energy, and coordination geometry, with performance metrics like reactive oxygen species (ROS) yield [218], enzyme-mimicking activity, or energy conversion efficiency. In photocatalytic systems, machine learning models trained on molecular fingerprints, electronic descriptors, and quantum chemical properties have accurately predicted light absorption characteristics, enabling the pre-synthesis optimization of hybrid structures like Pt-Mn nanocomposites [219,220]. More sophisticated deep learning models, such as graph neural networks, capture spatial and electronic features at the atomic level, supporting the prediction of adsorption energies and catalytic turnover rates under tumor-relevant conditions [221]. These models have been instrumental in identifying metal-organic frameworks with high drug loading capacities, and designing nanozymes with customized enzyme-mimetic activity adapted to specific TME [222,223]. When integrated with databases like the Materials Project, AI-driven virtual screening pipelines dramatically accelerate the discovery of high-potential candidates [224]. Furthermore, model interpretability tools provide mechanistic insights into how specific design parameters modulate therapeutic performance, bridging the gap between predictive modeling and rational material synthesis [225].

In addition to catalytic biomaterials design, a major frontier in catalytic tumor therapy lies in elucidating the "material-biology interface", which is the complex zone where nanomaterials interact with biomolecules, cells, and tissues. These interactions govern processes such as cellular uptake, biodistribution, immune recognition, and catalytic reactivity, ultimately determining therapeutic outcomes. However, conventional experimental approaches often fall short of capturing the full spatiotemporal dynamics of these interactions. AI offers the ability to decode this interface by integrating high-dimensional and multimodal datasets, often in conjunction with other physical simulations (*e.g.*, molecular dynamic simulation) [226]. For example, AI-assisted protein-protein interaction analyses have been used to identify synergistic drug candidates targeting pyroptosis regulators [227]. Omics-integrated models have elucidated how metabolic pathways (*e.g.*, lipid metabolism), cytoskeletal remodeling, and signaling cascades (*e.g.*, Notch/Akt) influence NP trafficking and therapeutic efficacy [228]. AI has also

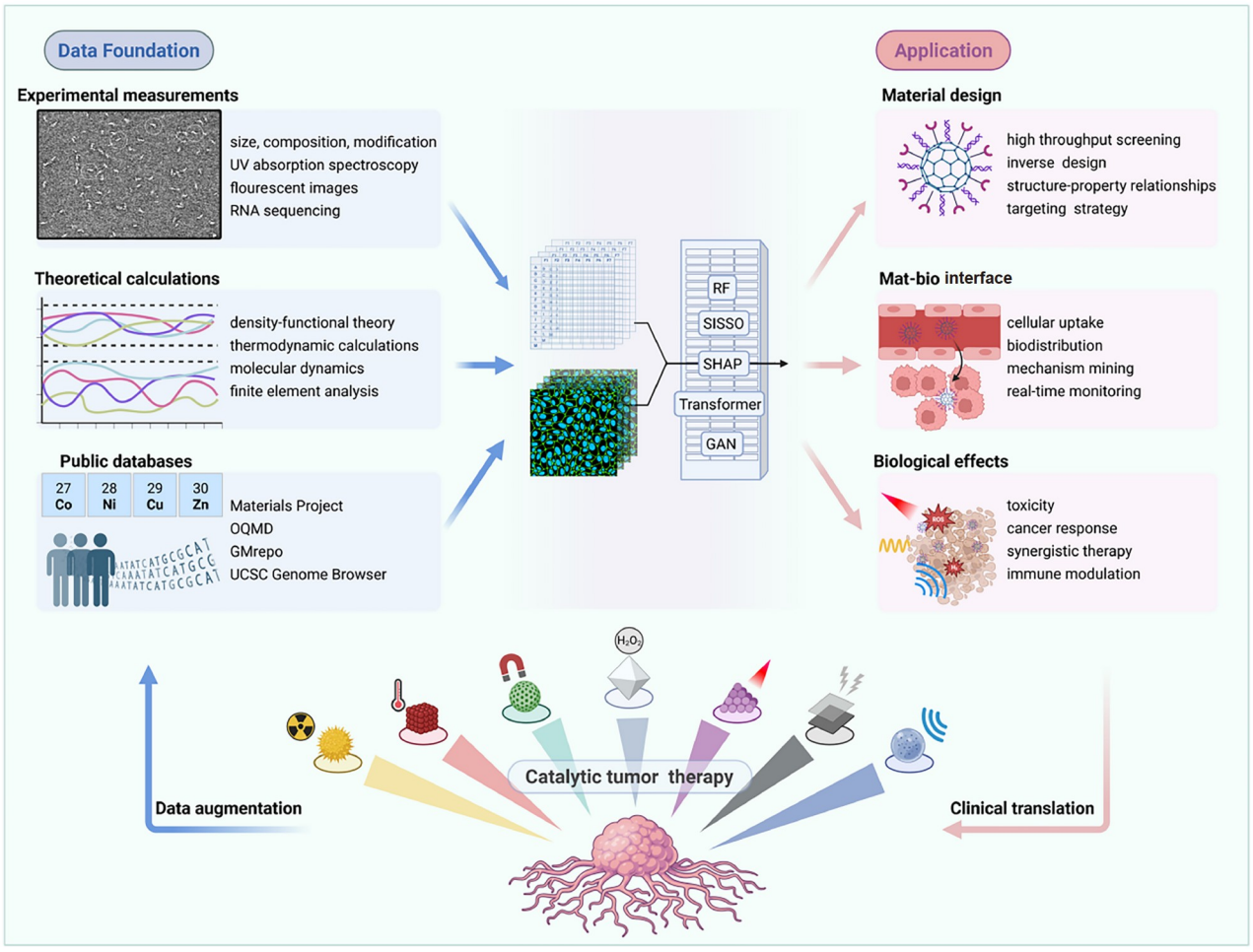

Figure 11 (Color online) Schematic illustration of the AI-enabled workflow for catalytic tumor therapy. The pipeline encompasses data collection, feature extraction, model training, interpretation, experimental validation, and clinical translation.

been applied to spatially resolve tumor heterogeneity by integrating histopathological imaging with molecular profiles, revealing how features such as stromal density and vascular architecture affect nanocatalyst penetration and local reactivity [222]. Active learning frameworks combined with fluorescence-based high-content imaging further enable iterative optimization of NP surface properties such as PEGylation and charge density as tailored to specific biological milieus [229]. Collectively, these AI-guided strategies transform static material design into a dynamic, systems-level engineering of therapeutic biomaterial platforms.

The ultimate objective of catalytic tumor therapy is to induce potent, tumor-specific cytotoxic effects while minimizing systemic toxicity. AI models have been instrumental in achieving this balance by predicting therapeutic efficacy and safety profiles based on integrated datasets. For instance, machine learning algorithms have identified oncolytic peptides that exhibit high selectivity for cancer cells while sparing healthy tissues [230]. In clinical oncology, multimodal AI frameworks, such as Multi-Modal model, successfully predicted patient-specific outcomes (*e.g.*, progression-free survival) in response to HER2-targeted therapies and their combinations with immunotherapies [231]. These tools enable dynamic adjustment of treatment regimens based on tumor responsiveness. AI also facilitates the design of synergistic therapeutic combinations, such as catalytic agents co-delivered with drugs that induce ferroptosis while avoiding counterproductive autophagy responses [232]. Moreover, AI-guided identification of immunomodulatory biomarkers, through network-based ML analysis of gene expression, has improved prediction of immune checkpoint inhibitor responses, surpassing traditional metrics such as PD-L1 expression [229,233]. Through accurate modeling of therapeutic efficacy, immunological interactions, and toxicity, AI has evolved into a critical component in the decision-making pipeline for catalytic tumor treatment.

Despite its transformative potential, the AI-driven catalytic tumor therapy still faces significant barriers, including the scarcity of standardized high-quality datasets, the inherent heterogeneity and dynamism of the TME, and challenges in integrating multimodal data types with varying dimension-

alities and noise levels. The lack of standardized and high-quality data limits the training and predictive accuracy of AI models. Moreover, the dynamic and heterogeneous nature of the TME complicates the accurate simulation of catalysis and drug interactions. The integration of diverse data types, such as clinical, imaging, and omics data, remains a challenge due to dimensional differences and data noise. Furthermore, the lack of model interpretability remains a significant challenge, as clinicians and researchers need transparent, understandable decision-making processes to trust and adopt AI-driven solutions. Looking ahead, the integration of AI with catalysis and other interdisciplinary fields, such as nanotechnology, material science, biology and clinical medicine, will foster the development of multifunctional, targeted catalytic agents with enhanced tumor specificity and therapeutic efficiency. Additionally, AI-driven adaptive treatment strategies, supported by real-time feedback systems, will allow for dynamic adjustments based on tumor progression and microenvironmental changes, improving treatment outcomes while minimizing side effects of catalytic tumor therapy. The synergy among AI, catalytic biomaterials and immunotherapy also presents a promising frontier, where AI can optimize combination therapies, such as pairing catalytic biomaterials with immune checkpoint inhibitors, to improve tumor response and reduce immune escape. In the future, the role of AI in catalytic tumor therapy will expand, leading to more efficient, adaptive, and personalized treatments, ultimately enhancing patient survival and quality of life.

5.3 Antibacterial

Inorganic nanomaterials have garnered increasing attention in the antibacterial field due to their diverse mechanisms of action, low likelihood of inducing resistance, and broad applicability across medical, environmental, and agricultural settings. These nanomaterials, including metal/metal oxide NPs (*e.g.*, Ag, Cu, ZnO), carbon-based nanostructures (*e.g.*, graphene oxide, carbon quantum dots), and emerging materials such as sulfur or enzyme-mimetic NPs, exert antibacterial effects primarily through membrane disruption, redox stress, metal ion release, and external stimulus-triggered responses. Depending on their physicochemical properties, these materials can be applied to various contexts —from clinical infection control to food preservation and crop protection. A more detailed classification, mechanism analysis, and application mapping of antibacterial inorganic NPs is provided in the Supplementary Information (Section S2).

5.4 Antioxidants

5.4.1 Oxidative stress and antioxidant inorganic NPs

Reactive species encompass a diverse group of extremely reactive substances that are produced as metabolic by-products. They include ROS and reactive nitrogen species (RNS), collectively known as RONS. Reactive species serve as signaling molecules in cells and tissues [234]. ROS are molecules generated during the aerobic processes in biological systems. These molecules typically comprise H_2O_2, $O_2^{\bullet -}$, $^{\bullet}OH$, ROOH, ROO$^{\bullet}$, and RO$^{\bullet}$ [235–237]. Reactive nitrogen species (RNS) are a distinct category of free radicals, including $ONOO^-$ and $^{\bullet}NO$ [238,239]. RONS interact to form molecular networks that link their signaling pathways. Their interaction is essential for regulating the cellular responses [240,241]. However, an imbalance of RONS content may lead to significant adverse effects. There are special compounds that maintain redox homeostasis, including low-molecular antioxidants, such as ascorbic acid, glutathione, and cysteine, and antioxidant enzymes, such as catalase (CAT), superoxide dismutase (SOD) [242], and glutathione peroxidase (GPx) [243,244]. In case the native antioxidant system cannot cope with maintaining redox homeostasis, the reactive species deal damage to biomolecules [245] and cellular organelles [246], causing oxidative stress. In turn, oxidative stress is involved in the pathogenesis of a wide variety of diseases [247]. Administration of therapeutic formulations endowed with antioxidant activity is a promising tool for alleviating such pathologies [248]. One of the advanced approaches in this field is the development of antioxidant inorganic NPs [249]. This kind of bioactive nanomaterials includes different formulations based on metals, metal oxides and other metal and nonmetal compounds [250]. Most of these NPs exhibit enzyme-like activities and are collectively referred to as nanozymes [251]. In this section, the different types of antioxidant inorganic NPs, their mechanisms of action and biomedical applications are reviewed. Furthermore, the roles of AI in their development and current perspectives and challenges are discussed (Figure 12).

5.4.2 Types of antioxidant inorganic NPs

(1) Metal

PtNPs possess CAT-like activity under neutral and alkaline conditions, SOD-like under neutral conditions, $^1O_2$-scavenging activity under neutral and alkaline conditions [252,253], and $HOO^{\cdot}$-scavenging activity [254]. Pt NPs combined with proteins show SOD- and CAT-like activities depending on pH and temperature [255–257].

PdNPs exhibit SOD- and CAT-like activities, depending on their surface facets: lower surface energy (111)-faceted Pd octahedrons demonstrate more efficient antioxidant activity than higher surface energy (100)-faceted Pd nanocubes [258]. Pd nanosheets show both CAT-like [259] and SOD-like activities [260].

AuNPs can act as SOD and CAT mimetics with pH-tunable activity [261]. There is also an approach to switch the peroxidase (POD)-like to CAT-like activity of Au NPs using

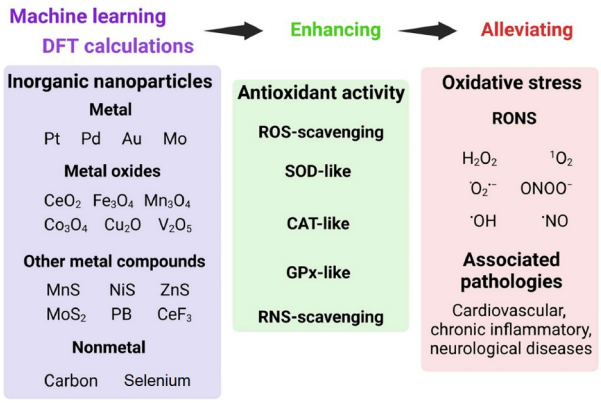

Figure 12 (Color online) AI-assisted development of antioxidant inorganic NPs for oxidative stress alleviating and adjuvant therapy of related diseases. Created with https://BioRender.com.

specific coatings [262].

Trimetallic nanozyme, consisting of Pt, Pd, and Mo, scavenge RONS, including $^1O_2$, H_2O_2, $^{\bullet}OH$, and $^{\bullet}NO$ at neutral pH [263]. Au@Pt nanostructures and nanocomposites demonstrate SOD- and CAT-like activities [264,265].

(2) Metal oxides

Cerium dioxide NPs (CeO_2 NPs, nanoceria) mimic activities of SOD [266–268] and CAT [269,270], depending on their size, shape, exposed facets, and Ce^{3+}/Ce^{4+} ratio [271,272]. Nanoceria remains active under various conditions, including pH and physiological environments [273]. CeO_2 NPs can be functionalized with various coatings, enhancing their biocompatibility and bioaccumulation [274].

Iron oxide NPs not only show POD-like activity [275] but also have antioxidant properties [276]. In particular, Fe_3O_4 and γ-Fe_2O_3 NPs exhibit pH-dependent POD-like and CAT-like activity: they decompose H_2O_2 at neutral conditions, while acting as POD at an acidic pH [277].

Mn_3O_4 nanoflowers possess ROS-scavenging capability, based on their SOD-, CAT- and GPx-like activities [278,279]. Manganese dioxide (MnO_2) NPs also mimic the activities of SOD and CAT [280]. Manganese oxide (MnO) NPs demonstrate SOD-like activity along with MRI-contrast properties [281].

Co_3O_4 NPs are CAT and SOD mimics, with their activity tunable by pH [282,283]. Cobalt oxide NPs demonstrate a remarkable stability when exposed to different pH and temperature [284]. The enzyme-like antioxidant activity depends on their size, shape, and exposed crystal planes [285].

Copper oxide (Cu_2O) and Au@Cu_2O nanostructures mimic the activities of SOD, CAT, and GPx [286,287]. Vanadia nanowires (V_2O_5) mimic GPx individually [288] and in combination with SOD- and CAT-mimicking MnO_2 NPs [289]. Yttrium oxide nanocrystals (Y_2O_3) scavenge $^{\bullet}OH$, depending on their size, shape, and dopants [290].

(3) Other metal compounds

Metal sulfide NPs, such as MnS, NiS, and ZnS NPs, are able to scavenge ROS [291,292]. Also, MoS_2 nanosheets mimic SOD and CAT under physiological conditions [293]. Prussian blue NPs (PB NPs) exhibit CAT- and SOD-like activities [294,295], which can be enhanced by doping them with Ni or by loading them with MoS_2 [296]. Cerium fluoride NPs (CeF_3 NPs) demonstrate H_2O_2- and $^{\bullet}OH$-scavenging activity under X-ray irradiation [297].

(4) Nonmetal

Graphene oxide NPs are able to effectively decrease the level of ROS [298]. They show CAT-like activity in the physiological microenvironment of healthy tissues such as neutral pH and low H_2O_2 content [299].

Fullerenes (C_{60}) and their derivatives exhibit ROS scavenging capability [300], which is based on their SOD- [238,301] and pH-switchable CAT-like activity [302]. There are metal-doped fullerenes that demonstrate improved antiradical capacity [303].

Carbon nanodots (CNDs), doped with different elements, are known for their antioxidant properties [304], mimicking CAT and SOD [305]. Carbon nanotubes (CNTs) also exert strong antiradical activities [306,307].

Mesoporous carbon decreases the level of intracellular ROS, particularly through its multienzyme-like activity [308,309].

Selenium NPs are known for their ability to scavenge various ROS, such as $O_2^{\bullet-}$, $^1O_2$, and $^{\bullet}OH$ [310–313]. This ability can be attributed to their GPx-like activity [314,315].

5.4.3 *Mechanisms and kinetics of the antioxidant activity*

The mechanisms of the antioxidant activity of inorganic NPs are mainly based on the redox transitions of their core elements at active sites or/and adsorption and rearrangement of the substrate [279,282,316,317]. For example, nanoceria exhibits enzyme-like activity through Ce^{3+}/Ce^{4+} redox switch in the presence of oxygen vacancies [267,269–271,313].

The catalytic activity of nanozymes is usually described by the Michaelis-Menten kinetics, which is typical for natural enzymes [87]. Therefore, when characterizing the antioxidant NPs, endowed with enzyme-like activity, their key parameters, including catalytic efficiency (k_{cat}), substrate affinity (K_M), and highest reaction velocity (V_{max}), are determined [286,318,319].

5.4.4 *Biomedical applications*

Antioxidant inorganic NPs are promising candidates for adjuvant therapy in a wide range of diseases associated with oxidative stress, including cardiovascular diseases (such as atherosclerosis [320], cardiovascular injury [321], and cardiac microvascular ischemia-reperfusion injury [322]); chronic inflammatory diseases (such as psoriasis [323], rheumatoid arthritis [324], and diabetic wounds [325]); as well as sepsis [84]. The NPs also have prospects for appli-

cation in the fields of neuroprotection against brain injury and stroke [326], Alzheimer's disease [327], Parkinson's disease [279], as well as wound healing [328] and cytoprotection [329].

5.4.5 The role of AI in the development of antioxidant inorganic NPs

Recently, data-driven approaches, including machine learning, and computationally-driven methods, including density functional theory (DFT) calculations, have been used to develop antioxidant inorganic NPs for various biomedical applications. In an early study, a data-informed approach was developed to discover hydrolytic nanozymes. The obtained Ce-FMA-MOF exhibited multiple substrate-cleaving activity (FMA, fumaric acid; MOF, metal-organic framework [330]) and demonstrated applications in biofilm elimination [331]. Recently, genetics-like evolutionary data-driven design of multienzyme-like nanozymes, mimicking SOD and CAT, among others, culminated in creating $CuMnCo_7O_{12}$ NPs (Figure 13) [224]. Machine learning-assisted high-throughput screening of nanozymes conditioned the development of $SrDy_2O_4$ NPs with remarkable ROS-scavenging ability for ulcerative colitis therapy [332]. Antioxidant property, acid stability, and zeta-potential parameters have been analyzed using machine learning, while intestinal barrier repair efficacy and biosafety were processed through high-throughput screening (Figure 14). Application of machine learning allowed for to prediction of the cytotoxicity of (Er,Yb)-doped ZnO NPs, depending on the NPs concentration and cell line type [333]. The extra tree and random forest models were used for this prediction (Figure 15). ChatGPT, combining machine learning, has been used to predict the catalytic activity of nanozymes, including antioxidant ones, endowed with SOD-, CAT-, and GPx-like activities (Figure 16A) [334]. The antioxidant activity of Nd-doped CeO_2 NPs has been elucidated using machine learning, using different techniques [335]. Among them, the random forest model showed the highest accuracy (Figure 16B). Rational design of bienzyme-mimicking (SOD and CAT) N_3S_4 NPs has been conducted using a nine-tier high-throughput screening strategy for inflammatory bowel disease therapy [336]. First-principles DFT calculations have been applied to develop N- and B-doped fullerene, exhibiting pH-switchable catalase-like activity [302]. A similar approach, based on DFT and machine learning, was used to predict 2D nanomaterials with CAT-like activity [337]. Manganese thiophosphite ($MnPS_3$) antioxidant nanozyme, which highly efficiently mimics SOD, was created using machine learning

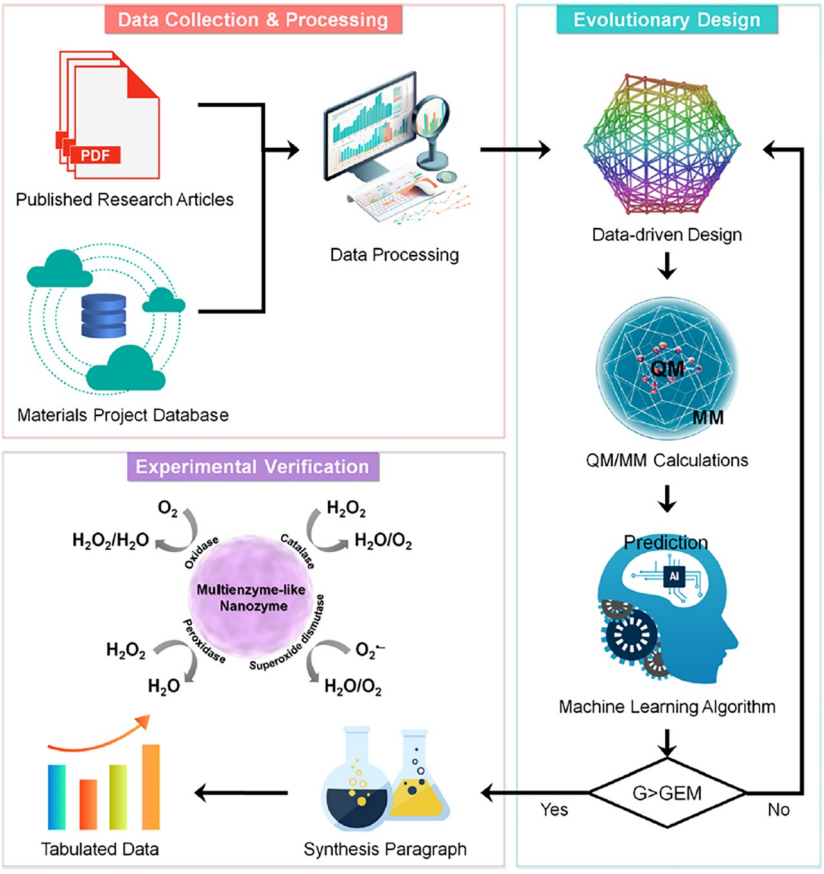

Figure 13 (Color online) Flowchart of the data-driven evolutionary design process for multienzyme-like NPs. Reproduced with permission from Ref. [224]. Copyright©2024, American Chemical Society.

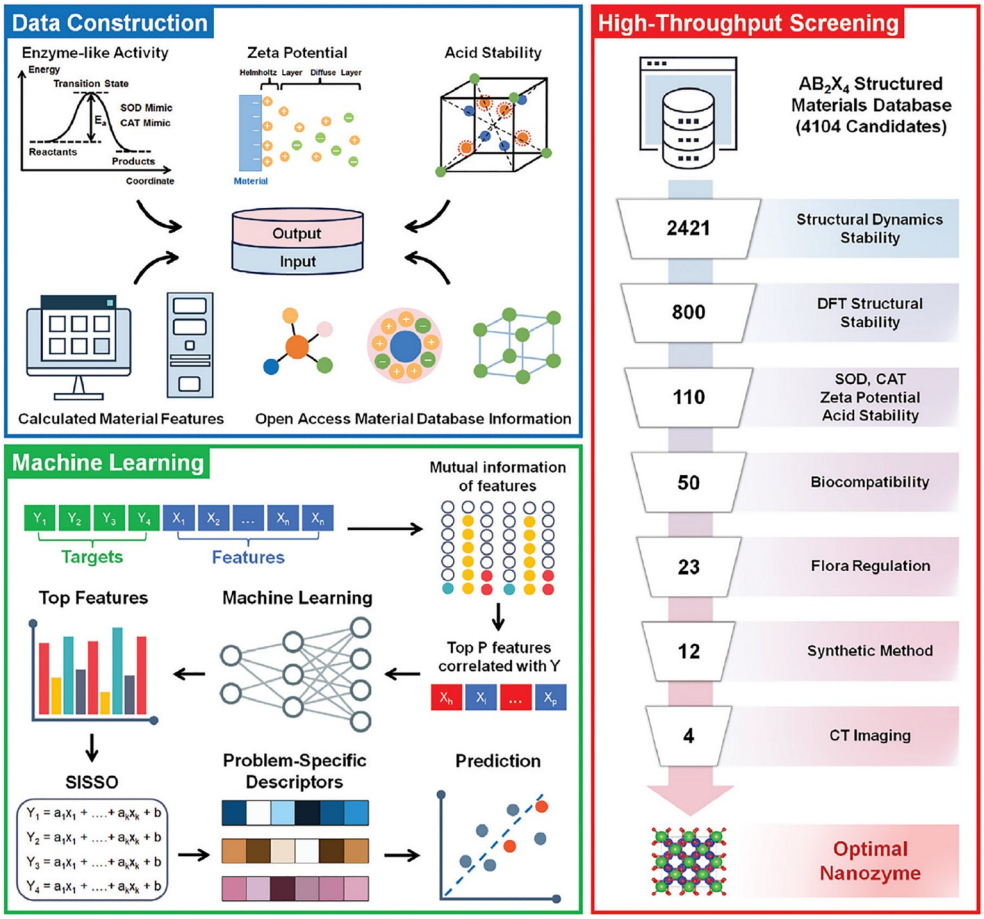

Figure 14 (Color online) Scheme of a rational design process for multi-featured nanozymes in ulcerative colitis therapeutics. Reproduced with permission from Ref. [332]. Copyright©2025, Wiley.

to treat androgenetic alopecia [338]. High-throughput computational screening, based on principles of energy level and adsorption energy, allowed for to computational prediction of NPs with the intrinsic SOD-like activity [339].

6 ADME and toxicity of NPs

6.1 ADME

The physiological journey of nanomaterials or nanomedicines *in vivo* typically encompasses four sequential phases: absorption, distribution, metabolism, and excretion (collectively termed ADME). The ADME profile fundamentally dictates the biomedical efficacy, toxicity profile, and safety parameters of nanomedicines [340,341]. Current technological approaches for ADME investigation can be categorized into three domains: Quantitative analytical techniques, including inductively coupled plasma mass spectrometry (ICP-MS), atomic absorption spectroscopy (AAS), fluorescence spectroscopy, and isotopic tracing; *in vivo* imaging modalities, such as photoacoustic imaging (PAI), bioluminescence/fluorescence imaging, magnetic resonance imaging (MRI), micro-computed tomography (micro-CT), and positron emission tomography/single-photon emission computed tomography (PET/SPECT-CT); chemical imaging and morphological characterization techniques, exemplified by synchrotron radiation imaging and X-ray spectroscopic analysis. While these technologies have proven indispensable in nanomaterial/nanomedicine research [342], they remain constrained by technical limitations including low throughput, labor-intensive workflows, and prohibitive operational costs. The evolution of computational methodologies has catalyzed the integration of AI into biomedical research. Recent years have witnessed growing interest in leveraging AI-driven approaches for ADME prediction [343]. Compared to conventional experimental paradigms, AI algorithms harness unparalleled computational power to achieve transformative improvements in both prediction speed and accuracy.

AI technology, leveraging its efficient data processing, pattern recognition, and predictive capabilities, has established a novel paradigm for nanomaterial ADME research. AI has demonstrated concrete applications across all ADME stages, with predictive dimensions spanning cellular uptake,

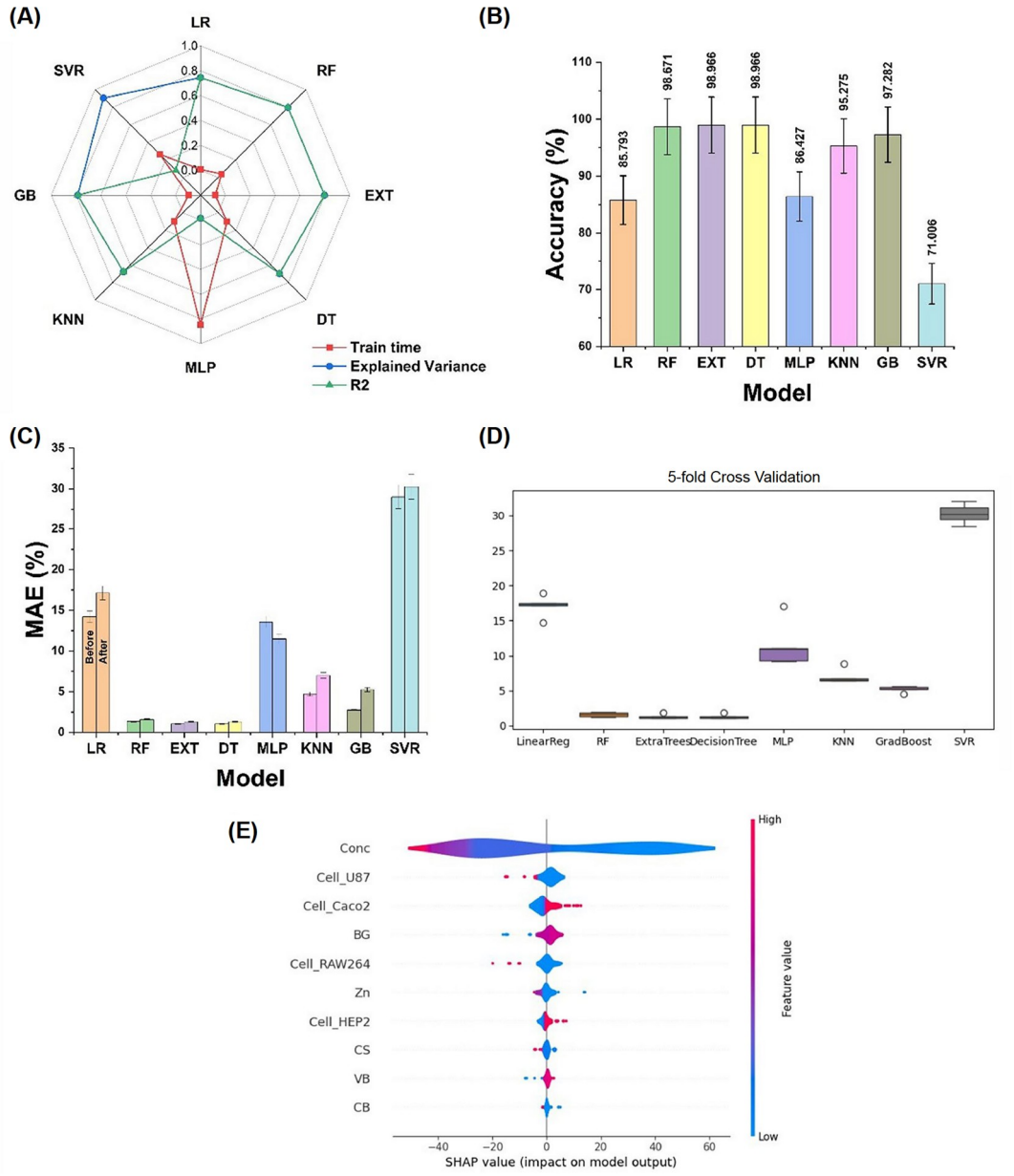

Figure 15 (Color online) (A–E) Overview of the machine learning experiment findings regarding (Er,Yb)-doped ZnO NPs cytotoxicity. Reproduced with permission from Ref. [333]. Copyright©2024, Springer Nature.

biodistribution, pharmacokinetics, and beyond [344,345]. Epa *et al*. [346] employed Bayesian-regularized artificial neural networks (ANNs) to successfully construct a quantitative predictive model for NP cellular uptake. The team compiled experimental data encompassing 50 types of NPs and approximately 3,200 experimental data points, achieving an accurate prediction of NP uptake in the pancreatic cancer cell line PaCa2. Results revealed a remarkable 90% prediction accuracy (Figure 17A). This predictive power facilitates the optimization of nanomedicine design to enhance specific cellular absorption *in vivo*, thereby improving therapeutic efficacy. Despite the 90% accuracy, the black-box nature of ANNs may limit mechanistic interpretability.

Tang *et al*. [347] developed a generative adversarial network for distribution analysis to predict the biodistribution of quantum dots post-intravenous injection. This methodology utilizes a generative-discriminative statistical framework capable of synthesizing new samples sharing key features with training datasets. By training on over 27,000 tumor image patches, the convolutional neural network (CNN)-based model generates QD distribution maps, precisely predicts intratumoral localization relative to vasculature, and employs a discriminator model to distinguish authentic *versus* synthetic images (Figure 17B). This work exemplifies big data generation from limited experimental datasets, advancing tumor-targeted nanomedicine design.

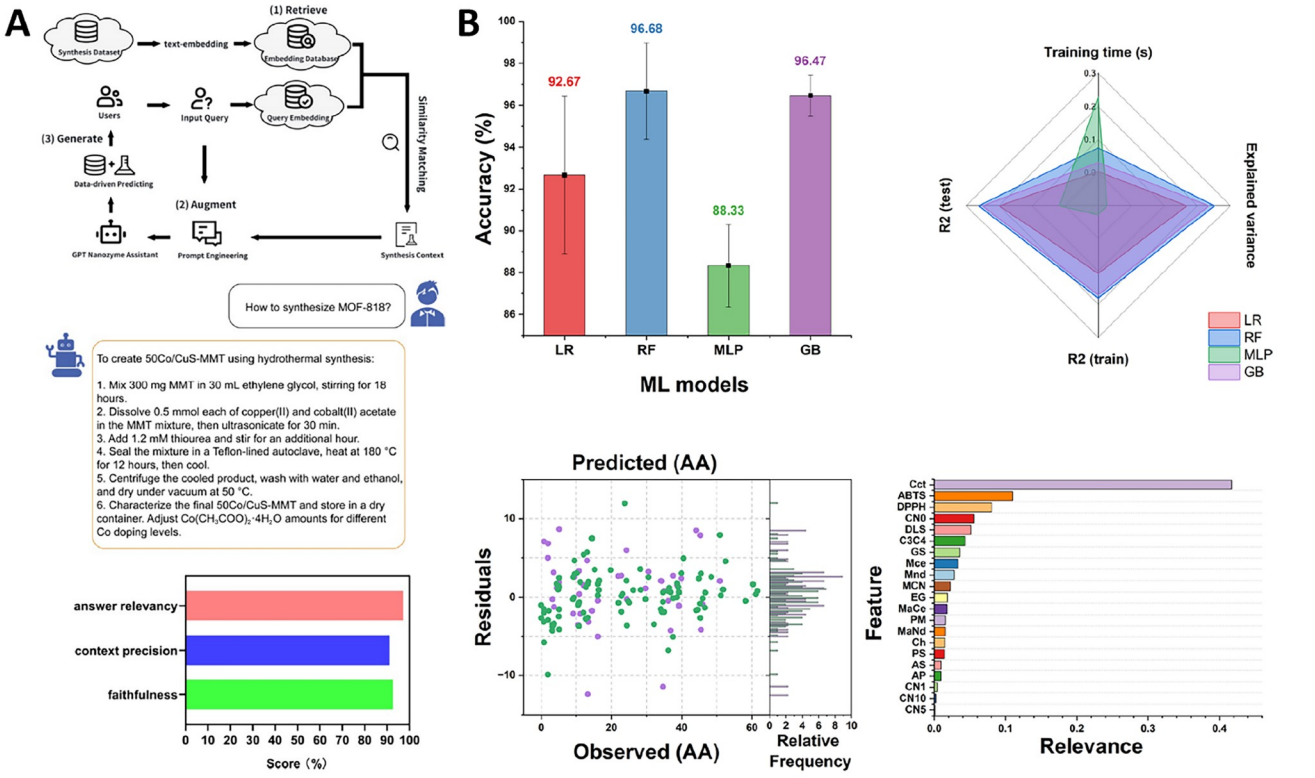

Figure 16 (Color online) (A) Operating principle and performance of ChatGPT-based nanozyme copilot. Reproduced with permission from Ref. [334]. Copyright©2024, American Chemical Society. (B) Results of machine learning modeling of scavenging activity. Reproduced with permission from Ref. [335]. Copyright©2024, Royal Society of Chemistry.

In complex biological fluids (*e.g.*, blood), proteins adsorb onto NP surfaces to form a protein corona, which alters NP physicochemical properties and influences interactions with biological systems, thereby modulating ADME processes. Liu *et al*. [348] devised a predictive model correlating protein corona fingerprints and NP physicochemical properties with cellular association/uptake. They screened 129 quantifiable serum proteins from 785 candidates, defining PCFs by relative abundance. Sequential forward floating selection was applied to identify optimal descriptors from 120 protein corona fingerprints and 19 NP properties. Subsequently, linear regression and nonlinear support vector regression models were developed to establish QSARs. Model validity was confirmed via bootstrapping, while robustness was verified through Y-randomization tests. Descriptor importance was assessed by randomized permutation-induced prediction accuracy decline (Figure 17C). Such models deepen the mechanistic understanding of nanomedicine metabolism.

AI also enables prediction of holistic pharmacokinetic parameters (*e.g.*, half-life, clearance, volume of distribution). Kaminskas *et al*. [349] created dendPoint, an open-access web platform for dendrimer-based therapeutic pharmacokinetic prediction. The platform evaluates dendrimer architectures and predicts parameters via critical scission molecular methodology, including hepatic uptake and urinary excretion. Triazine-cored dendrimers exhibited prolonged half-life and reduced clearance, with significant correlations observed between pharmacokinetic parameters and dendrimer molecular weight/PEGylation (positive for half-life, negative for clearance) (Figure 17D). Principal component analysis further highlighted the predictive dominance of dendrimer/PEG molecular weights and PEG group density (Table 4).

6.2 Toxicity

Unlike conventional materials assessed primarily by chemical composition, dosage, and exposure pathways, NPs demand a multidimensional framework for biological safety evaluation owing to their unique physicochemical attributes. This requires evaluating both inherent characteristics (size, morphology, surface properties, colloidal stability, crystallinity, quantum effects) and external variables (exposure metrics, administration routes, species-specific responses, and organ/cellular targeting interactions) [350].

6.2.1 The influence of surface properties of NPs on biological effects

Surface modifications critically regulate NP behavior, in-

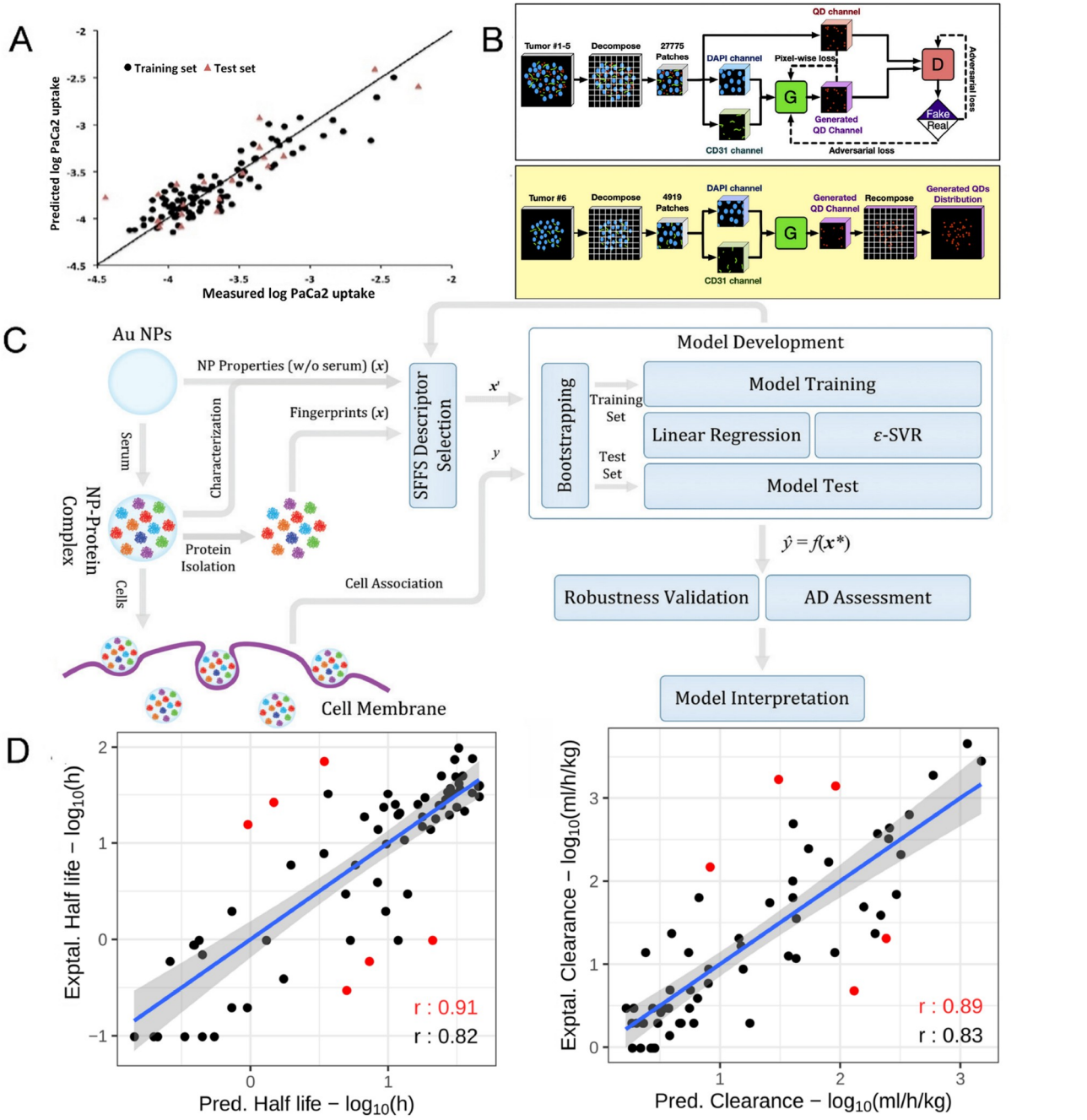

Figure 17 (Color online) Application cases of AI in ADME research. (A) Evaluation of NP uptake models in PaCa2 cells using training set (black circles) and test set (red triangles). Reproduced with permission from Ref. [346]. Copyright©2012, American Chemical Society. (B) Framework of generative adversarial network for distribution analysis (GANDA) during training and testing phases, enabling prediction of intratumoral nanomedicine distribution and vascular proximity assessment. Reproduced with permission from Ref. [347]. Copyright©2021, Elsevier. (C) QSAR development workflow: predictive modeling of NP cellular uptake based on protein corona fingerprints and nanomaterial physicochemical properties. Reproduced with permission from Ref. [348]. Copyright©2015, Royal Society of Chemistry. (D) DendPoint-predicted pharmacokinetic parameters (half-life and clearance rate) for dendrimer-based nanomedicines. Reproduced with permission from Ref. [349]. Copyright©2019, the Author(s).

fluencing cellular uptake, intracellular trafficking, and toxicity profiles. For instance, PDDAC-coated Au nanorods exhibit enhanced endocytosis with minimal cytotoxicity compared to CTAB- or PEI-modified counterparts, while CTAB-functionalized variants selectively localize in cancer cell mitochondria, inducing membrane depolarization, ROS elevation, and apoptosis—contrasting with lysosomal accumulation and safe excretion in normal cells [351,352]. Similarly, amino-modified polystyrene NPs disrupt cell cycle progression (G1 phase delay, cyclin D/E downregulation) and compromise membrane integrity more severely than carboxylated forms [353]. Unmodified graphene activates

Table 4 AI algorithms with demonstrated utility in ADME prediction

Algorithm	Core functionality & domain applications
Linear regression (LR)	Calculates significant interactions between continuous outcomes and data matrix features, applicable for predicting drug solubility, absorption rates, *etc*.
Logistic regression	Evaluates significant interactions between data matrix elements and categorical outcomes, applicable for optimizing molecular feature selection related to drug absorption
Principal component analysis (PCA)	Reduces dimensionality and extracts uncorrelated principal components, applicable for predicting drug absorption, distribution, metabolism, and excretion (ADME) properties
Linear discriminant analysis (LDA)	Identifies category-distinguishing features through data point projection, applicable for dimensionality reduction and classification of nanomedicine data
Support vector machine (SVM)	Separates different categories by finding an optimal hyperplane, advantageous for handling high-dimensional data and small sample sizes
Generative adversarial network (GAN)	Composed of two neural networks: a generator and a discriminator, capable of generating high-quality data through adversarial training
Convolutional neural network (CNN)	Automatically extracts image features through convolutional layers
K-nearest neighbors (KNN)	Predicts target sample categories/values by: Calculating distances to all training samples; Identifying K closest neighbors; Aggregating neighbor labels/values
Random forest	Performs classification/regression through multiple decision trees, reducing overfitting and enhancing generalization capability
Bayesian optimization	Finds global optima with minimal evaluations, applicable for searching optimal molecular descriptors or related parameters

mitochondrial apoptotic pathways via ROS generation and impairs macrophage function through TLR/NF-κB-mediated cytokine release [354,355]. Under light exposure, graphene oxide (GO) generates electron-hole pairs, depletes oxygen content, and amplifies antibacterial activity through redox-driven oxidative stress and antioxidant system disruption [356].

Once NPs enter the body, they inevitably encounter biomacromolecules, particularly proteins and interact with them with different mechanisms (Figure 18). Given the dynamic nature of various biological barriers, these NPs undergo continuous transformations throughout their journey, from initial bio-integration to eventual clearance. Currently, most studies in the field have focused on characterizing the dynamics, composition, and abundance of the protein corona that forms around NPs, as well as the acquired biological identity of these NPs. These factors significantly impact their recognition and distribution both *in vitro* and *in vivo*. In contrast, research on how the inherent chemical properties of NPs interact with the biotransformation of the NP-protein corona—and the holistic effects of these interactions on homeostasis and disease pathologies—has been surprisingly lacking. This is despite the fact that most NPs are functionalized with surface chemistry prior to their biomedical applications.

A series of studies have been conducted to advance the understanding of local and distal effects of NPs in hosts, focusing on their transportation and biotransformation from the perspective of the protein corona. For instance, Chen and colleagues [357] discovered that apolipoprotein E (ApoE), a key component of the protein corona, mediated the transport of molybdenum disulfide (MoS_2) NPs to the liver. There, the NPs underwent transformation, with molybdenum being incorporated into molybdenum enzymes and affecting their specific activities. This was achieved using *in situ* and highly sensitive techniques based on the synchrotron radiation facility. This finding revealed a protein corona-mediated chain of transport, transformation, and bioavailability for MoS_2

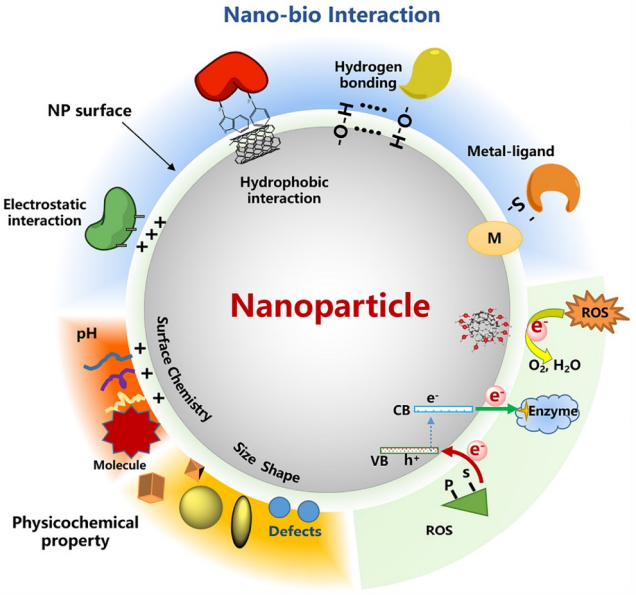

Figure 18 (Color online) NPs encounter several interactions in the presence of biomolecules, including electrostatic interaction, hydrogen bonding, hydrophobic interaction, ligand-receptor interaction, stereoselective interaction, coordination and membrane curvature effects.

in vivo. In other work, they demonstrated the feasibility of manipulating the ApoA-I protein corona *in vivo* to mitigate cardiovascular damage caused by silica NPs [358]. They also identified the crucial roles of intracellular coronal proteins, particularly STAT3 and C1q adsorbed on carbon NMs (graphdiyne oxide and Gd@$C_{82}(OH)_{22}$), This facilitated cancer immunotherapy *in vivo* [359,360]. Additionally, they showed that carbon nanotubes promoted breast cancer metastasis, with effects extending beyond local pulmonary pathologies to influence distal tissues [361]. These findings have unveiled a range of previously unknown behaviors governed by the acquired protein corona and their associated local and remote effects, significantly contributing to the field of nanosafety.

6.2.2 The influence of the size of NPs on biological effects

The size of NPs significantly impacts their biological effects and toxicity. For instance, the toxicity of carbon nanotubes (CNTs) is closely related to their length. Short multi-walled carbon nanotubes (MWNTs; 0.5–2 μm) promote endocytosis and cell efflorescence, enhance nerve growth factor signaling, and support neural cell differentiation without toxicity [362]. In contrast, longer CNTs (20–50 μm) induce alveolar macrophages to secrete TGF-β, stimulating fibroblast proliferation and collagen secretion, thereby causing pulmonary fibrosis. The TGF-β/Smad2/Collagen III signaling pathway is critical in this fibrotic process [363]. Additionally, long CNTs cannot be fully phagocytosed by macrophages and directly interact with fibroblasts and alveolar epithelial cells, activating fibroblasts and inducing myofibroblast differentiation and epithelial-mesenchymal transition via the TGF-β/Smad2 pathway [364]. Furthermore, cells can internalize larger particles (>5 μm) through phagocytosis and micropinocytosis, while submicron-sized particles enter cells via receptor-mediated endocytosis, depending on receptor type and particle size [365].

6.2.3 Other physicochemical factors affecting the biological effects of NPs

NP toxicity is critically influenced by structural parameters and degradation dynamics [366]. For instance, shape-dependent cellular uptake is exemplified by gold NPs in MCF-7 breast cancer cells, where increased aspect ratios correlate with reduced internalization [352]. Crystal plane engineering further modulates biological interactions: noble metal nanostructures with high surface energy facets (*e.g.*, cubic configurations) exhibit enhanced enzyme-mimetic activity compared to low-energy forms (*e.g.*, octahedrons), directly impacting antimicrobial efficacy. Notably, Gram-negative bacteria demonstrate crystal plane-selective accumulation of palladium NPs due to unimpeded membrane penetration, whereas Gram-positive counterparts show no such discrimination [365].

In addition, degradation pathways also determine NP biological fate and toxicity endpoints. For example, hepatic biotransformation of MoS_2@HSA nanocomplexes involves Mo(IV)-to-Mo(VI) oxidation, integrating molybdenum into metabolic enzymes to modulate hepatic activity [357]. Silver NPs undergo lipid raft-mediated endocytosis followed by oxidative dissolution to Ag^+, which binds sulfhydryl groups to induce cytotoxicity via oxidative stress—a process mitigated by surface modification or NAC chelation [367,368]. Interestingly, the products of carbon-based NP degradation and transformation mediated by gut microbiota or lipase affect the function of intestinal stem cells or directly elicit inflammation [369,370]. In contrast, gold nanorods demonstrate exceptional *in vivo* stability without degradation [371].

6.2.4 The use of artificial intelligence in nanotoxicity research

For the nanotoxicology research, the application of AI provides new ideas for addressing the challenges posed by large-scale data [372]. AI technology can transform vast amounts of nanotoxicity data into key information by constructing quantitative structure-toxicity relationships of NPs, thereby revealing the molecular mechanisms related to toxicity. For example, the team led by Yan *et al*. [373] successfully converted nanotoxicity data into information using AI and molecular simulations, offering new methods for nanotoxicology research. Additionally, AI is employed to develop predictive models for nanotoxicity. By analyzing the relationship between the physicochemical properties of NPs and their toxicity through machine learning algorithms, these models can predict the potential adverse effects of new NPs. Such AI-based predictive models not only enhance research efficiency but also reduce the reliance on animal experiments. In the future, with the development of high-quality nanotoxicity databases and more powerful nanodescriptors, AI is expected to play an even greater role in the field of nanotoxicology.

7 Summary, challenges and future perspective

Nanomedicine has emerged as a pivotal and dynamically evolving frontier in contemporary medical research, distinguished by its engineered nanoplatforms that enable unprecedented integration of cross-disciplinary knowledge and cutting-edge technologies. These sophisticated systems are revolutionizing therapeutic paradigms through innovative approaches to disease diagnosis, prognostic evaluation, and targeted treatment modalities. Nevertheless, the very interdisciplinary nature that empowers nanomedicine's transformative potential simultaneously introduces formidable scientific challenges. The necessity to reconcile molecular-scale design principles with macroscopic therapeutic out-

comes, optimize multifactorial nanoparticle synthesis parameters, and decipher complex nano-bio interactions across multiple biological scales creates substantial barriers to translational progress. These intrinsic complexities not only elevate the intellectual and technical demands of nanomedicine research but also inevitably extend development timelines from laboratory discovery to clinical implementation.

Artificial intelligence (AI), as a transformative technological paradigm of the new century, has fundamentally reshaped the landscape of scientific inquiry, with nanomedicine emerging as one of its most promising beneficiaries. The synergistic integration of AI is currently revolutionizing nanomedicine research methodologies while simultaneously unlocking unprecedented opportunities for therapeutic innovation. Over the past five years, AI applications have proliferated across critical nanomedicine subdomains, including intelligent nanobiosensors for precision diagnostics, AI-optimized nanocarriers for targeted drug delivery, machine learning-guided adjuvant therapy systems, and predictive computational models for nanosafety evaluation. While this review examines recent advancements in these areas, it must be acknowledged that the AI-nanomedicine convergence remains at a relatively nascent stage, presenting both formidable challenges and extraordinary potential for pioneering researchers. List below is the key challenges and emerging solutions.

(1) Data scarcity and heterogeneity. The integration of AI with nanomedicine primarily relies on AI methodologies to construct mathematical models from existing datasets, enabling prospective prediction of biomedical functionalities for nanodrugs. This paradigm accelerates the entire development pipeline—from rational design and synthesis optimization to precision clinical translation. Crucially, as a data-dependent methodology, AI demands exceptionally high standards of data integrity and standardization. However, when investigating novel nanotherapeutic entities, researchers confront a fundamental dilemma: The high-dimensional parameter space requiring optimization frequently exceeds the available experimental or clinical data volume. This data scarcity bottleneck severely constrains AI's capacity to generate robust predictive models, rendering comprehensive optimization of multivariate interactions computationally intractable. To address the challenge of data scarcity and heterogeneity in nanomedicine AI research, a multifaceted strategy must be implemented to expand data resources and enhance data utilization efficiency. This integrated approach encompasses three critical dimensions: historical knowledge mining, high-throughput computational simulation, and automated experimental data acquisition, which will be discussed in detail below. The synergistic implementation of these data-acquisition methodologies will establish a multidimensional data ecosystem, effectively overcoming current limitations in data volume, diversity, and interoperability—ultimately enabling robust AI models for predictive nanomedicine.

(2) Complexity in quality control. Nanomedicine formulations are intrinsically complex, characterized by multicomponent chemical compositions rather than pure single entities. This complexity presents substantial challenges for rigorous quality control during manufacturing, significantly complicating both synthesis and characterization processes. To overcome these barriers, the establishment of a systematic classification framework based on chemical composition and fabrication strategies is paramount. Such a framework is the essential foundation for developing modular, high-throughput manufacturing pipelines and automated characterization protocols, enabled by robotics and intelligent algorithms. This rational classification and the resulting automated processes are critical prerequisites for building robust databases of nanomedicine properties. Ultimately, this integrated approach enables a reverse-engineering paradigm, where nanomedicines are precisely engineered to meet predefined physicochemical properties, thereby facilitating targeted therapeutic applications.

(3) Prolonged safety and efficacy evaluation cycle. A critical bottleneck in AI-driven nanomedicine development is the extended timeframe required for safety and efficacy assessment. Conventional preclinical evaluation, heavily reliant on complex and time-consuming animal studies, generates critical data at a pace far too slow for effective AI model training. This data scarcity and latency severely hinder the iterative refinement of AI algorithms, limiting their predictive power and delaying the translation of promising nanomedicine candidates. To overcome this fundamental constraint, innovative *in vitro* models, particularly patient-derived organoids and organ-on-a-chip systems, offer a transformative potential. These sophisticated platforms recapitulate key aspects of human tissue architecture and function, enabling higher-throughput, more physiologically relevant screening of nanomedicine interactions. By generating rich, human-relevant datasets faster and more ethically than traditional animal models, these technologies can significantly shorten the evaluation cycle. This acceleration is crucial for feeding timely, high-quality data into AI training pipelines, ultimately enabling more robust model development, faster lead optimization, and a more efficient path towards clinically viable nanomedicines.

(4) Lack of interpretability and transferability. A significant limitation of current AI models in nanomedicine lies in their inherent "black-box" nature, which obscures the underlying physical and chemical mechanisms governing nanomaterial behavior. This lack of interpretability severely compromises model transferability and reuse across different nanoparticle types or biological contexts, hindering broader applicability. To tackle this challenge, the synergistic

integration of AI with accelerated molecular simulations presents a transformative path. By embedding classical physics-based theories and multiscale modeling frameworks within AI architectures, this approach can generate mechanistically interpretable descriptors that reflect fundamental interactions. This fusion not only enhances the predictive power and efficiency of simulations but is paramount for developing causally rooted, generalizable AI models that elucidate the governing principles of nanomedicine performance, enabling rational design and reliable extrapolation.

(5) Cross-modal data integration for disease-specific design. To realize predictive and rational design of nanocarriers tailored to specific disease models such as tumors, it is essential to integrate heterogeneous data across experimental characterization, molecular simulation, and therapeutic application using artificial intelligence. We propose a cross-modal, AI-driven framework composed of four key components. First, establish a unified and standardized database architecture that encodes nanomaterial physicochemical properties, biological interactions, and disease-model performance, enabling consistent cross-study data integration. Second, apply high-throughput molecular simulations (*e.g.*, MD, DFT, coarse-grained models) to generate mechanism-based descriptors that reflect nanocarrier behavior at molecular and cellular interfaces. Third, employ machine learning frameworks—such as graph neural networks and multimodal fusion architectures—that fuse these multiscale datasets, while embedding disease-specific constraints (*e.g.*, tumor targeting, EPR effect, immune modulation) to guide design. Finally, implement a closed-loop optimization system where AI-generated candidates are rapidly validated using organ-on-chip or *in vitro* tumor models, and new data are fed back into the model to enhance its performance. This integrative strategy transforms fragmented information into a cohesive and interpretable pipeline, enabling the construction of high-performance nanocarriers that are both biologically effective and clinically translatable.

While the fusion of AI and nanomedicine faces the substantial challenges outlined above, and will inevitably encounter further domain-specific hurdles as research advances into novel applications, the trajectory is clear. Continued advances in addressing data limitations, automating complex workflows, accelerating biological evaluation, and improving model interpretability are not just incremental steps—they have the potential to drive a fundamental shift in nanomedicine development. Crucially, this transformation hinges on the availability of high-quality, reproducible experimental data. Without reliable data, AI models are prone to being misled, leading to inaccurate predictions and suboptimal outcomes that may impede, rather than advance, progress in the field. The synergistic resolution of these challenges will empower the precise, AI-driven engineering of next-generation nanotherapeutics, fundamentally accelerating their path from conceptual design to clinical realization and ultimately enabling unprecedented levels of personalized and effective therapies.

Acknowledgements This work was supported by the Basic Science Center Project of the National Natural Science Foundation of China (22388101), the National Key Research and Development Program of China (2022YFA1207300), the National Natural Science Foundation of China (82204300, 32271452, 52425306, 22374071) and the State Key Laboratory of Analytical Chemistry for Life Science (5431ZZXM2501).

Conflict of interest The authors declare no conflict of interest.

Supporting information The supporting information is available online at http://chem.scichina.com and http://link.springer.com/journal/11426. The supporting materials are published as submitted, without typesetting or editing. The responsibility for scientific accuracy and content remains entirely with the authors.

1 Drexler KE, Peterson C, Pergamit G. *Unbounding the Future: The Nanotechnology Revolution*. New York: William Morrow & Company, 1991
2 Freitas Jr RA. *Nanomed-Nanotechnol Biol Med*, 2005, 1: 2–9
3 Kurul F, Turkmen H, Cetin AE, Topkaya SN. *Next Nanotechnol*, 2025, 7: 100129
4 Ge K, Chen G, Zhang D, Hao J, Li Y. *Angew Chem Int Ed*, 2024, 63: e202411956
5 Mao F, Su Y, Sun X, Li B, Liu PF. *ACS Omega*, 2023, 8: 2733–2739
6 Hao JN, Ge K, Chen G, Dai B, Li Y. *Chem Soc Rev*, 2023, 52: 7707–7736
7 Shi J, Kantoff PW, Wooster R, Farokhzad OC. *Nat Rev Cancer*, 2017, 17: 20–37
8 Szabó GT, Mahiny AJ, Vlatkovic I. *Mol Ther*, 2022, 30: 1850–1868
9 Karikó K, Buckstein M, Ni H, Weissman D. *Immunity*, 2005, 23: 165–175
10 Karikó K, Muramatsu H, Welsh FA, Ludwig J, Kato H, Akira S, Weissman D. *Mol Ther*, 2008, 16: 1833–1840
11 Anderson BR, Muramatsu H, Nallagatla SR, Bevilacqua PC, Sansing LH, Weissman D, Karikó K. *Nucleic Acids Res*, 2010, 38: 5884–5892
12 Wilhelm S, Tavares AJ, Dai Q, Ohta S, Audet J, Dvorak HF, Chan WCW. *Nat Rev Mater*, 2016, 1: 16014
13 Blanco E, Shen H, Ferrari M. *Nat Biotechnol*, 2015, 33: 941–951
14 Liu H, Ji M, Qin Y, Sun Y, Wang H, Xiao P, Zhao J, Deng Y, Zhang Z, Gou J, Yin T, He H, Chen G, Tang X, Zhang Y. *Nano Today*, 2024, 55: 102201
15 Ciccotti G, Dellago C, Ferrario M, Hernández ER, Tuckerman ME. *Eur Phys J B*, 2022, 95: 3
16 Kong S, Zhu K, Wen C, Li Y, Wu F, Yu J, Chang X. *Sci China Chem*, 2025, 68: 3484–3491
17 Schneider P, Walters WP, Plowright AT, Sieroka N, Listgarten J, Goodnow Jr. RA, Fisher J, Jansen JM, Duca JS, Rush TS, Zentgraf M, Hill JE, Krutoholow E, Kohler M, Blaney J, Funatsu K, Luebkemann C, Schneider G. *Nat Rev Drug Discov*, 2020, 19: 353–364
18 Hong X, Yang Q, Liao K, Pei J, Chen M, Mo F, Lu H, Zhang WB, Zhou H, Chen J, Su L, Zhang SQ, Liu S, Huang X, Sun YZ, Wang Y, Zhang Z, Yu Z, Luo S, Fu XF, You SL. *Sci China Chem*, 2024, 67: 2461–2496
19 Raffel C, Shazeer N, Roberts A, Lee K, Narang S, Matena M, Zhou Y, Li W, Liu PJ. *J Mach Learn Res*, 2020, 21: 1–67
20 Zhang Z, Gu Y, Han X, Chen S, Xiao C, Sun Z, Yao Y, Qi F, Guan J, Ke P. arXiv: 2106.10715
21 Wang Y, Zou Y, Li Z. *Nano Today*, 2024, 59: 102544
22 Zhou Y, Zhao J, Chen R, Lu P, Zhao W, Ma R, Xiao T, Dong Y,

Zheng W, Huang X, Tang BZ, Chen Y. *Nano Today*, 2024, 56: 102238
23 Li Y, Liu Z, Zheng Z, Bai L, Wang W, Min L, Hu H, Shi Y. *Nano Today*, 2025, 64: 102817
24 Adir O, Poley M, Chen G, Froim S, Krinsky N, Shklover J, Shainsky-Roitman J, Lammers T, Schroeder A. *Adv Mater*, 2020, 32: e1901989
25 Serov N, Vinogradov V. *Adv Drug Deliver Rev*, 2022, 184: 114194
26 Wilkinson MD, Dumontier M, Aalbersberg IJ, Appleton G, Axton M, Baak A, Blomberg N, Boiten JW, da Silva Santos LB, Bourne PE, Bouwman J, Brookes AJ, Clark T, Crosas M, Dillo I, Dumon O, Edmunds S, Evelo CT, Finkers R, Gonzalez-Beltran A, Gray AJG, Groth P, Goble C, Grethe JS, Heringa J, 't Hoen PAC, Hooft R, Kuhn T, Kok R, Kok J, Lusher SJ, Martone ME, Mons A, Packer AL, Persson B, Rocca-Serra P, Roos M, van Schaik R, Sansone SA, Schultes E, Sengstag T, Slater T, Strawn G, Swertz MA, Thompson M, van der Lei J, van Mulligen E, Velterop J, Waagmeester A, Wittenburg P, Wolstencroft K, Zhao J, Mons B. *Sci Data*, 2016, 3: 160018
27 Zhang X, Wang L, Helwig J, Luo Y, Fu C, Xie Y, Liu M, Lin Y, Xu Z, Yan K. arXiv: 2307.08423
28 Wan K, He J, Shi X. *Adv Mater*, 2024, 36: 2305758
29 Radford A, Narasimhan K. Improving language understanding by generative pre-training. 2018
30 Liu Z, Zhang W, Xia Y, Wu L, Xie S, Qin T, Zhang M, Liu T-Y. arXiv: 2305.10688
31 Devlin J, Chang M-W, Lee K, Toutanova K. arXiv: 1810.04805
32 Zeng Z, Yao Y, Liu Z, Sun M. *Nat Commun*, 2022, 13: 862
33 https://crfm.stanford.edu/2022/12/15/biomedlm.html
34 Singhal K, Tu T, Gottweis J, Sayres R, Wulczyn E, Amin M, Hou L, Clark K, Pfohl SR, Cole-Lewis H, Neal D, Rashid QM, Schaekermann M, Wang A, Dash D, Chen JH, Shah NH, Lachgar S, Mansfield PA, Prakash S, Green B, Dominowska E, Agüera y Arcas B, Tomašev N, Liu Y, Wong R, Semturs C, Mahdavi SS, Barral JK, Webster DR, Corrado GS, Matias Y, Azizi S, Karthikesalingam A, Natarajan V. *Nat Med*, 2025, 31: 943–950
35 Radford A, Wu J, Child R, Luan D, Amodei D, Sutskever I. *OpenAI Blog*, 2019, 1: 9
36 Chowdhery A, Narang S, Devlin J, Bosma M, Mishra G, Roberts A, Barham P, Chung HW, Sutton C, Gehrmann S. *J Mach Learn Res*, 2023, 24: 1–113
37 Liang Y, Zhang R, Zhang L, Xie P. arXiv: 2309.03907
38 Wang L, Gao Y, Chen X, Cui W, Zhou Y, Luo X, Xu S, Du Y, Wang B. *Sci Data*, 2023, 10: 175
39 Antunes LM, Butler KT, Grau-Crespo R. *Nat Commun*, 2024, 15: 1–6
40 Rubungo AN, Arnold C, Rand BP, Dieng AB. arXiv: 2310.14029
41 Nie Z, Liu Y, Yang L, Li S, Pan F. *Adv Energy Mater*, 2021, 11: 2003580
42 Nie Z, Zheng S, Liu Y, Chen Z, Li S, Lei K, Pan F. *Adv Funct Mater*, 2022, 32: 2201437
43 Dong WH, Zhang YY, Zhang YF, Sun JT, Liu F, Du S. *npj Comput Mater*, 2022, 8: 185
44 Ban Z, Yuan P, Yu F, Peng T, Zhou Q, Hu X. *Proc Natl Acad Sci USA*, 2020, 117: 10492–10499
45 Yu F, Wei C, Deng P, Peng T, Hu X. *Sci Adv*, 2021, 7: eabf4130
46 Boiko DA, MacKnight R, Kline B, Gomes G. *Nature*, 2023, 624: 570–578
47 Zhu Q, Zhang F, Huang Y, Xiao H, Zhao LY, Zhang XC, Song T, Tang XS, Li X, He G, Chong BC, Zhou JY, Zhang YH, Zhang B, Cao JQ, Luo M, Wang S, Ye GL, Zhang WJ, Chen X, Cong S, Zhou D, Li H, Li J, Zou G, Shang WW, Jiang J, Luo Y. *Natl Sci Rev*, 2022, 9: nwac190
48 Hegde VI, Borg CKH, del Rosario Z, Kim Y, Hutchinson M, Antono E, Ling J, Saxe P, Saal JE, Meredig B. *Phys Rev Mater*, 2023, 7: 053805
49 Axelrod S, Gómez-Bombarelli R. *Sci Data*, 2022, 9: 185
50 https://www.rdkit.org
51 Neese F. *Wires Comput Mol Sci*, 2012, 2: 73–78
52 Grimme S. *J Chem Theor Comput*, 2019, 15: 2847–2862
53 Okabe S, Ye S, Lan X, Nukada K, Zhang H, Kobayashi K, Oshiki M. *ISME Commun*, 2023, 3: 45
54 Petretto G, Dwaraknath S, Miranda PCH, Winston D, Giantomassi M, van Setten MJ, Gonze X, Persson KA, Hautier G, Rignanese GM. *Sci Data*, 2018, 5: 1–2
55 Xie F, Lu T, Meng S, Liu M. *Sci Bull*, 2024, 69: 3525–3532
56 Corso G, Stark H, Jegelka S, Jaakkola T, Barzilay R. *Nat Rev Methods Primers*, 2024, 4: 17
57 Veličković P. *Curr Opin Struct Biol*, 2023, 79: 102538
58 Rettie SA, Campbell KV, Bera AK, Kang A, Kozlov S, De La Cruz J, Adebomi V, Zhou G, DiMaio F, Ovchinnikov S, Bhardwaj G. *bioRxiv*, 2023, doi: 10.1101/2023.02.25.529956
59 Feng S, Chen Z, Zhang C, Xie Y, Ovchinnikov S, Gao YQ, Liu S. *Nat Mach Intell*, 2024, 6: 924–935
60 Xiao H, Li R, Shi X, Chen Y, Zhu L, Chen X, Wang L. *Nat Commun*, 2023, 14: 7027
61 Abramson J, Adler J, Dunger J, Evans R, Green T, Pritzel A, Ronneberger O, Willmore L, Ballard AJ, Bambrick J, Bodenstein SW, Evans DA, Hung CC, O'Neill M, Reiman D, Tunyasuvunakool K, Wu Z, Žemgulytė A, Arvaniti E, Beattie C, Bertolli O, Bridgland A, Cherepanov A, Congreve M, Cowen-Rivers AI, Cowie A, Figurnov M, Fuchs FB, Gladman H, Jain R, Khan YA, Low CMR, Perlin K, Potapenko A, Savy P, Singh S, Stecula A, Thillaisundaram A, Tong C, Yakneen S, Zhong ED, Zielinski M, Žídek A, Bapst V, Kohli P, Jaderberg M, Hassabis D, Jumper JM. *Nature*, 2024, 630: 493–500
62 Rouse I, Power D, Subbotina J, Lobaskin V. *J Chem Inf Model*, 2024, 64: 7525–7543
63 Tubiana J, Schneidman-Duhovny D, Wolfson HJ. *Nat Methods*, 2022, 19: 730–739
64 Wang Y, Li S, He X, Li M, Wang Z, Zheng N, Shao B, Liu T-Y, Wang T. arXiv: 2210.16518
65 Miao S, Luo Y, Liu M, Li P. arXiv: 2210.16966
66 Crabbé J, van der Schaar M. *Adv Neural Inf Process Syst*, 2023, 36: 71393–71429
67 Song X, Song Y, Lin M, Wang M, Jia T, Jin J, Sun J, Duan G, Gao X, Jiang S, Chen F, Gu N, Guo D. *Nano Today*, 2025, 64: 102774
68 Gao Z, Lu Z, Zhao S, You J, Wang J, Gao S, Zhang W, Cai R, Wang S, Wu Y, Wang Z, Li J, Bao Y, Han Q, Xianyu Y, Yu J, Gu Z, Zhang Y. *Nano Today*, 2025, 64: 102777
69 Liu L, Feng X, Zhao J, Li D, Yu F. *Nano Today*, 2025, 62: 102700
70 Kwong GA, Ghosh S, Gamboa L, Patriotis C, Srivastava S, Bhatia SN. *Nat Rev Cancer*, 2021, 21: 655–668
71 Chen L, Zhao L, Wang Z, Liu S, Pang D. *Small*, 2022, 18: 2104567
72 Hong G, Antaris AL, Dai H. *Nat Biomed Eng*, 2017, 1: 0010
73 Fang Z, Wang C, Yang J, Song Z, Xie C, Ji Y, Wang Z, Du X, Zheng Q, Chen C, Hu Z, Zhong Y. *Nat Nanotechnol*, 2024, 19: 124–130
74 Shen D, Wu G, Suk HI. *Annu Rev Biomed Eng*, 2017, 19: 221–248
75 Rao VM, Hla M, Moor M, Adithan S, Kwak S, Topol EJ, Rajpurkar P. *Nature*, 2025, 639: 888–896
76 Shmatko A, Ghaffari Laleh N, Gerstung M, Kather JN. *Nat Cancer*, 2022, 3: 1026–1038
77 Oumano M, Yu H. *Physica Medica*, 2021, 87: 83–89
78 Gleich B, Weizenecker J. *Nature*, 2005, 435: 1214–1217
79 Nigam S, Gjelaj E, Wang R, Wei G, Wang P. *Magn Reson Imag*, 2025, 61: 42–51
80 Tomitaka A, Vashist A, Kolishetti N, Nair M. *Nanoscale Adv*, 2023, 5: 4354–4367
81 Qian X, Pei J, Han C, Liang Z, Zhang G, Chen N, Zheng W, Meng F, Yu D, Chen Y, Sun Y, Zhang H, Qian W, Wang X, Er Z, Hu C, Zheng H, Shen D. *Nat Biomed Eng*, 2025, 9: 356–370
82 Ma Z, Wang F, Wang W, Zhong Y, Dai H. *Proc Natl Acad Sci USA*, 2021, 118: e2021446118
83 Bouchard C, Wiesner T, Deschênes A, Bilodeau A, Turcotte B, Gagné C, Lavoie-Cardinal F. *Nat Mach Intell*, 2023, 5: 830–844

84 Mangalwedhekar R, Singh N, Thakur CS, Seelamantula CS, Jose M, Nair D. *Nat Nanotechnol*, 2023, 18: 380–389
85 Kim M, Chen C, Wang P, Mulvey JJ, Yang Y, Wun C, Antman-Passig M, Luo HB, Cho S, Long-Roche K, Ramanathan LV, Jagota A, Zheng M, Wang YH, Heller DA. *Nat Biomed Eng*, 2022, 6: 267–275
86 Whitesides GM. *Nature*, 2006, 442: 368–373
87 Stern E, Vacic A, Rajan NK, Criscione JM, Park J, Ilic BR, Mooney DJ, Reed MA, Fahmy TM. *Nat Nanotech*, 2010, 5: 138–142
88 AbdElFatah T, Jalali M, Yedire SG, I. Hosseini I, del Real Mata C, Khan H, Hamidi SV, Jeanne O, Siavash Moakhar R, McLean M, Patel D, Wang Z, McKay G, Yousefi M, Nguyen D, Vidal SM, Liang C, Mahshid S. *Nat Nanotechnol*, 2023, 18: 922–932
89 Yang Y, Song Y, Bo X, Min J, Pak OS, Zhu L, Wang M, Tu J, Kogan A, Zhang H, Hsiai TK, Li Z, Gao W. *Nat Biotechnol*, 2020, 38: 217–224
90 Liu C, Zhao J, Tian F, Cai L, Zhang W, Feng Q, Chang J, Wan F, Yang Y, Dai B, Cong Y, Ding B, Sun J, Tan W. *Nat Biomed Eng*, 2019, 3: 183–193
91 Nitta N, Sugimura T, Isozaki A, Mikami H, Hiraki K, Sakuma S, Iino T, Arai F, Endo T, Fujiwaki Y, Fukuzawa H, Hase M, Hayakawa T, Hiramatsu K, Hoshino Y, Inaba M, Ito T, Karakawa H, Kasai Y, Koizumi K, Lee SW, Lei C, Li M, Maeno T, Matsusaka S, Murakami D, Nakagawa A, Oguchi Y, Oikawa M, Ota T, Shiba K, Shintaku H, Shirasaki Y, Suga K, Suzuki Y, Suzuki N, Tanaka Y, Tezuka H, Toyokawa C, Yalikun Y, Yamada M, Yamagishi M, Yamano T, Yasumoto A, Yatomi Y, Yazawa M, Di Carlo D, Hosokawa Y, Uemura S, Ozeki Y, Goda K. *Cell*, 2018, 175: 266–276.e13
92 Suzuki Y, Kobayashi K, Wakisaka Y, Deng D, Tanaka S, Huang CJ, Lei C, Sun CW, Liu H, Fujiwaki Y, Lee S, Isozaki A, Kasai Y, Hayakawa T, Sakuma S, Arai F, Koizumi K, Tezuka H, Inaba M, Hiraki K, Ito T, Hase M, Matsusaka S, Shiba K, Suga K, Nishikawa M, Jona M, Yatomi Y, Yalikun Y, Tanaka Y, Sugimura T, Nitta N, Goda K, Ozeki Y. *Proc Natl Acad Sci USA*, 2019, 116: 15842–15848
93 Yoon J, Jo YJ, Kim M, Kim K, Lee SY, Kang SJ, Park YK. *Sci Rep*, 2017, 7: 6654
94 Lamanna J, Scott EY, Edwards HS, Chamberlain MD, Dryden MDM, Peng J, Mair B, Lee A, Chan C, Sklavounos AA, Heffernan A, Abbas F, Lam C, Olson ME, Moffat J, Wheeler AR. *Nat Commun*, 2020, 11: 5632
95 Soteriou D, Kubánková M, Schweitzer C, López-Posadas R, Pradhan R, Thoma OM, Györfi AH, Matei AE, Waldner M, Distler JHW, Scheuermann S, Langejürgen J, Eckstein M, Schneider-Stock R, Atreya R, Neurath MF, Hartmann A, Guck J. *Nat Biomed Eng*, 2023, 7: 1392–1403
96 Chong LH, Ching T, Farm HJ, Grenci G, Chiam KH, Toh YC. *Lab Chip*, 2022, 22: 1890–1904
97 Paek K, Kim S, Tak S, Kim MK, Park J, Chung S, Park TH, Kim JA. *Bioeng Transla Med*, 2023, 8: e10313
98 Ma R, Li Y, Wei Y, Zhou J, Ma J, Zhang M, Tu J, Jiang J, Xie S, Tan W, Liu X. *Nano Today*, 2024, 57: 102325
99 Mehta M, Bui TA, Yang X, Aksoy Y, Goldys EM, Deng W. *ACS Mater Au*, 2023, 3: 600–619
100 He H, Liu L, Morin EE, Liu M, Schwendeman A. *Acc Chem Res*, 2019, 52: 2445–2461
101 Binici B, Rattray Z, Zinger A, Perrie Y. *J Control Release*, 2025, 377: 162–173
102 Yuan Y, Li Y, Li G, Lei L, Huang X, Li M, Yao Y. *Mol Pharm*, 2025, 22: 1142–1159
103 Zheng Y, Oz Y, Gu Y, Ahamad N, Shariati K, Chevalier J, Kapur D, Annabi N. *Nano Today*, 2024, 55: 102147
104 Wang H, Lan Z, Tian R, Liang X, Jia F, Ma M, Chen H. *Nano Today*, 2024, 56: 102301
105 Xu Y, Ma S, Cui H, Chen J, Xu S, Gong F, Golubovic A, Zhou M, Wang KC, Varley A, Lu RXZ, Wang B, Li B. *Nat Commun*, 2024, 15: 6305
106 Wang W, Chen K, Jiang T, Wu Y, Wu Z, Ying H, Yu H, Lu J, Lin J, Ouyang D. *Nat Commun*, 2024, 15: 10804
107 Witten J, Raji I, Manan RS, Beyer E, Bartlett S, Tang Y, Ebadi M, Lei J, Nguyen D, Oladimeji F, Jiang AY, MacDonald E, Hu Y, Mughal H, Self A, Collins E, Yan Z, Engelhardt JF, Langer R, Anderson DG. *Nat Biotechnol*, 2024, doi: 10.1038/s41587-024-02490-y
108 Barenholz YC. *J Control Release*, 2012, 160: 117–134
109 Zhang L, More KR, Ojha A, Jackson CB, Quinlan BD, Li H, He W, Farzan M, Pardi N, Choe H. *npj Vaccines*, 2023, 8: 156
110 Yuan Y, Wu Y, Cheng J, Yang K, Xia Y, Wu H, Pan X. *Particuology*, 2024, 90: 88–97
111 Fan Y, Yen CW, Lin HC, Hou W, Estevez A, Sarode A, Goyon A, Bian J, Lin J, Koenig SG, Leung D, Nagapudi K, Zhang K. *Int J Pharm*, 2021, 599: 120392
112 Eugster R, Orsi M, Buttitta G, Serafini N, Tiboni M, Casettari L, Reymond JL, Aleandri S, Luciani P. *J Control Release*, 2024, 376: 1025–1038
113 Liu X, Meng H. *VIEW*, 2021, 2: 20200190
114 Tomeh MA, Mansor MH, Hadianamrei R, Sun W, Zhao X. *Int J Pharm*, 2022, 620: 121762
115 Galan EA, Zhao H, Wang X, Dai Q, Huck WTS, Ma S. *Matter*, 2020, 3: 1893–1922
116 Yi J, You EM, Liu GK, Tian ZQ. *Nat Nanotechnol*, 2024, 19: 1758–1762
117 Mottafegh A, Joo JU, Na GS, Sharma V, Kim DP. *Chem Eng J*, 2024, 500: 157454
118 Yuan Z, Yan R, Fu Z, Wu T, Ren C. *Sci Total Environ*, 2024, 927: 172240
119 Aggarwal P, Hall JB, McLeland CB, Dobrovolskaia MA, McNeil SE. *Adv Drug Deliver Rev*, 2009, 61: 428–437
120 Qin M, Xia H, Xu W, Chen B, Wang Y. *Adv Drug Deliver Rev*, 2023, 203: 115137
121 Wang Y, Xiao Z, Wang Z, Lee DY, Ma Y, Wilhelm S, Wang H, Kim BYS, Jiang W. *Nat Rev Bioeng*, 2025, 3: 333–348
122 Nel AE, Mädler L, Velegol D, Xia T, Hoek EMV, Somasundaran P, Klaessig F, Castranova V, Thompson M. *Nat Mater*, 2009, 8: 543–557
123 Boehnke N, Straehla JP, Safford HC, Kocak M, Rees MG, Ronan M, Rosenberg D, Adelmann CH, Chivukula RR, Nabar N, Berger AG, Lamson NG, Cheah JH, Li H, Roth JA, Koehler AN, Hammond PT. *Science*, 2022, 377: eabm5551
124 Lazarovits J, Sindhwani S, Tavares AJ, Zhang Y, Song F, Audet J, Krieger JR, Syed AM, Stordy B, Chan WCW. *ACS Nano*, 2019, 13: 8023–8034
125 Ahmadi M, Ayyoubzadeh SM, Ghorbani-Bidkorpeh F. *Toxicology*, 2024, 501: 153697
126 Wang J, Li Y, Nie G. *Nat Rev Mater*, 2021, 6: 766–783
127 Rothemund PWK. *Nature*, 2006, 440: 297–302
128 Guo Y, Cao X, Zheng X, Abbas SJ, Li J, Tan W. *Natl Sci Rev*, 2022, 9: nwac006
129 Wan F, Liu Z, Zhang J, Zhang W, Dai B. *Nano Today*, 2024, 55: 102187
130 Qi Z, Wei C, Zhang F, Wang Z, Zuo X. *Nano Today*, 2024, 54: 102127
131 Singh M, Sharma D, Garg M, Kumar A, Baliyan A, Rani R, Kumar V. *Biotechnol Adv*, 2022, 61: 108052
132 Chiriboga M, Green CM, Hastman DA, Mathur D, Wei Q, Díaz SA, Medintz IL, Veneziano R. *Sci Rep*, 2022, 12: 3871
133 Kim Y, Lim J, Kim D. *Small*, 2022, 18: 2103779
134 Chen C, Nie J, Ma M, Shi X. *ACS Synth Biol*, 2023, 12: 524–532
135 Wanninger S, Asadiatouei P, Bohlen J, Salem CB, Tinnefeld P, Ploetz E, Lamb DC. *Nat Commun*, 2023, 14: 6564
136 Truong-Quoc C, Lee JY, Kim KS, Kim DN. *Nat Mater*, 2024, 23: 984–992
137 Wang Y, Jin X, Castro C. *Sci Rep*, 2023, 13: 15196
138 Cole DJ, Hine NDM. *J Phys-Condens Matter*, 2016, 28: 393001
139 Benson E, Lolaico M, Tarasov Y, Gådin A, Högberg B. *ACS Nano*, 2019, 13: 12591–12598

140 Lee AJ, Rackers JA, Bricker WP. *Biophys J*, 2022, 121: 3883–3895
141 Mahmoudi M, Landry MP, Moore A, Coreas R. *Nat Rev Mater*, 2023, 8: 422–438
142 Huzar J, Coreas R, Landry MP, Tikhomirov G. *ACS Nano*, 2025, 19: 4333–4345
143 Poppleton E, Mallya A, Dey S, Joseph J, Šulc P. *Nucleic Acids Res*, 2021, 50: D246–D252
144 Jumper J, Evans R, Pritzel A, Green T, Figurnov M, Ronneberger O, Tunyasuvunakool K, Bates R, Žídek A, Potapenko A, Bridgland A, Meyer C, Kohl SAA, Ballard AJ, Cowie A, Romera-Paredes B, Nikolov S, Jain R, Adler J, Back T, Petersen S, Reiman D, Clancy E, Zielinski M, Steinegger M, Pacholska M, Berghammer T, Bodenstein S, Silver D, Vinyals O, Senior AW, Kavukcuoglu K, Kohli P, Hassabis D. *Nature*, 2021, 596: 583–589
145 Baek M, DiMaio F, Anishchenko I, Dauparas J, Ovchinnikov S, Lee GR, Wang J, Cong Q, Kinch LN, Schaeffer RD, Millán C, Park H, Adams C, Glassman CR, DeGiovanni A, Pereira JH, Rodrigues AV, van Dijk AA, Ebrecht AC, Opperman DJ, Sagmeister T, Buhlheller C, Pavkov-Keller T, Rathinaswamy MK, Dalwadi U, Yip CK, Burke JE, Garcia KC, Grishin NV, Adams PD, Read RJ, Baker D. *Science*, 2021, 373: 871–876
146 Mandal D, Nasrolahi Shirazi A, Parang K. *Org Biomol Chem*, 2014, 12: 3544–3561
147 Lin Z, Akin H, Rao R, Hie B, Zhu Z, Lu W, Smetanin N, Verkuil R, Kabeli O, Shmueli Y, dos Santos Costa A, Fazel-Zarandi M, Sercu T, Candido S, Rives A. *Science*, 2023, 379: 1123–1130
148 Lee S, Kibler RD, Ahn G, Hsia Y, Borst AJ, Philomin A, Kennedy MA, Huang B, Stoddard B, Baker D. *Nature*, 2025, 638: 546–552
149 Brandes N, Ofer D, Peleg Y, Rappoport N, Linial M, Martelli PL. *Bioinformatics*, 2022, 38: 2102–2110
150 Elnaggar A, Heinzinger M, Dallago C, Rehawi G, Wang Y, Jones L, Gibbs T, Feher T, Angerer C, Steinegger M, Bhowmik D, Rost B. *IEEE Trans Pattern Anal Mach Intell*, 2022, 44: 7112–7127
151 Steichen SD, Caldorera-Moore M, Peppas NA. *Eur J Pharm Sci*, 2013, 48: 416–427
152 Batra R, Loeffler TD, Chan H, Srinivasan S, Cui H, Korendovych IV, Nanda V, Palmer LC, Solomon LA, Fry HC, Sankaranarayanan SKRS. *Nat Chem*, 2022, 14: 1427–1435
153 Madani A, Krause B, Greene ER, Subramanian S, Mohr BP, Holton JM, Olmos Jr. JL, Xiong C, Sun ZZ, Socher R, Fraser JS, Naik N. *Nat Biotechnol*, 2023, 41: 1099–1106
154 Ferruz N, Höcker B. *Nat Mach Intell*, 2022, 4: 521–532
155 An HW, Li LL, Wang Y, Wang Z, Hou D, Lin YX, Qiao SL, Wang MD, Yang C, Cong Y, Ma Y, Zhao XX, Cai Q, Chen WT, Lu CQ, Xu W, Wang H, Zhao Y. *Nat Commun*, 2019, 10: 4861
156 Yi Y, An H, Wang H. *Adv Mater*, 2024, 36: 2305099
157 Gao XJ, Ciura K, Ma Y, Mikolajczyk A, Jagiello K, Wan Y, Gao Y, Zheng J, Zhong S, Puzyn T, Gao X. *Adv Mater*, 2024, 36: e2407793
158 Cao L, Coventry B, Goreshnik I, Huang B, Sheffler W, Park JS, Jude KM, Marković I, Kadam RU, Verschueren KHG, Verstraete K, Walsh STR, Bennett N, Phal A, Yang A, Kozodoy L, DeWitt M, Picton L, Miller L, Strauch EM, DeBouver ND, Pires A, Bera AK, Halabiya S, Hammerson B, Yang W, Bernard S, Stewart L, Wilson IA, Ruohola-Baker H, Schlessinger J, Lee S, Savvides SN, Garcia KC, Baker D. *Nature*, 2022, 605: 551–560
159 Yang EC, Divine R, Miranda MC, Borst AJ, Sheffler W, Zhang JZ, Decarreau J, Saragovi A, Abedi M, Goldbach N, Ahlrichs M, Dobbins C, Hand A, Cheng S, Lamb M, Levine PM, Chan S, Skotheim R, Fallas J, Ueda G, Lubner J, Somiya M, Khmelinskaia A, King NP, Baker D. *Nat Struct Mol Biol*, 2024, 31: 1404–1412
160 Shah A, Malik MS, Khan GS, Nosheen E, Iftikhar FJ, Khan FA, Shukla SS, Akhter MS, Kraatz HB, Aminabhavi TM. *Chem Eng J*, 2018, 353: 559–583
161 Dowling QM, Park YJ, Fries CN, Gerstenmaier NC, Ols S, Yang EC, Wargacki AJ, Dosey A, Hsia Y, Ravichandran R, Walkey CD, Burrell AL, Veesler D, Baker D, King NP. *Nature*, 2025, 638: 553–561
162 Cheng J, Teply B, Sherifi I, Sung J, Luther G, Gu F, Levynissenbaum E, Radovicmoreno A, Langer R, Farokhzad O. *Biomaterials*, 2007, 28: 869–876
163 Schissel CK, Mohapatra S, Wolfe JM, Fadzen CM, Bellovoda K, Wu CL, Wood JA, Malmberg AB, Loas A, Gómez-Bombarelli R, Pentelute BL. *Nat Chem*, 2021, 13: 992–1000
164 Bennett NR, Coventry B, Goreshnik I, Huang B, Allen A, Vafeados D, Peng YP, Dauparas J, Baek M, Stewart L, DiMaio F, De Munck S, Savvides SN, Baker D. *Nat Commun*, 2023, 14: 2625
165 Hsueh HT, Chou RT, Rai U, Liyanage W, Kim YC, Appell MB, Pejavar J, Leo KT, Davison C, Kolodziejski P, Mozzer A, Kwon HY, Sista M, Anders NM, Hemingway A, Rompicharla SVK, Edwards M, Pitha I, Hanes J, Cummings MP, Ensign LM. *Nat Commun*, 2023, 14: 2509
166 Yue Y, Xu J, Li Y, Cheng K, Feng Q, Ma X, Ma N, Zhang T, Wang X, Zhao X, Nie G. *Nat Biomed Eng*, 2022, 6: 898–909
167 Vázquez Torres S, Leung PJY, Venkatesh P, Lutz ID, Hink F, Huynh HH, Becker J, Yeh AHW, Juergens D, Bennett NR, Hoofnagle AN, Huang E, MacCoss MJ, Expòsit M, Lee GR, Bera AK, Kang A, De La Cruz J, Levine PM, Li X, Lamb M, Gerben SR, Murray A, Heine P, Korkmaz EN, Nivala J, Stewart L, Watson JL, Rogers JM, Baker D. *Nature*, 2024, 626: 435–442
168 Rao L, Yuan Y, Shen X, Yu G, Chen X. *Nat Nanotechnol*, 2024, 19: 1769–1781
169 Wang Y, Tang H, Huang L, Pan L, Yang L, Yang H, Mu F, Yang M. *Nat Mach Intell*, 2023, 5: 845–860
170 Huddy TF, Hsia Y, Kibler RD, Xu J, Bethel N, Nagarajan D, Redler R, Leung PJY, Weidle C, Courbet A, Yang EC, Bera AK, Coudray N, Calise SJ, Davila-Hernandez FA, Han HL, Carr KD, Li Z, McHugh R, Reggiano G, Kang A, Sankaran B, Dickinson MS, Coventry B, Brunette TJ, Liu Y, Dauparas J, Borst AJ, Ekiert D, Kollman JM, Bhabha G, Baker D. *Nature*, 2024, 627: 898–904
171 Mendes BB, Zhang Z, Conniot J, Sousa DP, Ravasco JMJM, Onweller LA, Lorenc A, Rodrigues T, Reker D, Conde J. *Nat Nanotechnol*, 2024, 19: 867–878
172 Pandi A, Adam D, Zare A, Trinh VT, Schaefer SL, Burt M, Klabunde B, Bobkova E, Kushwaha M, Foroughijabbari Y, Braun P, Spahn C, Preußer C, Pogge von Strandmann E, Bode HB, von Buttlar H, Bertrams W, Jung AL, Abendroth F, Schmeck B, Hummer G, Vázquez O, Erb TJ. *Nat Commun*, 2023, 14: 7197
173 Xu T, Wang J, Zhao S, Chen D, Zhang H, Fang Y, Kong N, Zhou Z, Li W, Wang H. *Nat Commun*, 2023, 14: 3880
174 Beach MA, Nayanathara U, Gao Y, Zhang C, Xiong Y, Wang Y, Such GK. *Chem Rev*, 2024, 124: 5505–5616
175 McDonald SM, Augustine EK, Lanners Q, Rudin C, Catherine Brinson L, Becker ML. *Nat Commun*, 2023, 14: 4838
176 Bannigan P, Bao Z, Hickman RJ, Aldeghi M, Häse F, Aspuru-Guzik A, Allen C. *Nat Commun*, 2023, 14: 35
177 Santana R, Zuluaga R, Gañán P, Arrasate S, Onieva E, González-Díaz H. *Nanoscale*, 2019, 11: 21811–21823
178 Metwally AA, Hathout RM. *Mol Pharm*, 2015, 12: 2800–2810
179 Chaurawal N, Quadir SS, Joshi G, Barkat MA, Alanezi AA, Raza K. *Int J Biol Macromol*, 2024, 279: 135123
180 Stiepel RT, Pena ES, Ehrenzeller SA, Gallovic MD, Lifshits LM, Genito CJ, Bachelder EM, Ainslie KM. *J Control Release*, 2022, 351: 883–895
181 Jin S, Lan Z, Yang G, Li X, Shi JQ, Liu Y, Zhao C. *Aggregate*, 2024, 5: e606
182 Kumar R, Le N, Tan Z, Brown ME, Jiang S, Reineke TM. *ACS Nano*, 2020, 14: 17626–17639
183 Dalal RJ, Oviedo F, Leyden MC, Reineke TM. *Chem Sci*, 2024, 15: 7219–7228
184 Kumar R, Le N, Oviedo F, Brown ME, Reineke TM. *JACS Au*, 2022, 2: 428–442
185 Huwaimel B, Alqarni S. *Chemometrics Intelligent Lab Syst*, 2025, 258: 105335
186 Rezvantalab S, Mihandoost S, Rezaiee M. *Sci Rep*, 2024, 14: 1114

187 Almansour K, Alqahtani AS. *Sci Rep*, 2025, 15: 8840
188 Li Y, He Z, A S, Wang X, Li Z, Johnson M, Foley R, Sáez IL, Lyu J, Wang W. *ACS Appl Mater Interfaces*, 2023, 15: 36667–36675
189 Youshia J, Ali ME, Lamprecht A. *Eur J Pharm Biopharm*, 2017, 119: 333–342
190 Hashad RA, Ishak RAH, Fahmy S, Mansour S, Geneidi AS. *Int J Biol Macromol*, 2016, 86: 50–58
191 Abd-algaleel SA, Abdel-Bar HM, Metwally AA, Hathout RM. *Pharmaceuticals*, 2021, 14: 645
192 Mullis AS, Broderick SR, Binnebose AM, Peroutka-Bigus N, Bellaire BH, Rajan K, Narasimhan B. *Mol Pharm*, 2019, 16: 1917–1928
193 Siepmann J, Faisant N, Akiki J, Richard J, Benoit JP. *J Control Release*, 2004, 96: 123–134
194 Mendyk A, Szlęk J, Jachowicz R, Lau R, Paclawski A. *Int J Nanomed*, 2013, 8: 4601
195 Sun Y, Qin S, Li Y, Hasan N, Li YV, Liu J. *Sci Rep*, 2025, 15: 4218
196 Gong D, Ben-Akiva E, Singh A, Yamagata H, Est-Witte S, Shade JK, Trayanova NA, Green JJ. *Acta Biomater*, 2022, 154: 349–358
197 Loecher A, Bruyns-Haylett M, Ballester PJ, Borros S, Oliva N. *Biomater Sci*, 2023, 11: 5797–5808
198 Kingston BR, Syed AM, Ngai J, Sindhwani S, Chan WCW. *Proc Natl Acad Sci USA*, 2019, 116: 14937–14946
199 Pilié PG, Tang C, Mills GB, Yap TA. *Nat Rev Clin Oncol*, 2019, 16: 81–104
200 Piella J, Bastús NG, Puntes V. *Chem Mater*, 2016, 28: 1066–1075
201 Park J, Kim YM, Hong S, Han B, Nam KT, Jung Y. *Matter*, 2023, 6: 677–690
202 Tao H, Wu T, Aldeghi M, Wu TC, Aspuru-Guzik A, Kumacheva E. *Nat Rev Mater*, 2021, 6: 701–716
203 Schletz D, Breidung M, Fery A. *J Phys Chem C*, 2023, 127: 1117–1125
204 Li J, Chen T, Lim K, Chen L, Khan SA, Xie J, Wang X. *Adv Intelligent Syst*, 2019, 1: 1900029
205 Shafaei A, Khayati GR. *Measurement*, 2020, 151: 107199
206 Wahl CB, Aykol M, Swisher JH, Montoya JH, Suram SK, Mirkin CA. *Sci Adv*, 2021, 7: eabj5505
207 Huynh E, Hosny A, Guthier C, Bitterman DS, Petit SF, Haas-Kogan DA, Kann B, Aerts HJWL, Mak RH. *Nat Rev Clin Oncol*, 2020, 17: 771–781
208 Field M, Hardcastle N, Jameson M, Aherne N, Holloway L. *Phys Imag Radiat Oncol*, 2021, 19: 13–24
209 Li K, Liang J, Li N, Fang J, Zhou X, Zhang J, Lin A, Luo P, Meng H. *eLife*, 2024, 2024: 99849.2
210 Santoro M, Strolin S, Paolani G, Della Gala G, Bartoloni A, Giacometti C, Ammendolia I, Morganti AG, Strigari L. *Appl Sci*, 2022, 12: 3223
211 Zeng Z, Luo M, Li Y, Li J, Huang Z, Zeng Y, Yuan Y, Wang M, Liu Y, Gong Y, Xie C. *BMC Cancer*, 2022, 22: 1243
212 Wang H, He W, Liao J, Wang S, Dai X, Yu M, Xie Y, Chen Y. *Adv Mater*, 2025, 37: 2411967
213 Guo Y, Wang J, Wu X, Qiao Q, Liao T, Li L, Xu Z, Zheng DW, Kuang Y, Yu W, Li C. *Nano Today*, 2025, 65: 102848
214 Huang H, Zheng Y, Chang M, Song J, Xia L, Wu C, Jia W, Ren H, Feng W, Chen Y. *Chem Rev*, 2024, 124: 8307–8472
215 Huang H, Chen Y. *Sci Bull*, 2025, 70: 1554–1558
216 Wang Z, Song X, Huang H, Chang M, Chen Y. *MedComm-Biomater Appl*, 2023, 2: e53
217 Wu Q, Zhang H, Liu H. *BMEMat*, 2023, 1: e12010
218 He R, Yang B, Shi J. *Nano Today*, 2025, 65: 102820
219 He L, Dong J, Yang Y, Huang Z, Ye S, Ke X, Zhou Y, Li A, Zhang Z, Wu S, Wang Y, Cai S, Liu X, He Y. *J Mol Structure*, 2025, 1321: 139850
220 Vigna V, Cova TFGG, Pais AACC, Sicilia E. *J Cheminform*, 2025, 17: 1
221 Pablo-García S, Morandi S, Vargas-Hernández RA, Jorner K, Ivković Ž, López N, Aspuru-Guzik A. *Nat Comput Sci*, 2023, 3: 433–442
222 Zhu M, Zhuang J, Li Z, Liu Q, Zhao R, Gao Z, Midgley AC, Qi T, Tian J, Zhang Z, Kong D, Tian J, Yan X, Huang X. *Nat Nanotechnol*, 2023, 18: 657–666
223 Melle F, Menon D, Conniot J, Ostolaza-Paraiso J, Mercado S, Oliveira J, Chen X, Mendes BB, Conde J, Fairen-Jimenez D. *Adv Mater*, 2025, 37: 2412757
224 Jiang Y, Chen Z, Sui N, Zhu Z. *J Am Chem Soc*, 2024, 146: 7565–7574
225 Wu Y, Wang CF, Ju MG, Jia Q, Zhou Q, Lu S, Gao X, Zhang Y, Wang J. *Nat Commun*, 2024, 15: 138
226 Wang Z, Yuan A, Liu C, Liu Y, Qiao L, Xu Z, Bi S, Tian J, Yu B, Lin Z, Du J, Zhang Y. *Int J Biol Macromol*, 2025, 297: 139842
227 Ouyang B, Shan C, Shen S, Dai X, Chen Q, Su X, Cao Y, Qin X, He Y, Wang S, Xu R, Hu R, Shi L, Lu T, Yang W, Peng S, Zhang J, Wang J, Li D, Pang Z. *Nat Commun*, 2024, 15: 7560
228 Ortiz-Perez A, van Tilborg D, van der Meel R, Grisoni F, Albertazzi L. *Digital Discov*, 2024, 3: 1280–1291
229 Zhang YP, Chen HJ, Hu Y, Lin L, Wen HY, Pang DW, Zhang S, Wang ZG, Liu SL. *Nano Lett*, 2024, 24: 1816–1824
230 Yu XH, Yi JL, Zhang RL, Wang FY, Liu L. *Front Chem Sci Eng*, 2021, 15: 1380–1407
231 Chen Z, Chen Y, Sun Y, Tang L, Zhang L, Hu Y, He M, Li Z, Cheng S, Yuan J, Wang Z, Wang Y, Zhao J, Gong J, Zhao L, Cao B, Li G, Zhang X, Dong B, Shen L. *Sig Transduct Target Ther*, 2024, 9: 222
232 Li T, Cao B, Su T, Lin L, Wang D, Liu X, Wan H, Ji H, He Z, Chen Y, Feng L, Zhang T. *Small*, 2025, 21: 2408750
233 Kong JH, Ha D, Lee J, Kim I, Park M, Im SH, Shin K, Kim S. *Nat Commun*, 2022, 13: 3703
234 Fang FC. *Nat Rev Microbiol*, 2004, 2: 820–832
235 Nathan C, Cunningham-Bussel A. *Nat Rev Immunol*, 2013, 13: 349–361
236 Dickinson BC, Chang CJ. *Nat Chem Biol*, 2011, 7: 504–511
237 Winterbourn CC. *Nat Chem Biol*, 2008, 4: 278–286
238 Patel RP, McAndrew J, Sellak H, White CR, Jo H, Freeman BA, Darley-Usmar VM. *Biochim Biophys Acta (BBA)-Bioenergetics*, 1999, 1411: 385–400
239 Dedon PC, Tannenbaum SR. *Arch Biochem Biophys*, 2004, 423: 12–22
240 Midgley AC, Wei Y, Li Z, Kong D, Zhao Q. *Adv Mater*, 2020, 32: e1805818
241 Yang T, Zelikin AN, Chandrawati R. *Adv Sci*, 2018, 5: 1701043
242 Yan X, Song J, Zhang Y, Yang M, Deng Z, Gao B, Zhu Y, Xu C, Ding C, Zhang M, Zhang B. *Nano Today*, 2024, 54: 102139
243 MatÉs JÉM, Pérez-Gómez C, De Castro IN. *Clin Biochem*, 1999, 32: 595–603
244 Matés JM. *Toxicology*, 2000, 153: 83–104
245 Cooke MS, Evans MD, Dizdaroglu M, Lunec J. *FASEB J*, 2003, 17: 1195–1214
246 Sies H, Berndt C, Jones DP. *Annu Rev Biochem*, 2017, 86: 715–748
247 Ott M, Gogvadze V, Orrenius S, Zhivotovsky B. *Apoptosis*, 2007, 12: 913–922
248 Forman HJ, Zhang H. *Nat Rev Drug Discov*, 2021, 20: 689–709
249 Liu X, Xu H, Peng H, Wan L, Di D, Qin Z, He L, Lu J, Wang S, Zhao Q. *Coord Chem Rev*, 2024, 502: 215610
250 Kang T, Kim YG, Kim D, Hyeon T. *Coord Chem Rev*, 2020, 403: 213092
251 Wu J, Wang X, Wang Q, Lou Z, Li S, Zhu Y, Qin L, Wei H. *Chem Soc Rev*, 2019, 48: 1004–1076
252 Liu Y, Wu H, Li M, Yin JJ, Nie Z. *Nanoscale*, 2014, 6: 11904–11910
253 Moglianetti M, De Luca E, Pedone D, Marotta R, Catelani T, Sartori B, Amenitsch H, Retta SF, Pompa PP. *Nanoscale*, 2016, 8: 3739–3752
254 Watanabe A, Kajita M, Kim J, Kanayama A, Takahashi K, Mashino T, Miyamoto Y. *Nanotechnology*, 2009, 20: 455105
255 Liu X, Zhang Z, Zhang Y, Guan Y, Liu Z, Ren J, Qu X. *Adv Funct Mater*, 2016, 26: 7921–7928
256 Fan J, Yin JJ, Ning B, Wu X, Hu Y, Ferrari M, Anderson GJ, Wei J, Zhao Y, Nie G. *Biomaterials*, 2011, 32: 1611–1618

257 Hosaka H, Haruki R, Yamada K, Böttcher C, Komatsu T, Permyakov EA. *PLoS ONE*, 2014, 9: e110541
258 Ge C, Fang G, Shen X, Chong Y, Wamer WG, Gao X, Chai Z, Chen C, Yin JJ. *ACS Nano*, 2016, 10: 10436–10445
259 Wei J, Chen X, Shi S, Mo S, Zheng N. *Nanoscale*, 2015, 7: 19018–19026
260 Ding J, Luo W, Wu T, Cai S, Pan ZA, Li H, Tu B, Fang Q, Yan X, Yang R. *Nano Today*, 2024, 54: 102121
261 He W, Zhou YT, Wamer WG, Hu X, Wu X, Zheng Z, Boudreau MD, Yin JJ. *Biomaterials*, 2013, 34: 765–773
262 Kim HS, Lee S, Lee DY. *Small*, 2023, 19: 2302331
263 Mu X, Wang J, Li Y, Xu F, Long W, Ouyang L, Liu H, Jing Y, Wang J, Dai H, Liu Q, Sun Y, Liu C, Zhang XD. *ACS Nano*, 2019, 13: 1870–1884
264 He W, Liu Y, Yuan J, Yin JJ, Wu X, Hu X, Zhang K, Liu J, Chen C, Ji Y, Guo Y. *Biomaterials*, 2011, 32: 1139–1147
265 Xiong B, Xu R, Zhou R, He Y, Yeung ES. *Talanta*, 2014, 120: 262–267
266 Li Y, He X, Yin J, Ma Y, Zhang P, Li J, Ding Y, Zhang J, Zhao Y, Chai Z, Zhang Z. *Angew Chem Int Ed*, 2015, 54: 1832–1835
267 Heckert EG, Karakoti AS, Seal S, Self WT. *Biomaterials*, 2008, 29: 2705–2709
268 Korsvik C, Patil S, Seal S, Self WT. *Chem Commun*, 2007, 43: 1056
269 Baldim V, Bedioui F, Mignet N, Margaill I, Berret JF. *Nanoscale*, 2018, 10: 6971–6980
270 Pirmohamed T, Dowding JM, Singh S, Wasserman B, Heckert E, Karakoti AS, King JES, Seal S, Self WT. *Chem Commun*, 2010, 46: 2736–2738
271 Celardo I, De Nicola M, Mandoli C, Pedersen JZ, Traversa E, Ghibelli L. *ACS Nano*, 2011, 5: 4537–4549
272 Tan Z, Li G, Chou HL, Li Y, Yi X, Mahadi AH, Zheng A, Edman Tsang SC, Peng YK. *ACS Catal*, 2020, 10: 4003–4011
273 Singh S, Dosani T, Karakoti AS, Kumar A, Seal S, Self WT. *Biomaterials*, 2011, 32: 6745–6753
274 Liu X, Wei W, Yuan Q, Zhang X, Li N, Du Y, Ma G, Yan C, Ma D. *Chem Commun*, 2012, 48: 3155–3157
275 Gao L, Zhuang J, Nie L, Zhang J, Zhang Y, Gu N, Wang T, Feng J, Yang D, Perrett S, Yan X. *Nat Nanotech*, 2007, 2: 577–583
276 Zhang Y, Wang Z, Li X, Wang L, Yin M, Wang L, Chen N, Fan C, Song H. *Adv Mater*, 2016, 28: 1387–1393
277 Chen Z, Yin JJ, Zhou YT, Zhang Y, Song L, Song M, Hu S, Gu N. *ACS Nano*, 2012, 6: 4001–4012
278 Meng L, Feng J, Gao J, Zhang Y, Mo W, Zhao X, Wei H, Guo H. *ACS Appl Mater Interfaces*, 2022, 14: 50649–50663
279 Singh N, Savanur MA, Srivastava S, D'Silva P, Mugesh G. *Angew Chem Int Ed*, 2017, 56: 14267–14271
280 Li W, Liu Z, Liu C, Guan Y, Ren J, Qu X. *Angew Chem Int Ed*, 2017, 56: 13661–13665
281 Ragg R, Schilmann AM, Korschelt K, Wieseotte C, Kluenker M, Viel M, Völker L, Preiß S, Herzberger J, Frey H, Heinze K, Blümler P, Tahir MN, Natalio F, Tremel W. *J Mater Chem B*, 2016, 4: 7423–7428
282 Dong J, Song L, Yin JJ, He W, Wu Y, Gu N, Zhang Y. *ACS Appl Mater Interfaces*, 2014, 6: 1959–1970
283 Mu J, Wang Y, Zhao M, Zhang L. *Chem Commun*, 2012, 48: 2540–2542
284 Mu J, Zhang L, Zhao M, Wang Y. *J Mol Catal A-Chem*, 2013, 378: 30–37
285 Zhang W, Dong J, Wu Y, Cao P, Song L, Ma M, Gu N, Zhang Y. *Colloids Surfs B-Biointerfaces*, 2017, 154: 55–62
286 Hao C, Qu A, Xu L, Sun M, Zhang H, Xu C, Kuang H. *J Am Chem Soc*, 2019, 141: 1091–1099
287 Zeng J, Ding C, Chen L, Yang B, Li M, Wang X, Su F, Liu C, Huang Y. *ACS Appl Mater Interfaces*, 2023, 15: 378–390
288 Vernekar AA, Sinha D, Srivastava S, Paramasivam PU, D'Silva P, Mugesh G. *Nat Commun*, 2014, 5: 5301
289 Huang Y, Liu Z, Liu C, Ju E, Zhang Y, Ren J, Qu X. *Angew Chem Int Ed*, 2016, 55: 6646–6650
290 Nexha A, Díaz F, Aguiló M, Pujol MC, Carvajal JJ. *J Alloys Compd*, 2024, 980: 173565
291 Labiadh H, Lahbib K, Hidouri S, Touil S, Chaabane TB. *Asian Pac J Tropical Med*, 2016, 9: 757–762
292 Khalil AT, Khan MD, Razzaque S, Afridi S, Ullah I, Iqbal J, Tasneem S, Shah A, Shinwari ZK, Revaprasadu N, Ayaz M. *Appl Nanosci*, 2021, 11: 2489–2502
293 Chen T, Zou H, Wu X, Liu C, Situ B, Zheng L, Yang G. *ACS Appl Mater Interfaces*, 2018, 10: 12453–12462
294 Qin Z, Chen B, Mao Y, Shi C, Li Y, Huang X, Yang F, Gu N. *ACS Appl Mater Interfaces*, 2020, 12: 57382–57390
295 Zhang W, Hu S, Yin JJ, He W, Lu W, Ma M, Gu N, Zhang Y. *J Am Chem Soc*, 2016, 138: 5860–5865
296 Wang C, Ren G, Yuan B, Zhang W, Lu M, Liu J, Li K, Lin Y. *Anal Chem*, 2020, 92: 7822–7830
297 Chukavin NN, Filippova KO, Ermakov AM, Karmanova EE, Popova NR, Anikina VA, Ivanova OS, Ivanov VK, Popov AL. *Biomedicines*, 2023, 12: 11
298 Ren C, Hu X, Zhou Q. *Adv Sci*, 2018, 5: 1700595
299 Lin B, Chen H, Liang D, Lin W, Qi X, Liu H, Deng X. *ACS Appl Mater Interfaces*, 2019, 11: 11157–11166
300 Ma H, Zhao J, Meng H, Hu D, Zhou Y, Zhang X, Wang C, Li J, Yuan J, Wei Y. *ACS Appl Mater Interfaces*, 2020, 12: 16104–16113
301 Ali SS, Hardt JI, Dugan LL. *Nanomed-Nanotechnol Biol Med*, 2008, 4: 283–294
302 Hong SJ, Chun H, Hong M, Han B. *Appl Surf Sci*, 2022, 598: 153715
303 Andrade EB, Martínez A. *Comput Theor Chem*, 2017, 1115: 127–135
304 Zhang W, Chavez J, Zeng Z, Bloom B, Sheardy A, Ji Z, Yin Z, Waldeck DH, Jia Z, Wei J. *ACS Appl Nano Mater*, 2018, 1: 2699–2708
305 Xue S, Zhang T, Wang X, Zhang Q, Huang S, Zhang L, Zhang L, Zhu W, Wang Y, Wu M, Zhao Q, Li P, Wu W. *Small*, 2021, 17: 2102178
306 Watts PCP, Fearon PK, Hsu WK, Billingham NC, Kroto HW, Walton DRM. *J Mater Chem*, 2003, 13: 491–495
307 Vardakas P, Kartsonakis IA, Kyriazis ID, Kainourgios P, Trompeta AFA, Charitidis CA, Kouretas D. *Environ Res*, 2023, 220: 115156
308 Fan K, Xi J, Fan L, Wang P, Zhu C, Tang Y, Xu X, Liang M, Jiang B, Yan X, Gao L. *Nat Commun*, 2018, 9: 1440
309 Li F, Li T, Sun C, Xia J, Jiao Y, Xu H. *Angew Chem Int Ed*, 2017, 56: 9910–9914
310 Sentkowska A, Pyrzyńska K. *Molecules*, 2022, 27: 2486
311 Qiu WY, Wang YY, Wang M, Yan JK. *Colloids Surfs B-Biointerfaces*, 2018, 170: 692–700
312 Huang B, Zhang J, Hou J, Chen C. *Free Radical Biol Med*, 2003, 35: 805–813
313 Chen W, Li Y, Yang S, Yue L, Jiang Q, Xia W. *Carbohydrate Polyms*, 2015, 132: 574–581
314 Chen X, Zhu X, Gong Y, Yuan G, Cen J, Lie Q, Hou Y, Ye G, Liu S, Liu J. *Appl Mater Today*, 2021, 22: 100929
315 Huang Y, Liu Z, Liu C, Zhang Y, Ren J, Qu X. *Chem Eur J*, 2018, 24: 10224–10230
316 Lin SS, Gurol MD. *Environ Sci Technol*, 1998, 32: 1417–1423
317 Shen X, Liu W, Gao X, Lu Z, Wu X, Gao X. *J Am Chem Soc*, 2015, 137: 15882–15891
318 Zhang Y, Chen L, Sun R, Lv R, Du T, Li Y, Zhang X, Sheng R, Qi Y. *ACS BioMater Sci Eng*, 2022, 8: 638–648
319 Zhang X, Zhang S, Yang Z, Wang Z, Tian X, Zhou R. *Nanoscale*, 2021, 13: 12613–12622
320 Wang S, Zhou Y, Liang X, Xu M, Li N, Zhao K. *Chem Eng J*, 2022, 430: 132859
321 Li H, Yan J, Meng D, Cai R, Gao X, Ji Y, Wang L, Chen C, Wu X. *ACS Nano*, 2020, 14: 12854–12865
322 Ding L, Zhang S, Li Y, Wu Y, Liu X, Xu D, Zhao K, Xu C, Yu B, Huang X, Tang BZ, Zhang W. *Chem Eng J*, 2024, 486: 150177
323 Wang Y, Qin L, Li X, Wang L, Ling G, Zhang P. *Int J Biol Mac-*

romol, 2025, 291: 139210
324 Liu Y, Chen L, Chen Z, Liu M, Li X, Kou Y, Hou MM, Wang H, Li X, Tian B, Dong J. *ACS Nano*, 2023, 17: 8167–8182
325 Tu C, Lu H, Zhou T, Zhang W, Deng L, Cao W, Yang Z, Wang Z, Wu X, Ding J, Xu F, Gao C. *Biomaterials*, 2022, 286: 121597
326 Liao J, Li Y, Fan L, Sun Y, Gu Z, Xu QQ, Wang Y, Xiong L, Xiao K, Chen Z, Ma Z, Zhang C, Wang T, Lu Y. *ACS Nano*, 2024, 18: 5510–5529
327 Ma J, Tian Y, Du C, Zhu Y, Huang W, Ding C, Wei P, Yi X, Lin Z, Fang W. *J Nanobiotechnol*, 2025, 23: 181
328 Chen Y, Yang X, Li K, Feng J, Liu X, Li Y, Yang K, Li J, Ge S. *ACS Nano*, 2024, 18: 7024–7036
329 Hang C, Moawad MS, Lin Z, Guo H, Xiong H, Zhang M, Lu R, Liu J, Shi D, Xie D, Liu Y, Liang D, Chen YH, Yang J. *J Nanobiotechnol*, 2024, 22: 132
330 Zheng N, Li K, He L, Wang Q, Yang B, Mao C, Tang W, Liu S, Liu S. *Nano Today*, 2024, 58: 102404
331 Li S, Zhou Z, Tie Z, Wang B, Ye M, Du L, Cui R, Liu W, Wan C, Liu Q, Zhao S, Wang Q, Zhang Y, Zhang S, Zhang H, Du Y, Wei H. *Nat Commun*, 2022, 13: 827
332 Zhao X, Yu Y, Xu X, Zhang Z, Chen Z, Gao Y, Zhong L, Chen J, Huang J, Qin J, Zhang Q, Tang X, Yang D, Zhu Z. *Adv Mater*, 2025, 37: e2417536
333 Mejia-Mendez JL, Reza-Zaldívar EE, Sanchez-Martinez A, Ceballos-Sanchez O, Navarro-López DE, Marcelo Lozano L, Armendariz-Borunda J, Tiwari N, Jacobo-Velázquez DA, Sanchez-Ante G, López-Mena ER. *J Nanobiotechnol*, 2024, 22: 687
334 Sun L, Hu J, Yang Y, Wang Y, Wang Z, Gao Y, Nie Y, Liu C, Kan H. *J Chem Inf Model*, 2024, 64: 6736–6744
335 Ceballos-Sanchez O, Navarro-López DE, Mejía-Méndez JL, Sanchez-Ante G, Rodríguez-González V, Sánchez-López AL, Sanchez-Martinez A, Duron-Torres SM, Juarez-Moreno K, Tiwari N, López-Mena ER. *BioMater Sci*, 2024, 12: 2108–2120
336 Yu Y, Zhao X, Xu X, Cai C, Tang X, Zhang Q, Zhong L, Zhou F, Yang D, Zhu Z. *Adv Mater*, 2023, 35: 2304967
337 Gao XJ, Yan J, Zheng J, Zhong S, Gao X. *Adv Healthcare Mater*, 2023, 12: 2202925
338 Zhang C, Yu Y, Shi S, Liang M, Yang D, Sui N, Yu WW, Wang L, Zhu Z. *Nano Lett*, 2022, 22: 8592–8600
339 Wang Z, Wu J, Zheng JJ, Shen X, Yan L, Wei H, Gao X, Zhao Y. *Nat Commun*, 2021, 12: 6866
340 Su C, Liu Y, Li R, Wu W, Fawcett JP, Gu J. *Adv Drug Deliver Rev*, 2019, 143: 97–114
341 Zhang A, Meng K, Liu Y, Pan Y, Qu W, Chen D, Xie S. *Adv Colloid Interface Sci*, 2020, 284: 102261
342 Wang L, Yan L, Liu J, Chen C, Zhao Y. *Anal Chem*, 2018, 90: 589–614
343 Hassanzadeh P, Atyabi F, Dinarvand R. *Adv Drug Deliver Rev*, 2019, 151-152: 169–190
344 Serrano DR, Luciano FC, Anaya BJ, Ongoren B, Kara A, Molina G, Ramirez BI, Sánchez-Guirales SA, Simon JA, Tomietto G, Rapti C, Ruiz HK, Rawat S, Kumar D, Lalatsa A. *Pharmaceutics*, 2024, 16: 1328
345 Bannigan P, Aldeghi M, Bao Z, Häse F, Aspuru-Guzik A, Allen C. *Adv Drug Deliver Rev*, 2021, 175: 113806
346 Epa VC, Burden FR, Tassa C, Weissleder R, Shaw S, Winkler DA. *Nano Lett*, 2012, 12: 5808–5812
347 Tang Y, Zhang J, He D, Miao W, Liu W, Li Y, Lu G, Wu F, Wang S. *J Control Release*, 2021, 336: 336–343
348 Liu R, Jiang W, Walkey CD, Chan WCW, Cohen Y. *Nanoscale*, 2015, 7: 9664–9675
349 Kaminskas LM, Pires DEV, Ascher DB. *Sci Rep*, 2019, 9: 15465
350 Zhao F, Meng H, Yan L, Wang B, Zhao Y. *Sci Bull*, 2015, 60: 3–20
351 Wang L, Liu Y, Li W, Jiang X, Ji Y, Wu X, Xu L, Qiu Y, Zhao K, Wei T, Li Y, Zhao Y, Chen C. *Nano Lett*, 2011, 11: 772–780
352 Qiu Y, Liu Y, Wang L, Xu L, Bai R, Ji Y, Wu X, Zhao Y, Li Y, Chen C. *Biomaterials*, 2010, 31: 7606–7619
353 Liu Y, Li W, Lao F, Liu Y, Wang L, Bai R, Zhao Y, Chen C. *Biomaterials*, 2011, 32: 8291–8303
354 Zhou H, Zhao K, Li W, Yang N, Liu Y, Chen C, Wei T. *Biomaterials*, 2012, 33: 6933–6942
355 Li Y, Liu Y, Fu Y, Wei T, Le Guyader L, Gao G, Liu RS, Chang YZ, Chen C. *Biomaterials*, 2012, 33: 402–411
356 Chong Y, Ge C, Fang G, Wu R, Zhang H, Chai Z, Chen C, Yin JJ. *Environ Sci Technol*, 2017, 51: 10154–10161
357 Cao M, Cai R, Zhao L, Guo M, Wang L, Wang Y, Zhang L, Wang X, Yao H, Xie C, Cong Y, Guan Y, Tao X, Wang Y, Xu S, Liu Y, Zhao Y, Chen C. *Nat Nanotechnol*, 2021, 16: 708–716
358 Liu X, Wei W, Liu Z, Song E, Lou J, Feng L, Huang R, Chen C, Ke PC, Song Y. *Proc Natl Acad Sci USA*, 2021, 118: e2108131118
359 Ren J, Cai R, Wang J, Daniyal M, Baimanov D, Liu Y, Yin D, Liu Y, Miao Q, Zhao Y, Chen C. *Nano Lett*, 2019, 19: 4692–4701
360 Guo M, Zhao L, Liu J, Wang X, Yao H, Chang X, Liu Y, Liu J, You M, Ren J, Wang F, Wang L, Wang Y, Liu H, Li Y, Zhao Y, Cai R, Chen C. *Nano Lett*, 2021, 21: 6005–6013
361 Lu X, Zhu Y, Bai R, Wu Z, Qian W, Yang L, Cai R, Yan H, Li T, Pandey V, Liu Y, Lobie PE, Chen C, Zhu T. *Nat Nanotechnol*, 2019, 14: 719–727
362 Meng L, Chen R, Jiang A, Wang L, Wang P, Li C, Bai R, Zhao Y, Autrup H, Chen C. *Small*, 2013, 9: 1786–1798
363 Wang P, Nie X, Wang Y, Li Y, Ge C, Zhang L, Wang L, Bai R, Chen Z, Zhao Y, Chen C. *Small*, 2013, 9: 3799–3811
364 Zhao F, Zhao Y, Liu Y, Chang X, Chen C, Zhao Y. *Small*, 2011, 7: 1322–1337
365 Fang G, Li W, Shen X, Perez-Aguilar JM, Chong Y, Gao X, Chai Z, Chen C, Ge C, Zhou R. *Nat Commun*, 2018, 9: 129
366 Feculak M, Loureiro S, White JC, Xing B, Wu KCW, Sheteiwy MS, Gao Y, Oleszczuk P, Jośko I. *Nano Today*, 2025, 65: 102804
367 Jiang X, Miclăuș T, Wang L, Foldbjerg R, Sutherland DS, Autrup H, Chen C, Beer C. *Nanotoxicology*, 2015, 9: 181–189
368 Wang L, Zhang T, Li P, Huang W, Tang J, Wang P, Liu J, Yuan Q, Bai R, Li B, Zhang K, Zhao Y, Chen C. *ACS Nano*, 2015, 9: 6532–6547
369 Cui X, Wang X, Chang X, Bao L, Wu J, Tan Z, Chen J, Li J, Gao X, Ke PC, Chen C. *Proc Natl Acad Sci USA*, 2023, 120: e2218739120
370 Wang M, Li Q, Shi C, Lv J, Xu Y, Yang J, Chua SL, Jia L, Chen H, Liu Q, Huang C, Huang Y, Chen J, Fang M. *Nat Nanotechnol*, 2023, 18: 403–411
371 Wang L, Li YF, Zhou L, Liu Y, Meng L, Zhang K, Wu X, Zhang L, Li B, Chen C. *Anal Bioanal Chem*, 2010, 396: 1105–1114
372 Jarzynska K, Ciura K, Gao XJ, Mikolajczyk A, Gao X, Puzyn T. *Nano Today*, 2025, 64: 102783
373 Yan X, Yue T, Winkler DA, Yin Y, Zhu H, Jiang G, Yan B. *Chem Rev*, 2023, 123: 8575–8637